UNIVERSIDADE FEDERAL DE PERNAMBUCO
CENTRO DE CIÊNCIAS EXATAS E DA NATUREZA
PROGRAMA DE PÓS-GRADUAÇÃO EM FÍSICA

JOÃO LUCAS ROMÃO GOMES DARÉ

Characterization of a Fabry-Perot Cavity Using a Single-Frequency Laser

Recife
2025

JOÃO LUCAS ROMÃO GOMES DARÉ

Characterization of a Fabry-Perot Cavity Using a Single-Frequency Laser

Dissertação apresentada ao Programa de Pós-Graduação em Física da Universidade Federal de Pernambuco, como requisito parcial para obtenção do título de mestre(a) em Física. Área de concentração: Óptica.

Orientador (a): Márcio Heraclyto Gonçalves de Miranda,

Coorientador (a): Daniel Felinto Pires Barbosa.

Recife

2025

CATALOGAÇÃO DE PUBLICAÇÃO NA FONTE. UFPE - BIBLIOTECA CENTRAL

Daré, João Lucas Romão Gomes.

Characterization of a Fabry-Perot Cavity Using a Single-Frequency Laser / João Lucas Romão Gomes Daré. - Recife, 2025.
161f.: il.

Dissertação (mestrado) - Universidade Federal de Pernambuco, Centro de Ciências Exatas e da Natureza, Programa de Pós-Graduação em Física, 2025.
Orientação: Márcio Heraclyto Gonçalves de Miranda.
Coorientação: Daniel Felinto Pires Barbosa.
Inclui referências e apêndices.

1. Fabry-perot; 2. Óptica; 3. Metrologia; 4. Coeficiente de perda; 5. Tempo de vida do fóton; 6. Finesse. I. Miranda, Márcio Heraclyto Gonçalves de. II. Barbosa, Daniel Felinto Pires. III. Título.

UFPE - Biblioteca Central

JOÃO LUCAS ROMÃO GOMES DARÉ

CHARACTERIZATION OF A FABRY-PEROT CAVITY USING A SINGLE-FREQUENCY LASER

Dissertação apresentada ao Programa de Pós-Graduação em Física da Universidade Federal de Pernambuco, como requisito parcial para a obtenção do título de Mestre em Física.

Área de Concentração: Óptica

Data de aprovação: 10/04/2025.

BANCA EXAMINADORA

_____
Prof. Dr. Marcio Heraclyto Gonçalves de Miranda
Orientador
Universidade Federal de Pernambuco

_____
Prof. Dr. João Carlos de Aquino Carvalho
Examinador Interno
Universidade Federal de Pernambuco

_____
Prof. Dr. André de Lima Moura
Examinador Externo
Universidade Federal de Alagoas

DEDICATION

I dedicate this dissertation to my family. To my blood family, composed of my mom, dad and siblings, who, through their teachings of perseverance, gave me the strength to leave my home 8 years ago, pursue my undergraduate studies, and make it possible for me to be here today. And especially to my wife Bárbara Lavínia, who welcomed me, became my friend, and today is my companion for all the days of my life. Without her partnership and understanding, my life would not be the same.

ACKNOWLEGDMENTS

I thank my wife for her love and support throughout this research. Without her, I would not have been able to accomplish anything I have today. I also thank my family, my mother and father, because without their dedication, perseverance and endurance, I would not be the man I am today. To my sisters and brothers, who, in many ways, helped raise me, I will always be grateful. To my in-laws, who welcomed me into their family in a strange city and made my life much easier. To my friends, Ricardo Vasconcelos and Ruan Marinho, who made this path easier and lighter.

To my advisor, Márcio Miranda, who has guided me since the early days of my academic career. This journey made us not only colleagues but also friends. To my lab partners: Leandro de Andrade, Naudson Lopes and Nicolas Pessoa, who helped me at times when I didn't know what I should do. To the staff of the department's machine shop, Valdomiro and João, who assisted me in designing and building my ideas, making them more practical. I especially thank Alexandre Almeida and João Guilherme. They lent me a helping hand more times than I could ask, giving me the Fabry-Perot cavity that made this dissertation possible. I could not have done this without them. To the Fundação de Amparo à Ciência e Tecnologia de Pernambuco (FACEPE), which funded this research.

To God, who helped me along my path since my first breath. His tolerance, patience, generosity, grace, and, especially, love soothed me through good and bad times.

RESUMO

A presente dissertação obteve sucesso na caracterização de uma cavidade Fabry-Perot de baixa finesse. A cavidade foi construída localmente e acoplada a um laser comercial de frequência única da QPhotonics. Para realizar o experimento, desenvolvemos um aparato de estabilização de vibrações mecânicas. Conseguimos medir um valor de finesse de 720 ± 16, o tempo de vida do fóton de (50 ± 0,03) ns, a reflectância dos espelhos de 0.9966 ± 0.0006, um fator de qualidade de $8{,}86 \times 10^{7}$ e uma largura de linha de (4.0 ± 0.7) MHz. Também foi possível estimar um valor para o coeficiente de perdas da cavidade em (0,017 ± 0,003) m^{-1}.

Palavras-chave: metrologia; tempo de vida do fóton; coeficiente de perda da cavidade; fator de qualidade; finesse.

ABSTRACT

The present dissertation successfully characterized a low-finesse Fabry-Perot cavity. The cavity was locally constructed and coupled to a commercial single-frequency laser from QPhotonics. We needed to develop an apparatus to stabilize the mechanical vibrations to realize the experiment. We measured a finesse value of 720 ± 16, a photon lifetime of (50 ± 0.03) ns, a mirror reflectance of 0.9966 ± 0.0006, a quality factor of 8.86×10^7, and a cavity's linewidth of (4.0 ± 0.7) MHz. Estimating a value for the cavity propagation-loss coefficient of (0.017 ± 0.003) m^{-1} was also possible.

Keywords: metrology; photon lifetime; cavity loss coefficient; quality factor; finesse.

LIST OF FIGURES

LIST OF TABLES

LIST OF ABBREVIATIONS AND ACRONYMS

DTH	Diode Thermalization Housing
DFB	Distributed Feedback
EOM	Electro-Optic Modulator
ECDL	External Cavity Diode Laser
FSR	Free Spectral Range
FM	Frequency-Modulation Spectroscopy
FWHM	Full Width at Half Maximum
PZT	Piezoelectric Transducer
PBS	Polarized Beam-Splitter
PDH	Pound-Drever-Hall

CONTENTS

1 INTRODUCTION

The field of Metrology has witnessed significant advancements in the last two decades, especially in optics and laser systems. For example, the physics Nobel prizes from 2022[31] and 2023[32] came from metrological advancement, 2022 for experiments with entangled photons, establishing the violation of Bell inequalities and pioneering quantum information science and 2023 for the development of experimental methods for generating attosecond laser pulses (10^{-18} seconds). These are examples of high-precision experiments where optical metrology is essential. With growing interest in narrower linewidth lasers, methods to achieve it are very important. This dissertation aims to explore a Fabry-Perot cavity to acquire a narrow laser.

A narrow-frequency laser is essential for high-precision spectroscopy, and laser cooling and trapping. For example, for cooling and trapping Strontium atoms can deal with a natural linewidth of 7.6 kHz for the ${}^1S_0 - {}^3P_1$ transition[1]. An ultra-high finesse cavity can offer such narrow linewidth, or even narrower, such as sub-40mHz linewidth[6]. Despite these advantages, the coupling of a laser to an ultra-high finesse cavity is generally difficult and requires some properties from the laser, such as tunability in frequency. A tunable laser can be acquired from commercial means, or it can be homemade.

A tunable laser provides a range of workable wavelengths that make the laser useful in a variety of experiments. Generally, commercial tunable lasers are more stable through a wider range of wavelengths. However, the wider the range, more expensive they are. A stable laser is of great importance in experimental physics because it can hold its frequency for long periods. On the other hand, a stable cavity helps minimize laser frequency fluctuations primarily by serving as a stable reference. To serve as a reference, the cavity must have a low-frequency drift. Optical cavities that are employed for special relativity tests, can achieve low long-term frequency drifts of $40\ \mathrm{mHz \cdot s^{-1}}$ [2].

At first, the primary objectives of this dissertation were to couple a laser into an ultra-stable high-finesse cavity and characterize it, measuring its finesse, photon lifetime, frequency drift, and quality factor. To achieve this, we would employ a Pound-Drever-Hall (PDH) technique, which consists of a phase modulation of the incident

laser by an Electro-Optic Modulator (EOM). However, a succession of problems occurred and changed the main goal of this dissertation.

We discovered that the laser we were using was a single-frequency and was tunable only for a few kiloHertz range. Another difficulty was with the Fabry-Perot cavity, which has a fixed distance between the mirrors. Therefore, the setup was not suited for the experiment. The second step was to find an alternative, which was the construction of an External Cavity Diode Laser (ECDL), which would provide the tunability required. Due to importation bureaucracy and the delivery time of the needed equipment, the experiment was delayed some months, which was partially used to write the theoretical background of this dissertation.

The first attempt to construct the ECDL was to use a Littrow configuration, but it was thermally unstable. The second attempt was a Littman-Metcalf configuration, although it was thermally stable, could not be frequency stabilized and kept in a mono mode regime. Without a tunable laser to continue the experiment, the ultra-stable high-finesse cavity was not used. Instead, the solution was to use a low-finesse homemade cavity.

For the commercial laser, the central wavelength measured was 1063.27 nm with a linewidth limited by the spectrometer resolution of (1.00 $\pm$ 0.03) nm. For the low-finesse cavity, the original single-frequency laser was used, and the modulation was done at the cavity's PZT. For this cavity, we were able to measure a finesse value of (720 $\pm$ 16), a photon lifetime of (50 $\pm$ 0.03) ns, a reflectance of 0.9966, and a quality factor of $8.86 \cdot 10^7$. A greater photon lifetime means that the light lasts longer inside the cavity; consequently, the laser intensity is greater within the cavity, contributing to a greater enhancement factor, which means that the transmitted intensity would also be higher. The frequency drift could not be measured because the cavity was free-running. Using the values for finesse and photon lifetime inside the cavity, a cavity loss coefficient was estimated to be (0.017 $\pm$ 0.003) m^{-1}.

Here is an overview of this dissertation. Chapter 2 explores the theoretical foundations, discussing relevant literature and setting the backgrounds on the functioning of a Fabry-Perot cavity for both cases: with and without the losses of the cavity. Chapter 3 will discuss the method and theory of the construction of an ECDL and the three main approaches to do so: Littrow, Littman-Metcalf, and Double grating

configurations. The results and discussion are presented in Chapter 4, where key findings are interpreted considering the research objectives. Finally, Chapter 5 offers the conclusion.

2 THEORETICAL BACKGROUNDS

2.1 FABRY-PEROT CAVITY

A Fabry-Perot cavity is used for stabilizing the laser frequency. Its operation is straightforward, but it requires precise alignment. In this section, we will explain how a Fabry-Perot Cavity works. Let's start by discussing the structure of the cavity, as shown in Figure 1.

Figure 1: Representation of a Fabry-Perot Cavity. The quantities R, r_1 and r_2 are the curvature of the mirror, and the reflectivity of the mirrors 1 and 2, respectively. The curvature of the mirror 1 is exaggerated in the figure.

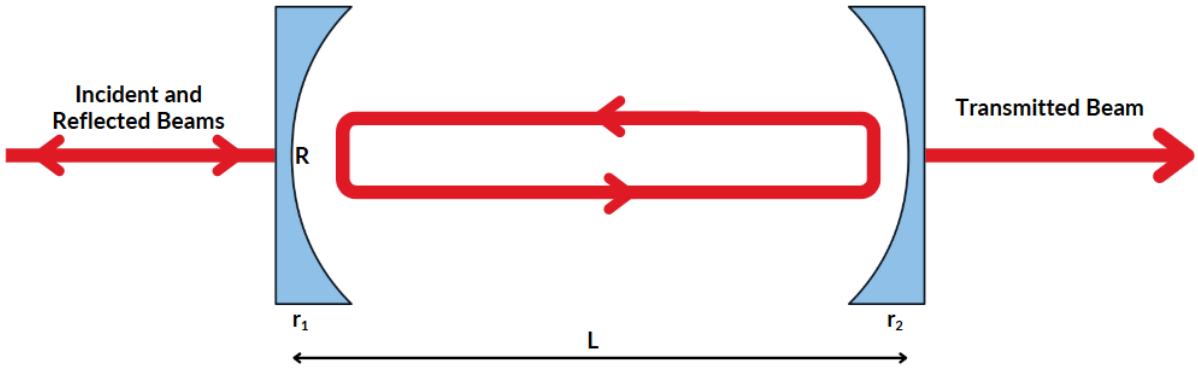

Source: Author, 2024.

Typically, Fabry-Perot mirrors possess high reflectivity, resulting in a transmitted beam with a narrow linewidth. Furthermore, at the cavity's resonance, the transmitted beam has power similar to the incident beam's. This is achievable by forming a standing wave inside the cavity. This standing wave is composed of numerous reflections, which have a slight leakage that can either constructively interfere to produce a transmitted beam in the order of the incident beam's power or destructively interfere in the reflected beam.

Let's investigate how it functions and its practical applications. A Fabry-Perot Cavity offers several remarkable properties, one of which is the ability to filter the laser beam's frequency spectrum. In essence, it can control the laser's linewidth by permitting only a specific frequency band, centered on the cavity's resonance, to pass through. The quality of the cavity directly influences the narrowness of the transmitted beam's linewidth. This is very important in experiments related to atomic physics, where a narrow linewidth is crucial, and in other applications[33],[34],[35]. For a more quantitative understanding, a rigorous approach is essential.

2.1.1 A QUANTITATIVE APPROACH TO THE FABRY-PEROT CAVITY

It's necessary to account for a system that resembles real-world conditions. This includes considering the presence of losses, primarily arising from the dispersion and absorption of light within the cavity. Hence, we will examine two scenarios: (a) a lossless system and (b) a scenario where losses play a significant role.

2.1.1.1 Lossless Fabry-Perot Cavity

The first case is the lossless Cavity. To proceed, we will depict the beam at a slight angle with respect to the normal of the mirrors. This simplification helps us visualize the problem more easily, even though such an angle is not present. This angulation is represented in Fig. 2:

Figure 2: Cavity diagram with exaggerated angulation of the reflected beams inside the cavity for better visualization.

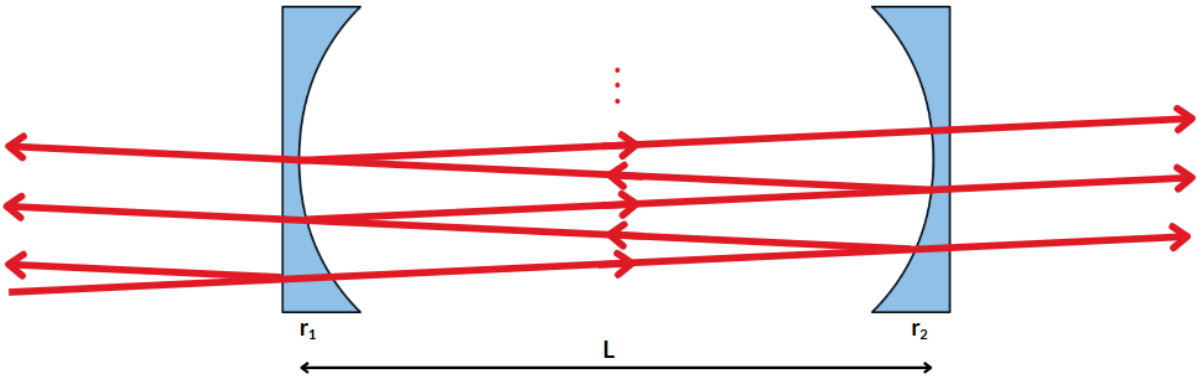

Source: Author, 2024.

Each time the beam hits the mirror surfaces, there will be a transmitted beam traveling in the same direction as the original and a reflected beam traveling backward to it. Considering that the absorption of the laser by the mirrors is negligible, we have:

$$\mathbb{T} + \mathbb{R} = 1,$$

Equation 2.1

where $\mathbb{T}$ is the transmission coefficient and $\mathbb{R}$ is the reflection coefficient. For simplicity, let's consider the incident beam traveling without a phase and in the positive direction of the z axis and that the mirrors have the same reflectivity, then we have:

For the input beam:

$$E_{in} = E_0 e^{i(kz-\omega t)}.$$

Equation 2.2

To find out the output Field, one must follow the path of the input field, as the reflectivity is considered the same for both mirrors. Then, $r_1 = r_2 \equiv r$ and $t_1 = t_2 \equiv t$ (transitivity). The first reflection occurs with the back of the mirror 1, E_{ref}, and there is a transmitted beam with field given by tE_{in}.

Figure 3: First reflection of the beam occurs with the back of the first mirror.

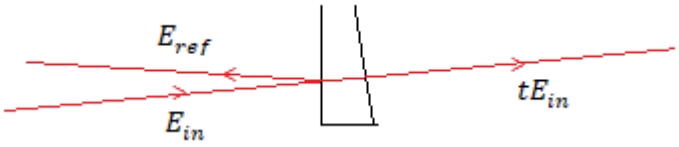

Source: Author, 2024.

The second interaction will be between the transmitted beam and the second mirror, so there will be a transmitted beam through the second mirror given by $t^2e^{ikL}E_{in}$ and a reflected beam given by $rte^{ikL}E_{in}$, where the term e^{ikL} is the phase shift originated by the cavity length.

Figure 4: Second interaction of the light beam with the front of the second mirror.

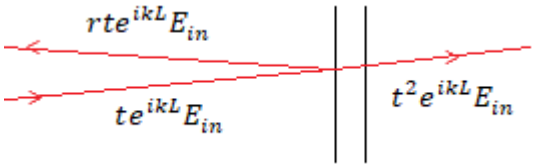

Source: Author, 2024.

Note that the backwards traveling beam gain a phase shift of e^{i2kL} until reach the second mirror one more time. Then, we have for each round trip an additional term of re^{i2kL}. Considering that there are an infinite number of round trips inside the cavity, then the output beam can be represented by:

$$E_{out} = t^2e^{ikL}E_{in} + t^2e^{ikL}E_{in} \cdot r^2e^{2ikL} + t^2e^{ikL}E_{in} \cdot \left(r^2e^{2ikL}\right)^2 + \cdots,$$

$$E_{out} = t^2e^{ikL}E_{in} \cdot \left[1 + \left(r^2e^{2ikL}\right) + \left(r^2e^{2ikL}\right)^2 + \cdots\right],$$

$$E_{out} = t^2e^{ikL}E_{in} \cdot \sum_{n=0}^{\infty}\left(r^2e^{2ikL}\right)^n.$$

Considering that $\mathbb{T} = |t|^2$ and $\mathbb{R} = |r|^2$, then:

$$E_{out} = (1-\mathbb{R})e^{ikL}E_{in} \cdot \sum_{n=0}^{\infty}\left(\mathbb{R}e^{2ikL}\right)^n,$$

identifying the geometric sum, which rises:

$$\sum_{n=0}^{\infty}\left(\mathbb{R}e^{2ikL}\right)^n = \frac{1}{1-\mathbb{R}e^{2ikL}},$$

that is true as long as $\left|\mathbb{R}e^{2ikL}\right| < 1$, which is true here. That brings for the output field:

$$E_{out} = \frac{(1-\mathbb{R})e^{ikL}}{1-\mathbb{R}e^{2ikL}}E_{in}.$$

Equation 2.3

Note that what the photodetector measures the intensity, but not the electric field. Similarly, to the electric field, there will be a reflected intensity and a transmitted intensity, that follows the same law:

$$\mathcal{T} + \mathcal{R} = 1.$$

Equation 2.4

Where $\mathcal{T}$ is the transmitted intensity coefficient (transmittance) and $\mathcal{R}$ is the reflected intensity coefficient (reflectance), they're given by: $\mathcal{T} = \left|\frac{E_{out}}{E_{in}}\right|^2$ and $\mathcal{R} = \left|\frac{E_{ref}}{E_{in}}\right|^2$ and the reflected electric field can be found in a analogous way to the transmitted field. Therefore:

$$\mathcal{T} = \left|\frac{E_{out}}{E_{in}}\right|^2 = \left|\frac{(1-\mathbb{R})e^{ikL}}{1-\mathbb{R}e^{2ikL}}\right|^2.$$

Where:

$$\left|(1-\mathbb{R})e^{ikL}\right|^2 = (1-\mathbb{R})^2.$$

And:

$$\left|1-\mathbb{R}e^{2ikL}\right|^2 = \left(1-\mathbb{R}e^{2ikL}\right)\left(1-\mathbb{R}e^{-2ikL}\right)$$

$$= 1-\mathbb{R}e^{-2ikL}-\mathbb{R}e^{2ikL}+\mathbb{R}^2 = 1+\mathbb{R}^2-2\mathbb{R}\cdot\left(\frac{\mathbb{R}e^{-2ikL}+\mathbb{R}e^{2ikL}}{2}\right)$$

$$= 1+\mathbb{R}^2-2\mathbb{R}\cdot\cos(2kL).$$

Using that $sin^2\,x = \frac{1-\cos(2x)}{2}$, we have:

$$\left|1 - \mathbb{R}e^{2ikL}\right|^2 = 1 + \mathbb{R}^2 - 2\mathbb{R}\cdot(1 - 2\,sin^2(kL)) = 1 + \mathbb{R}^2 - 2\mathbb{R} + 4\mathbb{R}\,sin^2(kL),$$

$$\therefore \left|1 - \mathbb{R}e^{2ikL}\right|^2 = (1-\mathbb{R})^2 + 4\mathbb{R}\,sin^2(kL).$$

Therefore, the transmitted intensity coefficient is:

$$\mathcal{T} = \frac{(1-\mathbb{R})^2}{(1-\mathbb{R})^2 + 4\mathbb{R}\,sin^2(kL)} = \frac{1}{1 + \left[\frac{4\mathbb{R}}{(1-\mathbb{R})^2}\right]\cdot sin^2(kL)}.$$

Equation 2.5

The function reveals an interesting behavior. Plotting it we begin to understand the role of a Fabry-Perot cavity in laser systems Fig. 5:

Figure 5: Graph of the transmittance of a Fabry-Perot Cavity. With the reflectivity of the mirrors being 94.8% (blue) and 77.4% (golden).

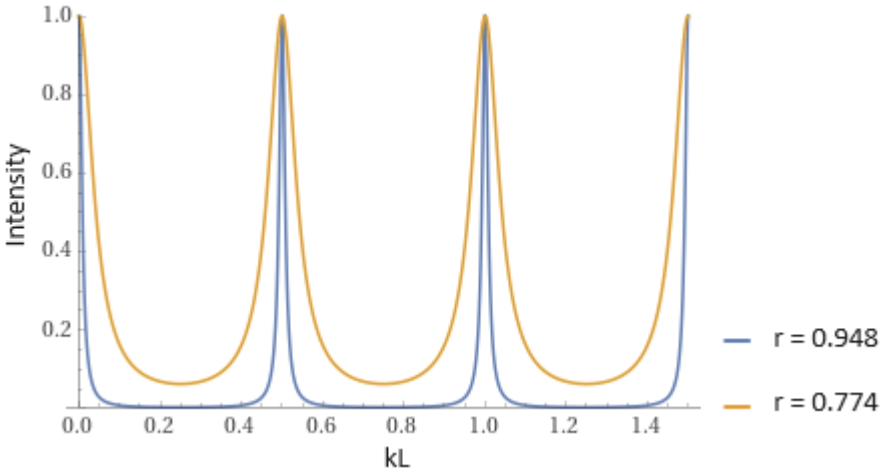

Source: Author, 2024.

It's important to note that increasing the reflectivity of the mirrors results in better frequency filtering. The formation of a standing wave inside the cavity plays a crucial role in ensuring that the transmitted intensity matches the incident intensity. This is achieved through the enhancement of the electric field within the cavity, which can be quantified using the internal resonance enhancement factor. Now, let's examine the field inside the cavity.

Figure 6: Internal electric fields of the Fabry-Perot cavity. The E_{circ} is the electric field that is circulating the cavity, the $E_{launched}$ in the filed that was launched into the cavity by the first mirror, the E_{RT} is the field after n round trips, the E_{trans} is the transmitted electric field and $E_{b-trans}$ is the filed transmitted back by the cavity.

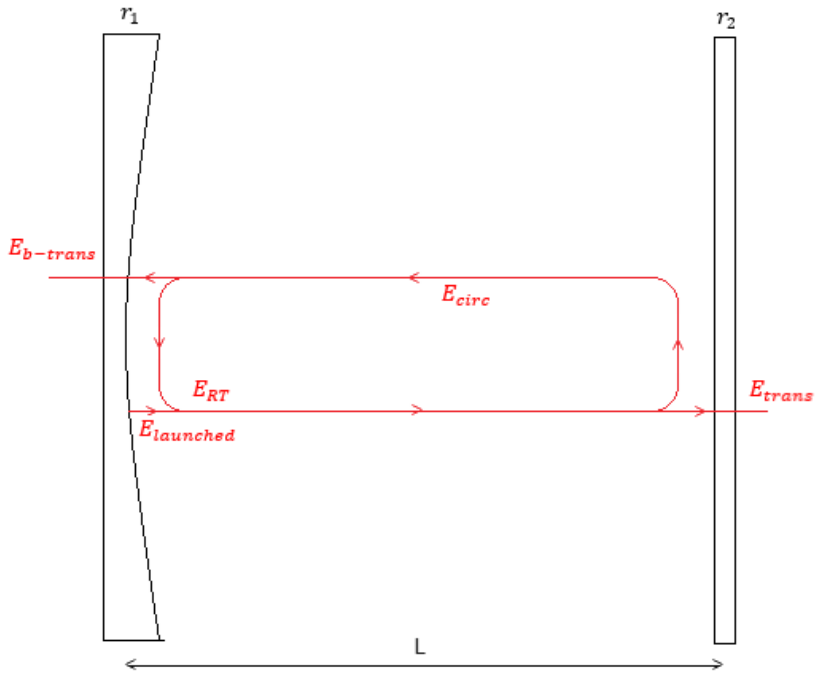

Source: Author, 2024.

In the context of the enhancement factor, our focus is on the electric field circulating within the cavity. This electric field is the cumulative result of the fields that are initially introduced into the cavity and the multiple round trips they make. Therefore:

$$E_{circ} = E_{launched} + E_{RT},$$

as E_{RT} is the result field after n round trips, then:

$$E_{circ} = E_{launched} + r^2 e^{2ikL} E_{launched} + \left(r^2 e^{2ikL}\right)^2 E_{launched} + \left(r^2 e^{2ikL}\right)^3 E_{launched} + \cdots,$$

$$E_{circ} = E_{launched} \cdot \sum_{n=0}^{\infty} \left(r^2 e^{2ikL}\right)^n = \frac{E_{launched}}{1 - r^2 e^{2ikL}}.$$

The intensities that are circulating within the cavity and launched into it are:

$$\mathrm{I}_{circ} = |E_{circ}|^2.$$

and

$$\mathrm{I}_{launched} = |E_{launched}|^2,$$

the internal resonance enhancement factor is defined as:

$$\mho_{int} \equiv \frac{|E_{circ}|^2}{|E_{launched}|^2}.$$

Then:

$$\mho_{int} = \frac{\left|\frac{E_{launched}}{1 - r^2 e^{2ikL}}\right|^2}{|E_{launched}|^2} = \left|\frac{E_{launched}}{1 - r^2 e^{2ikL}}\right|^2 \frac{1}{|E_{launched}|^2} = \frac{1}{|1 - r^2 e^{2ikL}|^2},$$

similarly to what was done for *Equation 2.5*:

$$\mho_{int} = \frac{1}{(1 - \mathbb{R})^2 + 4\mathbb{R}\, sin^2(kL)}.$$

Equation 2.6

Where $\mathbb{R}$ is the electric field reflection coefficient, $\mathbb{R} = r^2$. The internal resonance enhancement factor has its maximum value when $\sin(kL)$ is equal zero. This happens when the laser frequency is in resonance with the cavity. Therefore, $\mho_{int}$ is spectrally dependent. As k is the wave number, we can associate it to the frequency of the emitted light:

$$kL = \frac{2\pi}{\lambda} L = \frac{2\pi}{c/\nu} L = \frac{2\pi\nu}{c} L.$$

Where c if the light velocity in the vacuum and ν is the frequency of the emitted light. Then in terms of the frequency of the emitted light:

$$\mho_{int}(\nu) = \frac{1}{(1 - \mathbb{R})^2 + 4\mathbb{R}\, sin^2\left(\frac{2\pi\nu}{c} L\right)},$$

at the resonance:

$$\mho_{int}(\nu_{RES}) = \frac{1}{(1 - \mathbb{R})^2}.$$

For different values of reflectivity, we get the following graph:

Figure 7: spectrally dependent internal resonance enhancement factor which the resonator provides to light that is launched into it. The curves plotted are for $r = 0.4$ (blue), $r = 0.6$ (orange), $r = 0.75$ (red) and for $r = 0.9$ (green, $\mho_{int}(\nu) = 25$), outside the scale of the ordinate. The dashed red line marks the enhancement factor equal to one, that occurs when there is no reflectivity, that is $\mathbb{R} = 0$.

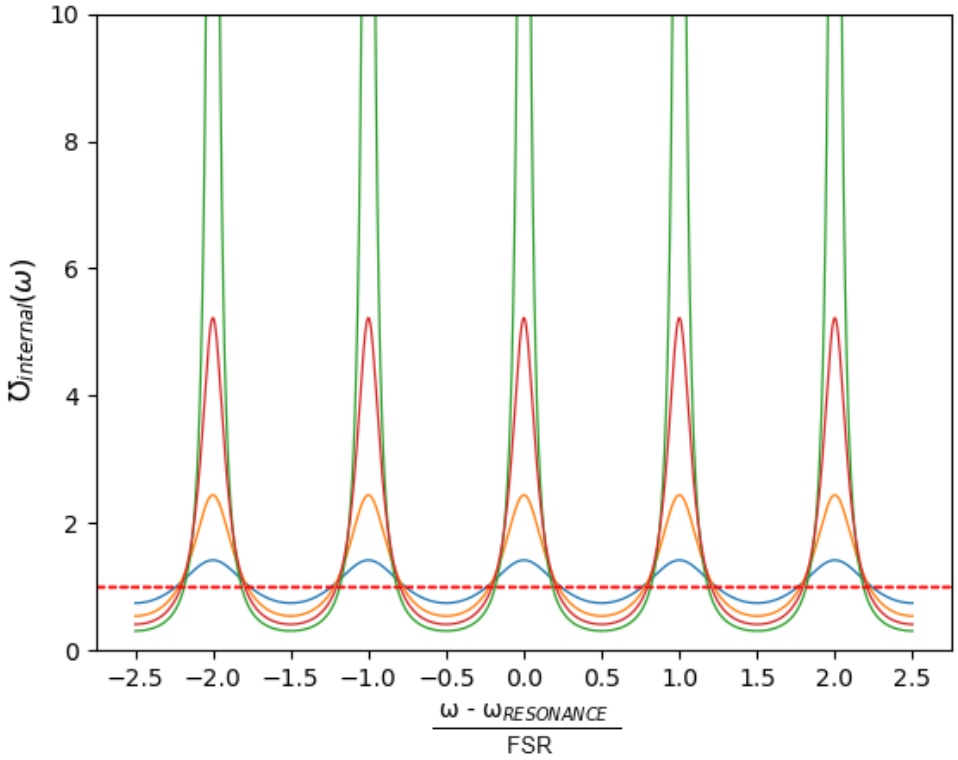

Source: Author, 2024.

The enhancement factor provides us with insight into the degree by which the electric field's intensity is amplified within the cavity. For instance, in a cavity with both mirrors having a reflectivity of 0.75, the electric field intensity within the cavity is approximately five times greater than the initial intensity launched into it, for mirrors with 0.95 the intensity is 100 times greater. This enhancement factor increases significantly with higher mirror reflectivities, playing a crucial role in high finesse cavities.

To have the enhancement factor linked to the incident intensity, we note that the incident intensity and the launched intensity are related by:

$$\mathrm{I}_{launched} = (1 - \mathbb{R})\mathrm{I}_{incident},$$

$$\mho'_{int}(\nu) = \frac{\mathrm{I}_{circ}}{\mathrm{I}_{incident}} = \frac{\mathrm{I}_{circ}}{\mathrm{I}_{launched}/(1-\mathbb{R})} = (1 - \mathbb{R})\frac{\mathrm{I}_{circ}}{\mathrm{I}_{launched}} = (1 - \mathbb{R})\mho_{int}(\nu).$$

Equation 2.7

Where the prime corresponds to the incident intensity. $\mho'_{int}(\nu)$ is the external intensity enhancement factor. This new factor is smaller than the enhancement of the intensity launched into the resonator (internal), as expected. Additionally, we can prove that in certain conditions the transmitted intensity matches the incident. Let us consider Fig. 6 again, the transmitted intensity in terms of the circulating intensity is given by:

$$\mathrm{I}_{trans} = (1 - \mathbb{R}_2)\mathrm{I}_{circ}.$$

From the definition of the enhancement factor:

$$\mathrm{I}_{trans} = (1 - \mathbb{R}_2)\mho_{int}(\nu)\mathrm{I}_{launched},$$

as seen in *Equation 2.7*:

$$\mathrm{I}_{trans} = (1 - \mathbb{R}_2)\mho_{int}(\nu)(1 - \mathbb{R}_1)\mathrm{I}_{incident},$$

then, for a cavity with mirrors with the same reflectivity:

$$\mathrm{I}_{trans} = \frac{(1 - \mathbb{R}_2)^2\mathrm{I}_{incident}}{(1 - \mathbb{R})^2 + 4\mathbb{R}\,sin^2\left(\frac{2\pi\nu}{c}L\right)}.$$

At resonance the sine term vanishes, so:

$$\therefore \mathrm{I}_{trans} = \mathrm{I}_{incident}.$$

If the laser frequency matches the resonance frequency of the cavity, the only condition for the output and input intensities be equal is mirrors with the same reflectivity. To continue obtaining information about the Fabry-Perot resonator, let's get back to the transmittance. Rewriting Equation 2.5 so $\mathcal{T}$ is explicitly dependent on the laser frequency:

$$\mathcal{T}(\nu) = \frac{1}{1 + \left[\frac{4\mathbb{R}}{(1 - \mathbb{R})^2}\right] \cdot sin^2\left(\frac{2\pi\nu}{c}L\right)}.$$

Equation 2.8

In this manner, there are periodically spaced frequencies that match the required configuration, which is the resonance frequency of the cavity. It can be found noticing that the peaks occur whenever the sine term is zero, then:

$$\sin^2\left(\frac{2\pi\nu}{c}L\right) = 0 \rightarrow sin\left(\frac{2\pi\nu}{c}L\right) = 0,$$

$$\frac{2\pi\nu}{c}L = m\pi \rightarrow \nu_m = m\frac{c}{2L},$$

Equation 2.9

where ν_m is the resonance frequency of the cavity. From this relation is possible to retrieve a relation between the wavelength and the length of the cavity:

$$\nu_m = \frac{c}{\lambda} = m\frac{c}{2L} \rightarrow m\lambda = 2L.$$

Equation 2.10

From that, we can inquire that the wavelength from the input beam must be an integer multiple of twice the cavity length. The spacing between peaks is known as the Free Spectral Range (FSR), which depends exclusively on the geometry of the cavity. It can be determined by examining the distance between two consecutive peaks in the transmitted intensity:

$$\nu_{m+1} - \nu_m = (m+1)\frac{c}{2L} - m\frac{c}{2L} = \frac{c}{2L},$$

$$\therefore FSR = \frac{c}{2L}.$$

Equation 2.11

The FSR is a fascinating quantity, as it is inversely proportional to the length of the cavity. When the mirrors are positioned closer to each other, the spacing between the resonances becomes larger. Another important characteristic of the transmitted intensity is the linewidth of the peaks. While maintaining a fixed distance between the mirrors, the linewidth changes through alterations in the reflectivity of the mirrors. This behavior is demonstrated by analyzing $\mathcal{T}$ near the peaks. To do this, we will use the approximation that sin(x) ~ x for x << 1. This approximation holds true near the peaks. Therefore, we have:

$$\mathcal{T} = \frac{1}{1 + \left[\frac{4\mathbb{R}}{(1-\mathbb{R})^2}\right] \cdot sin^2\left(\frac{2\pi\nu}{c}L\right)} = \frac{1}{1 + \left[\frac{4\mathbb{R}}{(1-\mathbb{R})^2}\right] \cdot \left(\frac{2\pi\nu}{c}L\right)^2}.$$

Note that this function follows the law of $(1 + ax^2)^{-1}$, a Lorentzian curve. Then, looking more carefully to the varying term we have:

$$\left[\frac{4\mathbb{R}}{(1-\mathbb{R})^2}\right]\cdot\left(\frac{2\pi\nu}{c}L\right)^2=\left[\frac{2\sqrt{\mathbb{R}}}{1-\mathbb{R}}\right]^2\cdot\left(\frac{2\pi\nu}{c}L\right)^2=\left[2\frac{\pi\sqrt{\mathbb{R}}}{1-\mathbb{R}}\cdot\frac{2L}{c}\nu\right]^2,$$

we can identify some terms and label another:

$$\left[\frac{4\mathbb{R}}{(1-\mathbb{R})^2}\right]\cdot\left(\frac{2\pi\nu}{c}L\right)^2=4\left(\frac{\mathcal{F}}{FSR}\right)^2\cdot\nu^2,$$

where:

$$\mathcal{F}\equiv\frac{\pi\sqrt{\mathbb{R}}}{1-\mathbb{R}},$$

Equation 2.12

$\mathcal{F}$ is the finesse of the cavity. Then near the peaks we have:

$$\mathcal{T}=\frac{1}{1+4\left(\frac{\mathcal{F}}{FSR}\right)^2\cdot\nu^2}.$$

From that, it is possible to find the Full Width at Half Maximum (FWHM) of the transmitted intensity by finding it for a Lorentzian curve and comparing the functions:

$$\frac{1}{2}=\frac{1}{1+ax^2}\rightarrow 2=1+ax^2\rightarrow 1=ax^2,$$

$$x^2=\frac{1}{a}\rightarrow x=\frac{1}{\sqrt{a}},$$

then the width is twice as much:

$$\Delta x=\frac{2}{\sqrt{a}},$$

as a is given by $a=4\left(\frac{\mathcal{F}}{FSR}\right)^2$, then:

$$\Delta\nu_{FWHM}=\frac{2}{\sqrt{4\left(\frac{\mathcal{F}}{FSR}\right)^2}}=\frac{2}{2\frac{\mathcal{F}}{FSR}}\therefore\Delta\nu_{FWHM}=\frac{FSR}{\mathcal{F}},$$

Equation 2.13

where $\Delta\nu_{FWHM}$ is the Full Width at Half Maximum of the beam's transmitted intensity. Note that this approximation works only near the resonances, therefore this result is good if the linewidth is narrow. In terms of the reflectivity of the cavity:

$$\Delta\nu_{FWHM} = \frac{FSR}{\frac{\pi\sqrt{\mathbb{R}}}{1-\mathbb{R}}} = \frac{(1-\mathbb{R})FSR}{\pi\sqrt{\mathbb{R}}}.$$

Equation 2.14

Figure 8: Dependence of the Linewidth of the peaks with the reflectivity coefficient of the cavity.

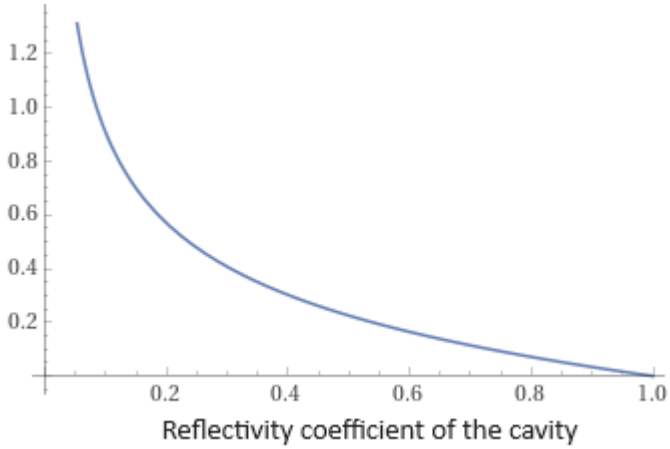

Source: Author, 2024.

As the reflectivity of the mirrors increases, the peaks become narrower. From *Equation 2.13*, it is possible to derive the meaning of finesse. Finesse is a measurement of how narrow the resonances are in relation to their frequency distance, with high finesse indicating sharp resonances. This quality is important for various applications, such as the excitation of ultracold rubidium gas[3] and Rydberg atom experiments[4],[5]. The ability to resolve peaks is essential in spectroscopy[6] and atomic physics.

Another important characteristic of a Fabry-Perot cavity is the Quality Factor, often referred to as the $\mathcal{Q}$ factor. As light becomes trapped within the Fabry-Perot cavity, it stores energy. While a significant amount of optical energy is stored at resonant wavelengths as the light bounces back and forth between the mirrors, some light still leaks out. In a steady state, the power being coupled into the cavity must be equal to the sum of the power leaving the cavity, quantifying how effectively the cavity stores energy is of interest. A high $\mathcal{Q}$ cavity is exceptionally efficient at storing energy, which experiences minimal loss. Following this, we can define the $\mathcal{Q}$ factor as:

$$\mathcal{Q} = 2\pi\frac{\mathcal{W}_{stored}}{\mathcal{W}_{lost}}.$$

Equation 2.15

Where $\mathcal{W}_{stored}$ is the energy stored in the resonator at resonance frequency and $\mathcal{W}_{lost}$ is the energy lost per oscillation cycle. Our attention, now, turns to the mentioned energies. As we're looking the case for lossless resonator, the energy loss in the cycles is due to the decay of the photons from the beam inside the cavity. The relationship between the energy inside of the cavity and the photon-decay is given by the following equation[16]:

$$\frac{d\mathcal{W}}{dt} = -\frac{\mathcal{W}}{\tau_c},$$

Equation 2.16

where τ_c is the photon-decay time of the resonator. Therefore, trying a solution of the form $\mathcal{W}(t) = \mathcal{W}_0 e^{at}$:

$$\frac{d\mathcal{W}_0 e^{at}}{dt} = -\frac{\mathcal{W}_0 e^{at}}{\tau_c},$$

$$a\mathcal{W}_0 e^{at} = -\frac{\mathcal{W}_0 e^{at}}{\tau_c} \rightarrow a = -\frac{1}{\tau_c},$$

where $\mathcal{W}_0$ is the energy of the electric field that was launched into the cavity. Then, we will work with energy given by $\mathcal{W}(t) = \mathcal{W}_{launched} e^{-t/\tau_c}$. For the energy loss, we can relate it to the power dissipated by the cavity as[15][16]:

$$\mathcal{W}_{lost} = \frac{1}{\nu_{RES}} P_{lost},$$

here ν_{RES} is the center frequency of the resonance peak. Also, by the definition of dissipated power:

$$P_{lost} = -\frac{d\mathcal{W}(t)}{dt},$$

then, we can rewrite the quality factor as:

$$\mathcal{Q} = 2\pi \frac{\mathcal{W}_{stored}}{-\frac{1}{\nu_{RES}} \frac{d\mathcal{W}(t)}{dt}} = -2\pi\nu_{RES} \frac{\mathcal{W}(t)}{\frac{d\mathcal{W}(t)}{dt}},$$

$$\mathcal{Q} = -2\pi\nu_{RES} \frac{\mathcal{W}_{launched} e^{-t/\tau_c}}{\left(-\frac{\mathcal{W}_{launched} e^{-t/\tau_c}}{\tau_c}\right)},$$

$$\therefore Q = 2\pi\nu_{RES}\tau_c.$$

Equation 2.17

In the lossless case, the photon-decay time is related only to the outcoupling of the mirrors[15]. The Quality factor can be related to the full width at half maximum by[15]:

$$Q = \frac{\nu_{RES}}{\Delta\nu_{FWHM}}.$$

Equation 2.18

The Q factor is a commonly used parameter to assess the overall performance of Fabry-Perot cavities. It provides valuable information about both the selectivity of resonant frequencies and the efficiency in energy storage within the cavity. A high Q value suggests that the cavity is exceptionally selective when it comes to resonant frequencies, meaning it allows only very specific and narrow frequencies to pass through. Additionally, it denotes that the cavity can store a significant amount of the energy. As the Q factor presents a higher value, the Fabry-Perot cavity exhibits better overall quality, regarding selectivity, narrower resonance frequency, in energy storage and overall performance. These attributes are very important for applications in high-resolution spectroscopy and high-precision lasers.

2.1.1.2 Fabry-Perot Cavity with Losses

Typically, a resonator experiences various optical losses along the path of light propagation. These losses can be categorized as discrete or continuous and often exhibit variation with frequency ν. Discrete outcoupling losses stem from the imperfect reflectivity of the resonator mirrors, which is often the case[15].

$$|r_i|^2 = \mathbb{R}_i = 1 - \left|t_{out,i}\right|^2 = 1 - \mathbb{T}_{out,i} = e^{-t_{RT}/\tau_{out,i}}.$$

Where r_i and $\mathbb{R}_i$ are the electric field and intensity reflection coefficients of the mirror i, respectively[14][15]. Analogously, $t_{out,i}$ and $\mathbb{T}_{out,i}$ are the electric field and intensity transmission coefficients of the mirror i, respectively. The index “out” in $t_{out,i}$ refers to outcoupling. Furthermore, t_{RT} is the time for a round trip and $\tau_{out,i}$ is the exponential decay-time resulting from the outcoupling loss at the mirror i. From the equation above:

$$\mathbb{R}_i = e^{-t_{RT}/\tau_{out,i}} \rightarrow -\frac{t_{RT}}{\tau_{out,i}} = ln(\mathbb{R}_i) \rightarrow \frac{1}{\tau_{out,i}} = \frac{-ln(\mathbb{R}_i)}{t_{RT}} = \frac{-ln(1-\mathbb{T}_{out,i})}{t_{RT}},$$

defining the mirror coupling coefficient as:

$$\delta_{out,i} = -\ln(\mathbb{R}_i) = \frac{t_{RT}}{\tau_{out,i}}.$$

Equation 2.19

Considering the entire cavity, with two mirrors characterized by their respective reflectivities $\mathbb{R}_1$ and $\mathbb{R}_2$, the overall outcoupling losses arise from the transmission of light through these mirrors.

$$\mathbb{R}_1\mathbb{R}_2 = e^{-t_{RT}/\tau_{out}} \rightarrow \ln(\mathbb{R}_1\mathbb{R}_2) = \frac{-t_{RT}}{\tau_{out}} \rightarrow \frac{1}{\tau_{out}} = -\frac{\ln(\mathbb{R}_1) + \ln(\mathbb{R}_2)}{t_{RT}} = \frac{1}{\tau_{out,1}} + \frac{1}{\tau_{out,2}}.$$

Rewriting in terms of the mirror coupling coefficients:

$$\delta_{out} = -\ln(\mathbb{R}_1\mathbb{R}_2) = \delta_{out,1} + \delta_{out,2}.$$

There are additional losses from two other natures that can be considered in the general case. First, are the individual discrete losses that can occur due to various factors, such as: (a) absorption and scattering losses in the mirror coatings or (b) diffraction losses at the mirrors with finite lateral dimensions. Although exists losses related to the presence of an active medium inside the cavity, this is not the scenario in this dissertation and will be completely discarded.

On the other hand, we have continuous losses that can be characterized by the intensity propagation-loss coefficient per unit length, denoted as α_{prop}. These losses can be caused by various factors within the cavity, such as: (a) Scattering losses resulting from material imperfections, (b) waveguide propagation losses due to interface roughness[1] at the mirrors[26], or (c) losses in the propagation within the cavity due to non-perfect vacuum.

These losses, whether from discrete or continuous nature, represent intrinsic resonator losses and are often quantified using the intrinsic round-trip loss coefficient,

[1] the surface roughness is regarded as the quality of a surface of not being smooth, presence of imperfections.

denoted as $\mathbb{L}_{RT}$. This coefficient incorporates any possible losses during the round-trip regardless its nature. In one round-trip:

$$1 - \mathbb{L}_{RT} \equiv e^{-\alpha_{prop}(2L)} = e^{-t_{RT}/\tau_{loss}},$$

Equation 2.20

from *Equation 2.20*:

$$-\ln(1 - \mathbb{L}_{RT}) = \frac{t_{RT}}{\tau_{loss}} = \alpha_{prop}(2L),$$

$$\frac{1}{\tau_{loss}} = \frac{-\ln(1 - \mathbb{L}_{RT})}{t_{RT}} = \frac{2L}{t_{RT}}\alpha_{prop} = c\alpha_{prop},$$

Where c is the velocity of the light within the cavity. As we did to the mirror coupling coefficient, we can define an intrinsic loss coefficient:

$$\delta_{loss} \equiv -\ln(1 - \mathbb{L}_{RT}) = \frac{t_{RT}}{\tau_{loss}}.$$

Equation 2.21

The overall decay-rate constant, which encompasses both the outcoupling losses and the intrinsic losses, can be expressed as the sum of the decay rates we've identified above:

$$\frac{1}{\tau_c} = \frac{1}{\tau_{out}} + \frac{1}{\tau_{loss}} = -\frac{\ln(\mathbb{R}_1\mathbb{R}_2)}{t_{RT}} + c\alpha_{prop},$$

Equation 2.22

where τ_c is the photon-decay time of the resonator. We can express it in terms of the coupling and intrinsic loss coefficients as:

$$\delta_c = \delta_{out} + \delta_{loss} = \frac{t_{RT}}{\tau_c}.$$

Now, let's turn our attention to the internal resonance enhancement factor and consider the implications of the losses by outcoupling and intrinsic nature. Similar to the lossless scenario, the enhancement factor represents the ratio between the field circulating within the cavity and the field initially launched into the cavity. The circulating field is the outcome of its interference with the fields from multiple round trips. Therefore:

$$E_{circ} = E_{launched} + r_1 r_2 e^{-\alpha_{prop}(2L)} e^{i2kL} E_{launched} + \left(r_1 r_2 e^{-\alpha_{prop}(2L)} e^{i2kL}\right)^2 E_{launched} + \left(r_1 r_2 e^{-\alpha_{prop}(2L)} e^{i2kL}\right)^3 E_{launched} + \cdots,$$

$$E_{circ} = E_{launched} \sum_{n=0}^{\infty} \left(r_1 r_2 e^{-\alpha_{prop}(2L)} e^{i2kL}\right)^n,$$

$$E_{circ} = \frac{1}{1 - r_1 r_2 e^{-\alpha_{prop}(2L)} e^{i2kL}} E_{launched},$$

Equation 2.23

then:

$$\mho_{int}^{loss} \equiv \frac{\mathrm{I}_{circ}}{\mathrm{I}_{launched}} = \frac{\left|\frac{E_{launched}}{1 - r_1 r_2 e^{-\alpha_{prop}(2L)} e^{i2kL}}\right|^2}{|E_{launched}|^2} = \frac{1}{\left|1 - r_1 r_2 e^{-\alpha_{prop}(2L)} e^{i2kL}\right|^2},$$

from the denominator:

$$\left|1 - r_1 r_2 e^{-\alpha_{prop}(2L)} e^{i2kL}\right|^2 = \left(1 - r_1 r_2 e^{-\alpha_{prop}(2L)} e^{i2kL}\right)\left(1 - r_1 r_2 e^{-\alpha_{prop}(2L)} e^{-i2kL}\right)$$

$$= 1 - r_1 r_2 e^{-\alpha_{prop}(2L)} e^{-i2kL} - r_1 r_2 e^{-\alpha_{prop}(2L)} e^{i2kL} + (r_1 r_2)^2 e^{-2\alpha_{prop}(2L)}$$

$$= 1 + (r_1 r_2)^2 e^{-4\alpha_{prop}L} - 2 r_1 r_2 e^{-2\alpha_{prop}L} cos(2kL)$$

$$= 1 + (r_1 r_2)^2 e^{-4\alpha_{prop}L} - 2 r_1 r_2 e^{-2\alpha_{prop}L} [1 - 2sin^2(kL)]$$

$$= 1 + (r_1 r_2)^2 e^{-4\alpha_{prop}L} - 2 r_1 r_2 e^{-2\alpha_{prop}L} + 4 r_1 r_2 e^{-2\alpha_{prop}L} sin^2(kL)$$

$$= (1 - r_1 r_2 e^{-2\alpha_{prop}L})^2 + 4 r_1 r_2 e^{-2\alpha_{prop}L} sin^2(kL),$$

finally:

$$\mho_{int}^{loss} = \frac{1}{(1 - r_1 r_2 e^{-2\alpha_{prop}L})^2 + 4 r_1 r_2 e^{-2\alpha_{prop}L} sin^2(kL)}.$$

In terms of the laser frequency:

$$\mho_{int}^{loss}(\nu) = \frac{1}{\left(1 - r_1 r_2 e^{-\frac{c\alpha_{prop}}{FSR}}\right)^2 + 4 r_1 r_2 e^{-\frac{c\alpha_{prop}}{FSR}} sin^2\left(\frac{\pi\nu}{FSR}\right)}.$$

For the case of a cavity with both mirror with equal reflectivity:

$$\mathfrak{V}_{int}^{loss}(\nu) = \frac{1}{\left(1 - r^2 e^{-\frac{c\alpha_{prop}}{FSR}}\right)^2 + 4r^2 e^{-\frac{c\alpha_{prop}}{FSR}} sin^2\left(\frac{\pi\nu}{FSR}\right)}.$$

Plotting the curve for $\mathfrak{V}_{int}^{loss}(\omega)$:

Figure 9: spectrally dependent internal resonance enhancement factor when there are propagation losses which the resonator provides to light that is launched into it. The curves plotted are for $r = 0.4$ (blue), $r = 0.6$ (orange), $r = 0.75$ (red) and for $r = 0.9$ (green) that isn't outside the scale anymore. Here the α_{prop} is assumed to be 0.01m^{-1} and the cavity length to be 0.1m. The dashed line represents the value one, that would mean no enhancement.

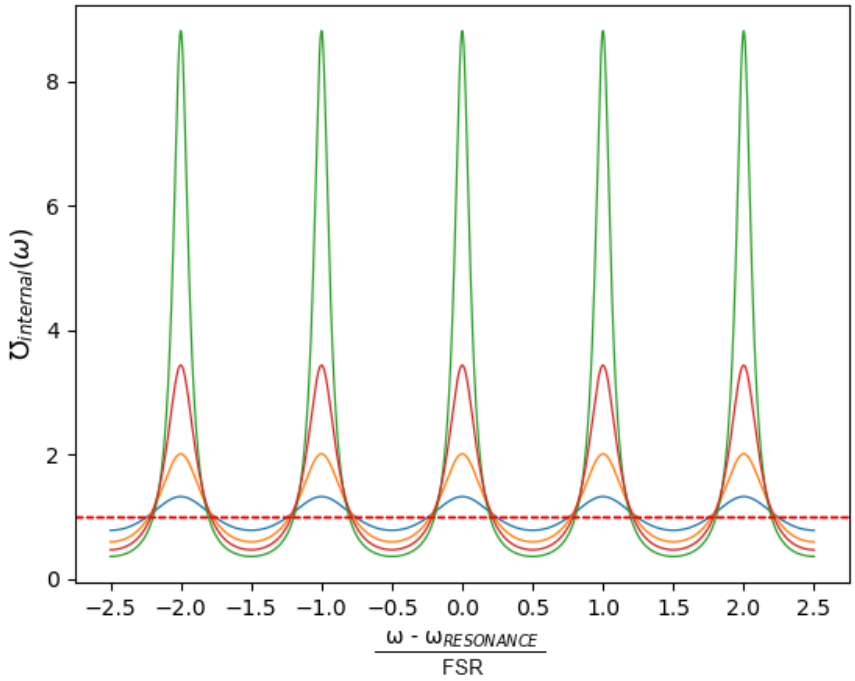

Source: Author, 2024.

In the presence of losses, the enhancement of the electric field experiences a significant reduction, depending on the propagation-loss coefficient. In the lossless scenario, a reflectivity of 0.9 yielded an enhancement of approximately 25 times the launched intensity. However, with propagation losses considered, this enhancement drops to around 9 times for the same reflectivity for $\alpha_{prop} = 0.01\text{m}^{-1}$.

Similarly, we can determine the transmittance in the presence of losses using a method analogous to the one described above for the circulating and launched intensity. For the transmittance, we will use the transmitted intensity and the circulating intensity.

$$\mathcal{T} = \frac{\text{I}_{trans}}{\text{I}_{inc}},$$

note that:

$$\mathrm{I}_{trans} = (1 - \mathbb{R}_2)e^{-\alpha_{prop}(2L)}\mathrm{I}_{circ},$$

$$\mathrm{I}_{launched} = (1 - \mathbb{R}_1)\mathrm{I}_{inc},$$

then:

$$\mathcal{T}(\nu) = \frac{\mathrm{I}_{trans}}{\mathrm{I}_{inc}} = \frac{(1 - \mathbb{R}_2)e^{-\alpha_{prop}(2L)}\mathrm{I}_{circ}}{\mathrm{I}_{launched}/(1 - \mathbb{R}_1)} = (1 - \mathbb{R}_2)(1 - \mathbb{R}_1)e^{-\alpha_{prop}(2L)}\mho_{int}^{loss}(\nu),$$

finally, for mirrors with same reflectivities:

$$\mathcal{T}(\nu) = \frac{(1 - r^2)^2 e^{-\frac{c\alpha_{prop}}{FSR}}}{\left(1 - r^2 e^{-\frac{c\alpha_{prop}}{FSR}}\right)^2 + 4r^2 e^{-\frac{c\alpha_{prop}}{FSR}} sin^2\left(\frac{\pi\nu}{FSR}\right)}.$$

Equation 2.24

So, plotting it gives us:

Figure 10: Graph of the transmittance of a Fabry-Perot Cavity with propagation losses given by $\alpha_{prop} = 0.001\mathrm{m}^{-1}$. With the reflectivity of the mirrors being 0.9 (blue) and 0.75 (orange).

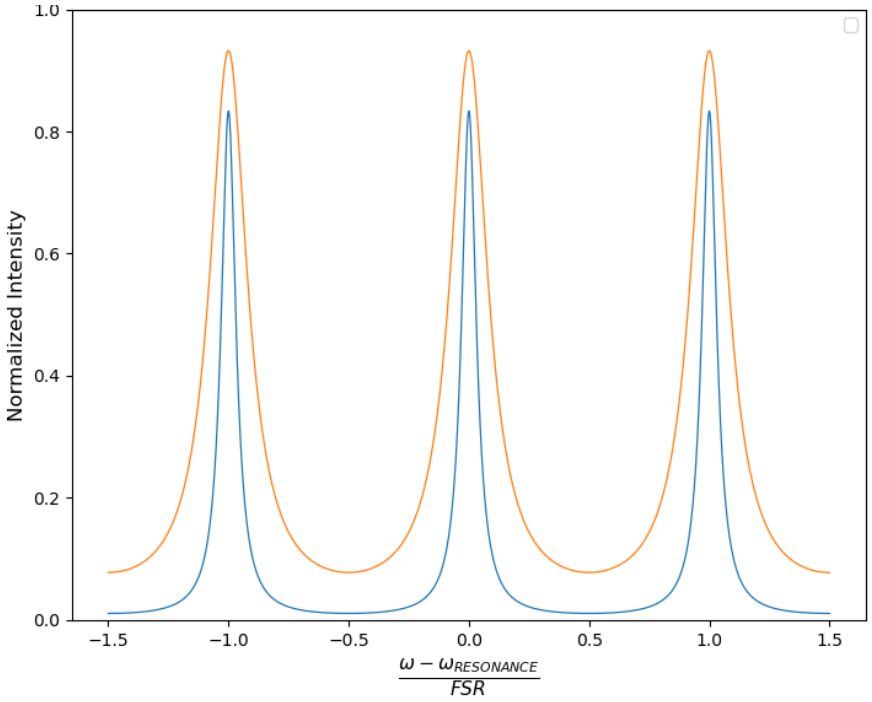

Source: Author, 2024.

As depicted in Figure 10, it's evident that the transmittance doesn't approach unity in the presence of propagation losses, meaning that the transmitted intensity is

not equal to the input beam intensity, even at resonance. Additionally, for mirrors with lower reflectivity, there is greater transmittance, mainly due to the light that can pass through them. In the limit where α_{prop} approaches zero, the transmittance approaches unity at resonance.

In the absence of propagation losses, and when only outcoupling losses are considered, the sum of transmitted and reflected intensities equals unity, as we previously examined in the lossless scenario. However, when propagation losses are introduced, this relationship adjusts to accommodate an intrinsic propagation-loss. This adjustment is due to the consideration of propagation losses, and it can be expressed as:

$$\mathcal{R} + \mathcal{T} + \mathfrak{L} = 1.$$

Equation 2.25

To find the intrinsic propagation-loss intensity we must first find the reflectance. For this, we're going to look to the first reflected, reflected by the back of the first mirror, and back-transmitted fields, that is, the field that is transmitted by the first mirror:

$$E_{reflec} = E_{reflec,1} + E_{b-trans}.$$

The first reflected electric field is easy to obtain, it is just the reflected incident field:

$$E_{reflec,1} = r_1 E_{inc} e^{i\pi}.$$

Here $e^{i\pi}$ is introduced to account for the opposite directions of the reflected and incident fields. The back-transmitted field:

$$\begin{aligned} E_{b-trans} = {} & t_1 r_2 e^{-\alpha_{prop}(2L)} e^{i2kL} E_{launched} + t_1 r_2 e^{-\alpha_{prop}(2L)} e^{i2kL} E_{launched} \\ & \cdot \left(r_1 r_2 e^{-\alpha_{prop}(2L)} e^{i2kL}\right) + t_1 r_2 e^{-\alpha_{prop}(2L)} e^{i2kL} E_{launched} \\ & \cdot \left(r_1 r_2 e^{-\alpha_{prop}(2L)} e^{i2kL}\right)^2 + \cdots, \end{aligned}$$

here we have a minus signal to represent that the back-transmitted field is propagating in the opposite direction of the launched field. Considering that $E_{launched} = t_1 E_{inc}$, then:

$$E_{b-trans} = t_1 r_2 e^{-\alpha_{prop}(2L)} e^{i2kL} E_{launched} \sum_{n=0}^{\infty} \left(r_1 r_2 e^{-\alpha_{prop}(2L)} e^{i2kL}\right)^n$$

$$= \frac{t_1 r_2 e^{-\alpha_{prop}(2L)} e^{i2kL} E_{launched}}{1 - r_1 r_2 e^{-\alpha_{prop}(2L)} e^{i2kL}} = \frac{t_1^2 r_2 e^{-2\alpha_{prop}L} e^{i2kL} E_{inc}}{1 - r_1 r_2 e^{-2\alpha_{prop}L} e^{i2kL}},$$

then the total reflected field is:

$$E_{reflec} = -r_1 E_{inc} + \frac{t_1^2 r_2 e^{-2\alpha_{prop}L} e^{i2kL} E_{inc}}{1 - r_1 r_2 e^{-2\alpha_{prop}L} e^{i2kL}} = \left(-r_1 + \frac{t_1^2 r_2 e^{-2\alpha_{prop}L} e^{i2kL}}{1 - r_1 r_2 e^{-2\alpha_{prop}L} e^{i2kL}}\right) E_{inc}$$

$$= \frac{-r_1\left(1 - r_1 r_2 e^{-2\alpha_{prop}L} e^{i2kL}\right) + t_1^2 r_2 e^{-2\alpha_{prop}L} e^{i2kL}}{1 - r_1 r_2 e^{-2\alpha_{prop}L} e^{i2kL}} E_{inc},$$

as $t_1^2 = 1 - r_1^2$, then:

$$= \frac{-r_1\left(1 - r_1 r_2 e^{-2\alpha_{prop}L} e^{i2kL}\right) + (1 - r_1^2) r_2 e^{-2\alpha_{prop}L} e^{i2kL}}{1 - r_1 r_2 e^{-2\alpha_{prop}L} e^{i2kL}} E_{inc}$$

$$= \frac{-r_1 + r_1^2 r_2 e^{-2\alpha_{prop}L} e^{i2kL} + r_2 e^{-2\alpha_{prop}L} e^{i2kL} - r_1^2 r_2 e^{-2\alpha_{prop}L} e^{i2kL}}{1 - r_1 r_2 e^{-2\alpha_{prop}L} e^{i2kL}} E_{inc}$$

$$E_{reflec} = \frac{-r_1 + r_2 e^{-2\alpha_{prop}L} e^{i2kL}}{1 - r_1 r_2 e^{-2\alpha_{prop}L} e^{i2kL}} E_{inc},$$

then the reflectance is given by:

$$\mathcal{R} = \frac{\left|E_{reflec}\right|^2}{|E_{inc}|^2} = \frac{\left|-r_1 + r_2 e^{-2\alpha_{prop}L} e^{i2kL}\right|^2}{|1 - r_1 r_2 e^{-2\alpha_{prop}L} e^{i2kL}|^2}$$

$$= \frac{\left(-r_1 + r_2 e^{-2\alpha_{prop}L} e^{i2kL}\right)\left(-r_1 + r_2 e^{-2\alpha_{prop}L} e^{-i2kL}\right)}{(1 - r_1 r_2 e^{-2\alpha_{prop}L} e^{i2kL})(1 - r_1 r_2 e^{-2\alpha_{prop}L} e^{-i2kL})}$$

$$= \frac{r_1^2 - r_1 r_2 e^{-2\alpha_{prop}L} e^{-i2kL} - r_1 r_2 e^{-2\alpha_{prop}L} e^{i2kL} + r_2^2 e^{-4\alpha_{prop}L}}{1 - r_1 r_2 e^{-2\alpha_{prop}L} e^{-i2kL} - r_1 r_2 e^{-2\alpha_{prop}L} e^{i2kL} + r_1^2 r_2^2 e^{-4\alpha_{prop}L}}$$

$$= \frac{r_1^2 + r_2^2 e^{-4\alpha_{prop}L} - r_1 r_2 e^{-2\alpha_{prop}L} 2cos(2kL)}{1 + r_1^2 r_2^2 e^{-4\alpha_{prop}L} - r_1 r_2 e^{-2\alpha_{prop}L} 2cos(2kL)},$$

using trigonometric identities:

$$\mathcal{R} = \frac{r_1^2 + r_2^2 e^{-4\alpha_{prop}L} - 2r_1 r_2 e^{-2\alpha_{prop}L}(1 - 2sin^2(kL))}{1 + r_1^2 r_2^2 e^{-4\alpha_{prop}L} - 2r_1 r_2 e^{-2\alpha_{prop}L}(1 - 2sin^2(kL))}$$

$$= \frac{r_1^2 + r_2^2 e^{-4\alpha_{prop}L} - 2r_1 r_2 e^{-2\alpha_{prop}L} + 4r_1 r_2 e^{-2\alpha_{prop}L} sin^2(kL)}{1 + r_1^2 r_2^2 e^{-4\alpha_{prop}L} - 2r_1 r_2 e^{-2\alpha_{prop}L} + 4r_1 r_2 e^{-2\alpha_{prop}L} sin^2(kL)}$$

$$= \frac{(r_1 - r_2 e^{-2\alpha_{prop}L})^2 + 4r_1 r_2 e^{-2\alpha_{prop}L} sin^2(kL)}{(1 - r_1 r_2 e^{-2\alpha_{prop}L})^2 + 4r_1 r_2 e^{-2\alpha_{prop}L} sin^2(kL)},$$

in terms of the laser frequency and considering both mirrors to have equal reflectivity:

$$\mathcal{R}(\nu) = \frac{r^2\left(1 - e^{-\frac{c\alpha_{prop}}{FSR}}\right)^2 + 4r^2 e^{-\frac{c\alpha_{prop}}{FSR}} sin^2(\frac{\pi\nu}{FSR})}{\left(1 - r^2 e^{-\frac{c\alpha_{prop}}{FSR}}\right)^2 + 4r^2 e^{-\frac{c\alpha_{prop}}{FSR}} sin^2(\frac{\pi\nu}{FSR})}.$$

Equation 2.26

Where Equation 2.26 gives the cavity's spectrally dependent reflectance on the presence of propagation losses. Plotting it with the spectrally dependent transmittance:

Figure 11: Transmittance (blue), Reflectance (orange) and the resulting sum of the transmitted and reflected intensities (green) for a reflectivity of 0.9 and a propagation-loss coefficient of 0.1$\mathbf{m^{-1}}$.

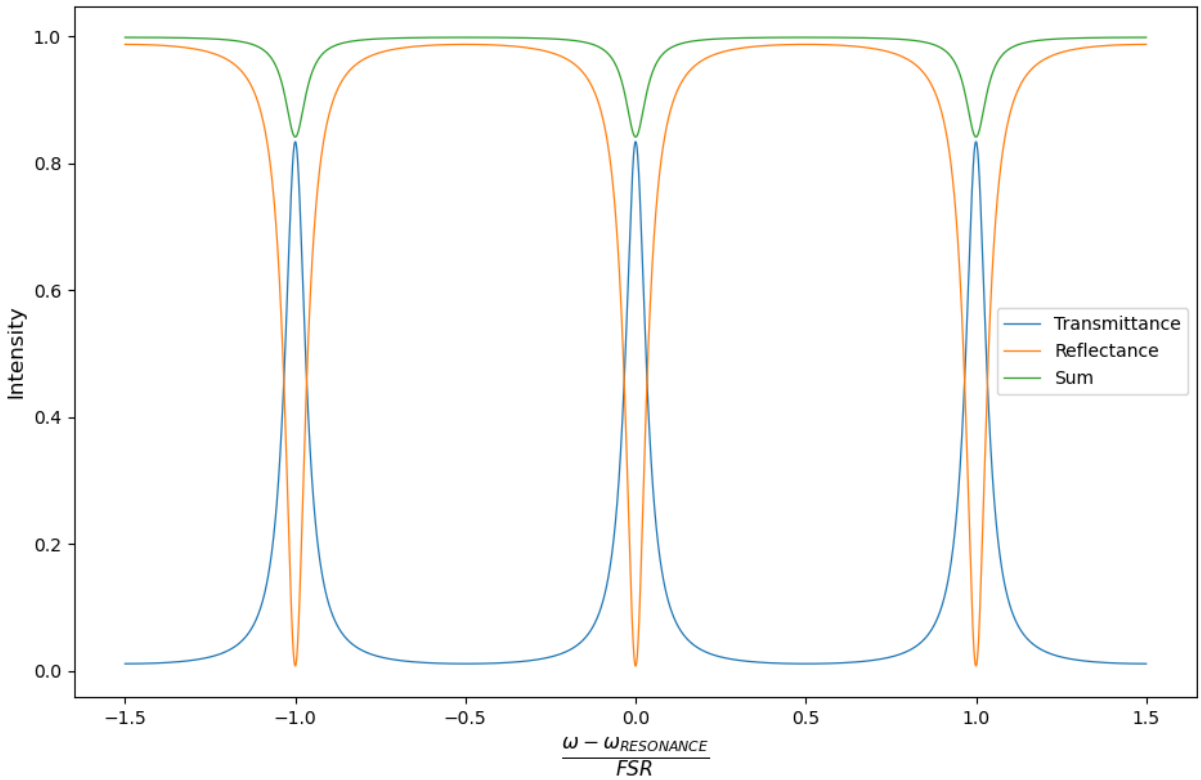

Source: Author, 2024.

The sum of the reflectance and transmittance does not sum up to unity as it did before. For that, we need to consider *Equation 2.25*[15] and from that we get:

Figure 12: Transmittance (blue), Reflectance (orange), Intrinsic propagation-loss Intensity (red) and the resulting sum of these intensities (green) for a reflectivity of 0.9 and a propagation-loss coefficient of $0.1\mathrm{m}^{-1}$.

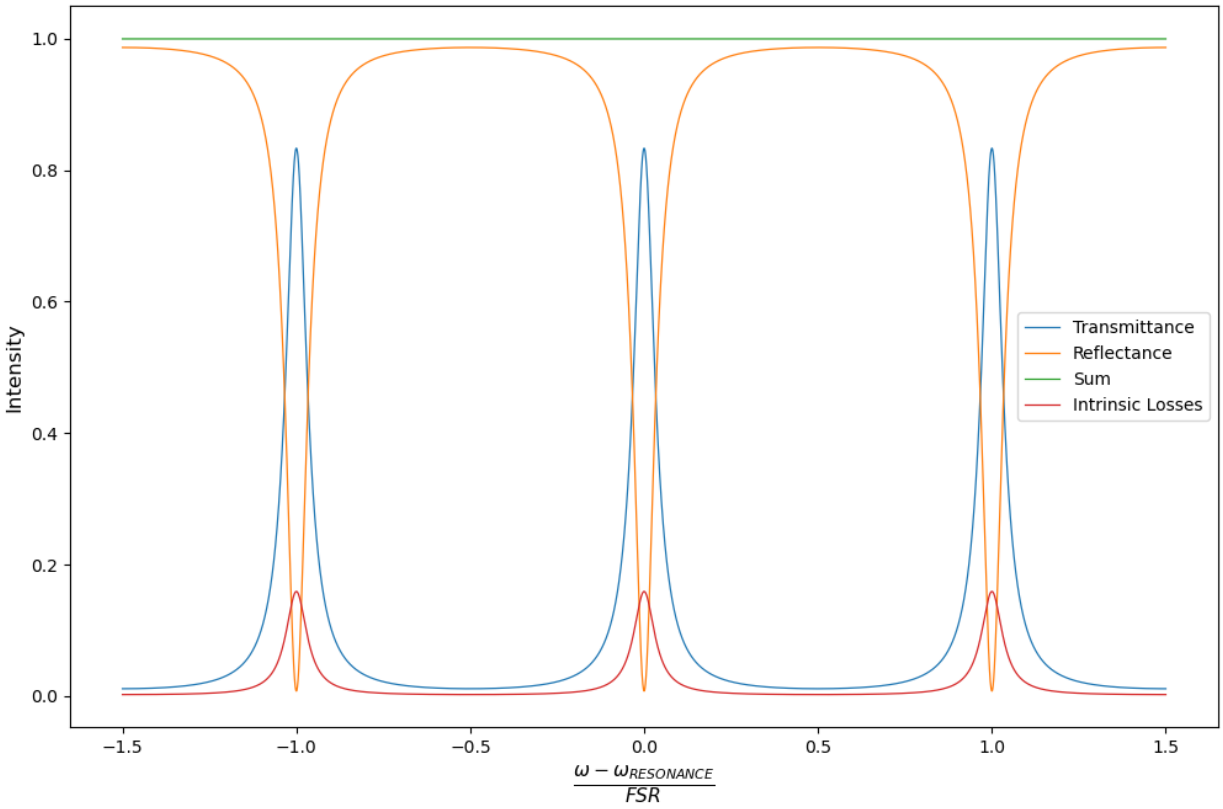

Source: Author, 2024.

To proceed with our analysis, it's essential to consider the parameters associated with Fabry-Perot Cavities. The Free Spectral Range (FSR), which depends solely on the cavity's geometry, remains unchanged when transitioning from the lossless case to the scenario with propagation losses. Consequently, the condition for resonance, which stipulates that twice the cavity length must be equal to an integer multiple of the laser's wavelength, also remains unaltered.

For the linewidth, we must be careful. Considering the region near the peaks of the transmittance and making the approximation for the sin(x) when $x \ll 1$, we get:

$$\mathcal{T}(\nu) = \frac{(1-r^2)^2 e^{-\frac{c\alpha_{prop}}{FSR}}}{\left(1 - r^2 e^{-\frac{c\alpha_{prop}}{FSR}}\right)^2 + 4r^2 e^{-\frac{c\alpha_{prop}}{FSR}} sin^2\left(\frac{\pi\nu}{FSR}\right)}.$$

Unlike what we did in the case of no losses, we cannot directly associate a Lorentzian curve with the transmittance due to the presence of the propagation-loss term. Instead, we will work directly with the expression for transmittance. Initially, we

will consider the Full Width at Half Maximum (FWHM). To do this, we will use high-reflectivity mirrors, so that the transmittance curve exhibits narrow peaks, as shown by the blue curve in Figure 10. In this scenario, the frequency variation required to go from the maximum of the peak to its half value is very small, making the approximation for the sine function suitable. Therefore:

$$\mathcal{T}(\nu) = \frac{(1-r^2)^2 e^{-\frac{c\alpha_{prop}}{FSR}}}{\left(1-r^2 e^{-\frac{c\alpha_{prop}}{FSR}}\right)^2 + 4r^2 e^{-\frac{c\alpha_{prop}}{FSR}}\left(\frac{\pi\nu}{FSR}\right)^2},$$

as we are interested in the half value of the transmittance at resonance, then:

$$\frac{(1-r^2)^2 e^{-\frac{c\alpha_{prop}}{FSR}}}{\left(1-r^2 e^{-\frac{c\alpha_{prop}}{FSR}}\right)^2 + 4r^2 e^{-\frac{c\alpha_{prop}}{FSR}}\left(\frac{\pi\nu_{1/2}}{FSR}\right)^2} = \frac{\mathcal{T}(\nu_{RES})}{2},$$

at resonance $sin^2\left(\frac{\pi\nu_{RES}}{FSR}\right) = 0$, then:

$$\frac{(1-r^2)^2 e^{-\frac{c\alpha_{prop}}{FSR}}}{\left(1-r^2 e^{-\frac{c\alpha_{prop}}{FSR}}\right)^2 + 4r^2 e^{-\frac{c\alpha_{prop}}{FSR}}\left(\frac{\pi\nu_{1/2}}{FSR}\right)^2} = \frac{(1-r^2)^2 e^{-\frac{c\alpha_{prop}}{FSR}}}{2\left(1-r^2 e^{-\frac{c\alpha_{prop}}{FSR}}\right)^2},$$

$$\frac{1}{\left(1-r^2 e^{-\frac{c\alpha_{prop}}{FSR}}\right)^2 + 4r^2 e^{-\frac{c\alpha_{prop}}{FSR}}\left(\frac{\pi\nu_{1/2}}{FSR}\right)^2} = \frac{1}{2\left(1-r^2 e^{-\frac{c\alpha_{prop}}{FSR}}\right)^2},$$

$$\left(1-r^2 e^{-\frac{c\alpha_{prop}}{FSR}}\right)^2 + 4r^2 e^{-\frac{c\alpha_{prop}}{FSR}}\left(\frac{\pi\nu_{1/2}}{FSR}\right)^2 = 2\left(1-r^2 e^{-\frac{c\alpha_{prop}}{FSR}}\right)^2,$$

$$4r^2 e^{-\frac{c\alpha_{prop}}{FSR}}\left(\frac{\pi\nu_{1/2}}{FSR}\right)^2 = \left(1-r^2 e^{-\frac{c\alpha_{prop}}{FSR}}\right)^2,$$

$$\left(\frac{\pi\nu_{1/2}}{FSR}\right)^2 = \frac{\left(1-r^2 e^{-\frac{c\alpha_{prop}}{FSR}}\right)^2}{4r^2 e^{-\frac{c\alpha_{prop}}{FSR}}},$$

using $\mathbb{R} = |r|^2$, then:

$$\frac{\pi\nu_{1/2}}{FSR} = \frac{\left(1-\mathbb{R}e^{-\frac{c\alpha_{prop}}{FSR}}\right)}{2\sqrt{\mathbb{R}e^{-\frac{c\alpha_{prop}}{FSR}}}},$$

finally:

$$\Delta\nu_{FWHM}^{loss} = 2\nu_{1/2},$$

$$\therefore \Delta\nu_{FWHM}^{loss} = \frac{\left(1 - \mathbb{R}e^{-\frac{c\alpha_{prop}}{FSR}}\right)}{\pi\sqrt{\mathbb{R}e^{-\frac{c\alpha_{prop}}{FSR}}}} FSR.$$

Equation 2.27

In the scenario where the propagation-loss coefficient is equal to zero, *Equation 2.27* reverts to *Equation 2.14*, and we obtain the linewidth for the lossless case, as expected. Using the definition of Finesse, we can derive:

$$\mathcal{F} = \frac{FSR}{\Delta\nu_{FWHM}},$$

therefore:

$$\mathcal{F}^{loss} = \frac{FSR}{\Delta\nu_{FWHM}^{loss}} = \frac{FSR}{\frac{\left(1 - \mathbb{R}e^{-\frac{c\alpha_{prop}}{FSR}}\right)}{\pi\sqrt{\mathbb{R}e^{-\frac{c\alpha_{prop}}{FSR}}}} FSR},$$

$$\mathcal{F}^{loss} = \frac{\pi\sqrt{\mathbb{R}e^{-\frac{c\alpha_{prop}}{FSR}}}}{1 - \mathbb{R}e^{-\frac{c\alpha_{prop}}{FSR}}}.$$

Equation 2.28

When the propagation-loss coefficient is equal to zero, *Equation 2.28* reverts to *Equation 2.12*, and we obtain the finesse for the lossless case, as expected. The losses represent a great drop in the finesses. For example, when the propagation-loss coefficient is $\alpha_{prop} = 0.1\mathrm{m}^{-1}$ the Finesse in the lossless case is about 10 times of the case with losses. Plotting both cases:

Figure 13: Finesse of the Fabry-Perot Cavity without propagation losses (orange, off scale, Equation 2.12) and with the propagation-loss coefficient is $\alpha_{prop} = 0.1\mathrm{m}^{-1}$ (blue, Equation 2.28).

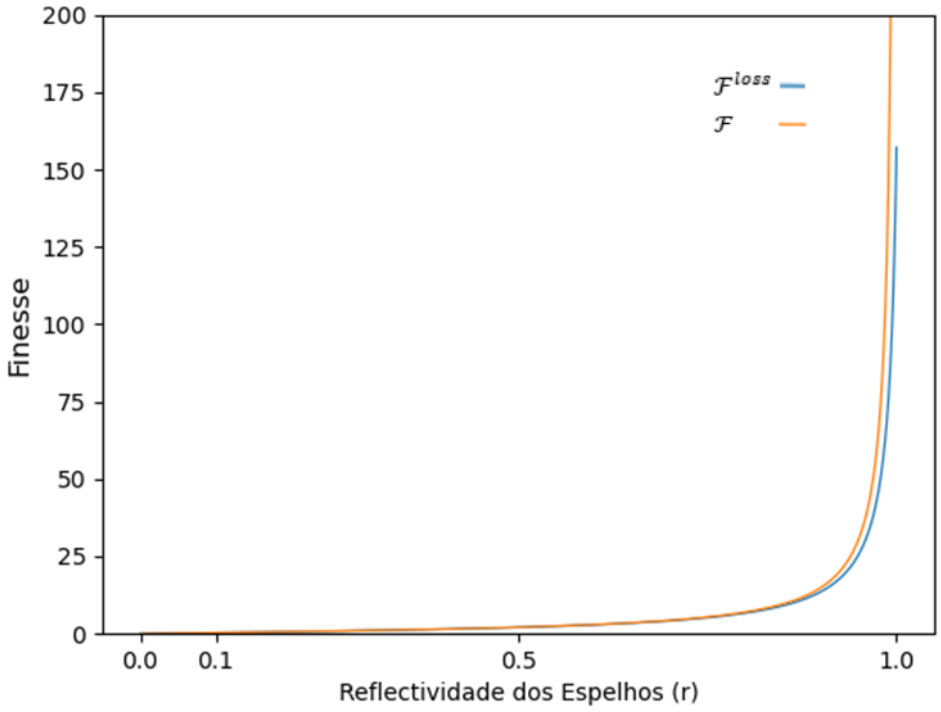

Source: Author, 2024.

Indeed, as finesse decreases in the presence of losses while the FSR remains constant, the linewidth becomes wider. This broadening of the linewidth is not desirable for experiments that demand a stable and narrow frequency linewidth. It underscores the importance of minimizing losses in such experiments to maintain the required frequency stability.

Finally, we have the quality factor. For the case with losses, we going to use the equations 2.15 and 2.16. The *Equation 2.15* remains equal as it was, however, the *Equation 2.16* suffers a change in the photon-decay time, that now englobes not only the outcoupling but also the propagation-loss time, given by *Equation 2.22*. Then, the quality factor is given by:

$$Q = -2\pi\nu_{RES}\frac{\mathcal{W}(t)}{\frac{d\mathcal{W}(t)}{dt}},$$

where $\frac{1}{\tau_c} \rightarrow \frac{1}{\tau_{out}} + \frac{1}{\tau_{loss}}$, then:

$$Q = -2\pi\nu_{RES}\frac{\mathcal{W}_{launched}e^{-t\left(\frac{1}{\tau_{out}}+\frac{1}{\tau_{loss}}\right)}}{\left(-\frac{\mathcal{W}_{launched}e^{-t\left(\frac{1}{\tau_{out}}+\frac{1}{\tau_{loss}}\right)}}{\frac{1}{\tau_{out}}+\frac{1}{\tau_{loss}}}\right)},$$

from *Equation 2.22*:

$$Q = 2\pi\nu_{RES}\frac{1}{\left(\frac{1}{-\frac{\ln(\mathbb{R}_1\mathbb{R}_2)}{t_{RT}}+c\alpha_{prop}}\right)} = 2\pi\nu_{RES}\left(-\frac{\ln(\mathbb{R}_1\mathbb{R}_2)}{t_{RT}}+c\alpha_{prop}\right),$$

the round-trip time can be rewritten in terms of the light velocity and the cavity length by $t_{RT} = \frac{2L}{c}$, then:

$$Q = 2\pi c\nu_{RES}\left(\alpha_{prop}-\frac{\ln(\mathbb{R}_1\mathbb{R}_2)}{2L}\right),$$

Equation 2.29

and using *Equation 2.18* and adapting the FWHM to the loss case:

$$Q = \frac{\nu_{RES}}{\Delta\nu_{FWHM}^{loss}}.$$

Equation 2.30

3 EXTERNAL CAVITY LASER DIODE

Shifting our focus to the laser itself, let's begin by considering the type of laser that aligns with our interest – Distributed Feedback (DFB) Lasers. Monolithic DFB lasers can operate in both a single transverse mode and a single longitudinal mode. However, their spectral linewidth can be relatively large since the Schawlow–Townes linewidth is proportional to the square of the cavity linewidth, that is, the FWHM of the resonator, which can be significant in monolithic DFB lasers[17].

An important obstacle is that achieving a significant electronic tuning range in a DFB laser is challenging. The tuning range resulting from changes in the injection current is relatively small, and one is often compelled to use a slower mechanism to do so, like diode temperature changes to tune the diode over a large range.

To address these challenges, one approach is to extend the diode cavity by coupling it with an external cavity, essentially forming a much larger compound cavity. In this configuration, the diode serves as the gain medium in this expanded cavity. To achieve this, optical elements such as mirrors, gratings can be used. Due to the presence of an additional cavity, this modified laser is called External Cavity Diode Laser (ECDL).

Firstly, a longer cavity brings about a reduction in the Laser Shawlow–Townes width, due to its inverse proportionality with the square of the cavity length, the greater the cavity length, the smaller the Shawlow–Townes width of that cavity will be. Additionally, the increase in cavity length significantly mitigates the impact of the α parameter, as the active medium length becomes a very small fraction of the overall cavity length. To overcome the challenges associated with the limited tuning range resulting from changes in injection current and the slow temperature tuning process, tunability can be transferred to other elements. For instance, the incorporation of a coarse frequency-selecting element, typically a grating, along with adjustments to the cavity length, by a Piezoelectric Transducer (PZT), provides a broad tuning range without the need to alter the diode current or temperature.

The arrangement of optical elements in an ECDL can be constructed in various ways, with common configurations including the Littrow configuration, the Littman configuration, or a combination of both. In the subsequent sections of this dissertation,

we will explore these configurations. For now, let's use a simplified illustration (shown in Figure 14) to establish the basic theory.

Figure 14: Schematic of the overall cavity reflective surfaces. Here r_1 and r_2 are the reflectivities of the first and second surfaces of the diode laser, and r_3 is the reflectivity of the second surface of the external cavity.

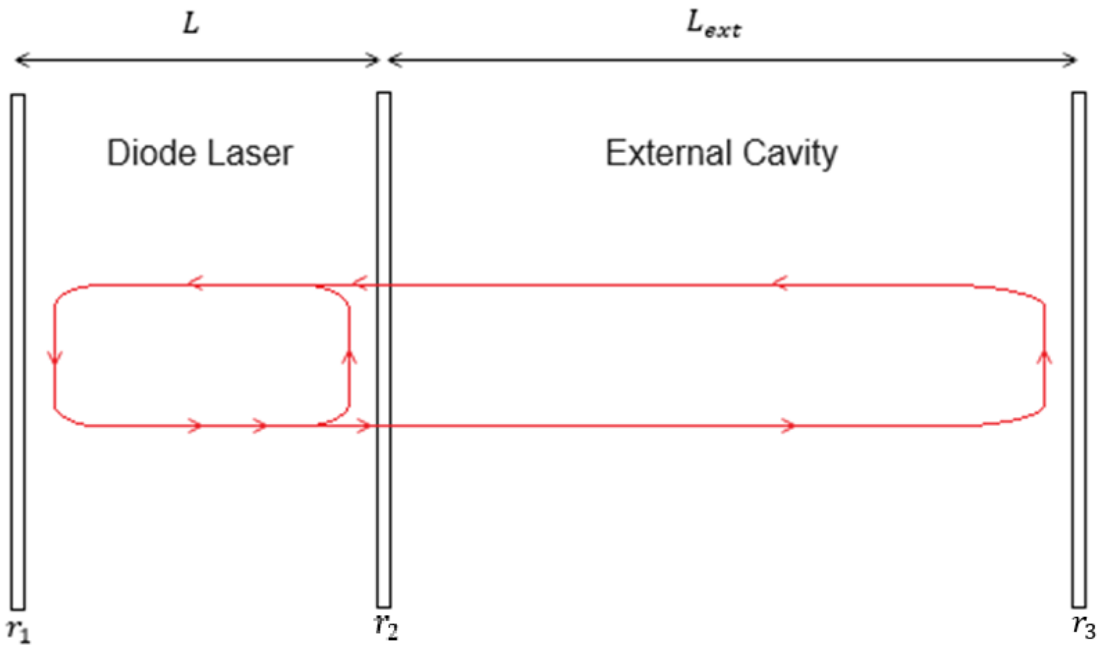

Source: Author, 2024.

The construction of an ECDL can be intricate, and opting for a commercial one may be a practical alternative. Here, we will look into the basic theory for the construction of an ECDL. A fundamental consideration that can significantly impact the analysis is the coating problem, specifically the presence or absence of antireflection coating on the diode laser cavity. Optimal results are typically achieved when one of the diode facets has zero reflectivity, and the other is highly reflecting. This aspect is crucial because if there is an antireflection coating on the diode, it essentially acts as a gain element in a larger cavity. If there isn't, the problem must be treated as a composite cavity formed by the coupling of the diode cavity and the external cavity, presenting a more complex scenario. Nevertheless, the complex scenario is our case.

In the absence of an antireflection coating, small amounts of feedback into the diode can lead to adverse effects. To analyze these effects, let's initially focus on the second surface of the external cavity, r_3, without specifying its nature (mirror, grating, etc.) but considering only its reflectivity and its distance to the diode output facet, L_{ext}. Making a realistic assumption that the external cavity can accommodate only a single

reflection aligns with the fact that the second diode facet is uncoated, yielding a reflectivity, r_2, of around 0.6 (using GaAs)[17]. With only one reflection from the external cavity, we can associate the output facet of the diode with an effective reflectivity, considering both the first reflected beam and the one that was reflected by the external cavity and re-entered the diode. This effective reflectivity is given by:

$$r_{2,eff} = r_2 + |t_2|^2 r_3 e^{-i2kL_{ext}}.$$

Here we're considering that there are two transmissions at the diode output facet, one leaving the diode cavity towards r_3 and other that enters back to the diode cavity coming back from r_3, and the phase shift given by the round-trip in the external cavity. Considering that $k = \omega/c$ and $2L_{ext} = c\tau_{ext}$, where τ_{ext} is the round-trip time of the external cavity. Therefore, only in terms of reflectivity:

$$r_{2,eff}(\omega) = r_2 + (1 - |r_2|^2) r_3 e^{-i\omega\tau_{ext}}.$$

Equation 3.1

The optical coherence from lasers offers numerous advantages compared to conventional light sources, including a narrower monochromatic light, and directionality. These characteristics, however, are tied to the processes of laser oscillation. Laser light is produced through the stimulated emission of electromagnetic waves resulting from these oscillations in a specific mode[18]. To attain the necessary oscillations, the diode laser must satisfy two key conditions for laser oscillation. Firstly, the optical gain must surpass losses. Secondly, the presence of an external cavity must introduce feedback (reflected light) that aligns in phase with the recently emitted light. These conditions can be expressed as:

$$r_1 \left| r_{2,eff} \right| e^{(g'_{th} - \alpha)L} = 1,$$

$$2k'L + \varphi_r = 2\pi m.$$

Equation 3.2

Here, g'_{th} is the threshold gain of the diode's medium, α is the loss of the compound cavity, k' is the wave number of the diode's medium (the prime is to differentiate from the free space wave number) and φ_r is the phase of the complex number $r_{2,eff}$. It is interesting to define a coupling parameter:

$$\kappa_{ext} \equiv \frac{r_3}{r_2}(1 - |r_2|^2),$$

Equation 3.3

then, rewriting *Equation 3.1*:

$$r_{2,eff}(\omega) = r_2\left[1 + \kappa_{ext}e^{-i\omega\tau_{ext}}\right],$$

Equation 3.4

from *Equation 3.4,* we can extract some quantities, like the modulus and the phase of the complex number, φ_r. When $\kappa_{ext} \ll 1$:

$$\left|r_{2,eff}(\omega)\right|^2 = r_2\left[1 + \kappa_{ext}e^{-i\omega\tau_{ext}}\right] \cdot r_2\left[1 + \kappa_{ext}e^{i\omega\tau_{ext}}\right]$$

$$= r_2^2\left[1 + \kappa_{ext}e^{-i\omega\tau_{ext}} + \kappa_{ext}e^{i\omega\tau_{ext}} + \kappa_{ext}^2\right],$$

considering that $\kappa_{ext} \ll 1$:

$$\left|r_{2,eff}(\omega)\right|^2 = r_2^2\left[1 + \kappa_{ext}e^{-i\omega\tau_{ext}} + \kappa_{ext}e^{i\omega\tau_{ext}}\right]$$

$$= r_2^2[1 + 2\kappa_{ext}cos(\omega\tau_{ext})],$$

then:

$$\left|r_{2,eff}(\omega)\right| = r_2\sqrt{1 + 2\kappa_{ext}cos(\omega\tau_{ext})},$$

once again, $\kappa_{ext} \ll 1$, then using a Taylor expansion:

$$\sqrt{1 + x} \approx 1 + \frac{1}{2}x,$$

finally:

$$\left|r_{2,eff}(\omega)\right| \approx r_{2,d}[1 + \kappa_{ext}cos(\omega\tau_{ext})],$$

Equation 3.5

for the phase φ_r in the regime of $\kappa_{ext} \ll 1$, we have by definition:

$$\varphi_r = \arctan\left(\frac{\Im m\left[r_{2,eff}(\omega)\right]}{\Re e\left[r_{2,eff}(\omega)\right]}\right).$$

Expanding *Equation 3.4*:

$$r_{2,eff}(\omega) = r_2\left[1 + \kappa_{ext}e^{-i\omega\tau_{ext}}\right] = r_2[1 + \kappa_{ext}cos(\omega\tau_{ext}) - i\kappa_{ext}sin(\omega\tau_{ext})],$$

then the phase is given by:

$$\varphi_r = \arctan\left(\frac{-r_2\kappa_{ext}sin(\omega\tau_{ext})}{r_2[1 + \kappa_{ext}cos(\omega\tau_{ext})]}\right) = \arctan\left(\frac{-\kappa_{ext}sin(\omega\tau_{ext})}{[1 + \kappa_{ext}cos(\omega\tau_{ext})]}\right).$$

Considering $\kappa_{ext} \ll 1$ and $cos(\omega\tau_{ext}) \leq 1$, then $[1 + \kappa_{ext}cos(\omega\tau_{ext})] \approx 1$, which gives:

$$\varphi_r = \arctan\left(-\kappa_{ext}sin(\omega\tau_{ext})\right),$$

using a Taylor expansion for the arctan(x):

$$\arctan(x) \approx x - \frac{x^3}{3} + \cdots,$$

up to the first order:

$$\varphi_r = -\kappa_{ext}sin(\omega\tau_{ext}).$$

Equation 3.6

In our analysis, we want to quantify the effects of an external cavity, and consequently the presence of feedback on the diode. In that manner, we seek the change in the threshold gain and phase due to the presence of the feedback. For the threshold gain we will use the *Equations 3.2* and *3.5*:

With the presence of the external cavity:

$$r_1\left|r_{2,eff}\right|e^{(g'_{th}-\alpha)L} = 1,$$

$$\left|r_{2,eff}(\omega)\right| \approx r_2[1 + \kappa_{ext}cos(\omega\tau_{ext})],$$

then:

$$r_1r_2[1 + \kappa_{ext}cos(\omega\tau_{ext})]e^{(g'_{th}-\alpha)L} = 1.$$

Without the presence of the external cavity the effective reflectivity is just r_2, then:

$$r_1r_2e^{(g_{th}-\alpha)L} = 1.$$

Here g_{th} is the threshold gain in the absence of the external cavity. Subtracting one of the other:

$$r_1 r_2[1 + \kappa_{ext} cos(\omega\tau_{ext})]e^{(g'_{th}-\alpha)L} - r_1 r_2 e^{(g_{th}-\alpha)L} = 0,$$

$$[1 + \kappa_{ext} cos(\omega\tau_{ext})]e^{(g'_{th}-\alpha)L} - e^{(g_{th}-\alpha)L} = 0,$$

$$[1 + \kappa_{ext} cos(\omega\tau_{ext})]e^{(g'_{th}-\alpha)L} = e^{(g_{th}-\alpha)L},$$

$$ln\left\{[1 + \kappa_{ext} cos(\omega\tau_{ext})]e^{(g'_{th}-\alpha)L}\right\} = (g_{th} - \alpha)L,$$

$$ln[1 + \kappa_{ext} cos(\omega\tau_{ext})] + (g'_{th} - \alpha)L = (g_{th} - \alpha)L,$$

$$(g'_{th} - \alpha)L - (g_{th} - \alpha)L = -ln[1 + \kappa_{ext} cos(\omega\tau_{ext})].$$

Considering, again, that $\kappa_{ext} \ll 1$, then a Taylor expansion represents a good approach:

$$\ln(1 + x) \approx x - \frac{x^2}{2} + \cdots,$$

up to the first order:

$$(g'_{th} - g_{th})L \approx -\kappa_{ext} cos(\omega\tau_{ext}),$$

therefore:

$$g'_{th} - g_{th} = -\frac{\kappa_{ext}}{L} cos(\omega\tau_{ext}).$$

Equation 3.7

In the other hand, the condition for phase in the absence of feedback is given by:

$$\frac{2nL\omega_{th}}{c} = 2\pi m.$$

Equation 3.8

Here, n represents the index of refraction in the diode cavity, ω_{th} is the angular frequency at threshold, and m is an integer. The introduction of feedback and an external cavity leads to slight changes in the frequency at threshold ($\Delta\omega = \omega - \omega_{th}$) and the index of refraction (Δn), respectively. Thus, the modified condition can be expressed as:

$$\frac{2L}{c}(n+\Delta n)(\omega_{th}+\Delta\omega)+\varphi_r=2\pi m+\Delta\varphi.$$

Equation 3.9

The presence of φ_r is due to the effective reflectivity that must be considered in the case when there is feedback. The $\Delta\varphi$ is the difference between the round-trip phase and $2\pi m$. For laser oscillation to occur, we will require that $\Delta\varphi$ is either a multiple of 2π or zero. Using the equation for no feedback (*Equation 3.8*) in *Equation 3.9*, we have:

$$\frac{2L}{c}(n+\Delta n)(\omega_{th}+\Delta\omega)+\varphi_r=\frac{2nL\omega_{th}}{c}+\Delta\varphi,$$

$$\frac{2L}{c}(n\omega_{th}+n\Delta\omega+\omega_{th}\Delta n+\Delta n\Delta\omega)+\varphi_r=\frac{2nL\omega_{th}}{c}+\Delta\varphi,$$

$$\frac{2Ln\omega_{th}}{c}+\frac{2L}{c}(n\Delta\omega+\omega_{th}\Delta n+\Delta n\Delta\omega)+\varphi_r=\frac{2nL\omega_{th}}{c}+\Delta\varphi,$$

$$\frac{2L}{c}(n\Delta\omega+\omega_{th}\Delta n+\Delta n\Delta\omega)+\varphi_r=\Delta\varphi.$$

Considering that Δn and $\Delta\omega$ are small, keeping only the terms up to the first order in small quantities:

$$\Delta\varphi=\frac{2L}{c}(n\Delta\omega+\omega_{th}\Delta n)+\varphi_r.$$

Equation 3.10

To quantify Δn, we can consider the expansion of the refractive index around the threshold values of frequency and carrier density[17]:

$$n=n_0+\frac{\partial n}{\partial\omega}(\omega-\omega_{th})+\frac{\partial n}{\partial N}(N-N_{th}),$$

$$\Delta n=\frac{\partial n}{\partial\omega}(\omega-\omega_{th})+\frac{\partial n}{\partial N}(N-N_{th}).$$

Here, N_{th} is the carrier density at threshold without feedback. Inserting it into *Equation 3.10*:

$$\Delta\varphi=\frac{2L}{c}\left(n\Delta\omega+\omega_{th}\left[\frac{\partial n}{\partial\omega}(\omega-\omega_{th})+\frac{\partial n}{\partial N}(N-N_{th})\right]\right)+\varphi_r,$$

$$\Delta\varphi = \frac{2L}{c}\left(n\Delta\omega + \omega_{th}\Delta\omega\frac{\partial n}{\partial\omega} + \omega_{th}\frac{\partial n}{\partial N}(N - N_{th})\right) + \varphi_r,$$

$$\Delta\varphi = \frac{2L}{c}\left[\Delta\omega\left(n + \omega_{th}\frac{\partial n}{\partial\omega}\right) + \omega_{th}\frac{\partial n}{\partial N}(N - N_{th})\right] + \varphi_r.$$

Now, we can recognize the group index of refraction, where:

$$n_g = n + \omega_{th}\frac{\partial n}{\partial\omega}.$$

Equation 3.11

Then:

$$\Delta\varphi = \frac{2L}{c}\left[n_g\Delta\omega + \omega_{th}\frac{\partial n}{\partial N}(N - N_{th})\right] + \varphi_r.$$

For the carrier density, we can associate it to the difference in gain and the linewidth enhancement factor by using the relations given by Nagourney[17]:

$$\nu - \nu_{th} = -\frac{\nu_{th}}{n_g}\frac{\partial n}{\partial N}(N - N_{th}),$$

Equation 3.12

and

$$\nu - \nu_{th} = \frac{\upsilon_g\alpha}{4\pi}\frac{\partial g}{\partial N}(N - N_{th}),$$

Equation 3.13

where υ_g is the laser's group velocity and α is the linewidth enhancement factor, that besides quantifying the amplitude-phase coupling, also helps characterize to which degree variations in the carrier density, N, alter the index of refraction of the active layer, n[27]. Moreover, α is related to how the laser linewidth is bigger than the Schawlow-Townes linewidth by the factor of $(1 + \alpha^2)$[28]. Comparing these equations:

$$\frac{\upsilon_g\alpha}{4\pi}\frac{\partial g}{\partial N}(N - N_{th}) = -\frac{\nu_{th}}{n_g}\frac{\partial n}{\partial N}(N - N_{th}),$$

$$\frac{\partial n}{\partial N}(N - N_{th}) = -\frac{n_g\upsilon_g}{4\pi\nu_{th}}\alpha\frac{\partial g}{\partial N}(N - N_{th}),$$

by the definition of group index of refraction, $n_g \equiv c/v_g$, then:

$$\frac{\partial n}{\partial N}(N - N_{th}) = -\frac{c\alpha}{2\omega_{th}}\frac{\partial g}{\partial N}(N - N_{th}) = -\frac{c\alpha}{2\omega_{th}}(g'_{th} - g_{th}),$$

where we used that the product of $\partial g/\partial N$ and $N - N_{th}$ is the increment in the gain above threshold, $g'_{th} - g_{th}$[17]. Therefore:

$$\Delta\varphi = \frac{2L}{c}\left[n_g\Delta\omega - \omega_{th}\frac{c\alpha}{2\omega_{th}}(g'_{th} - g_{th})\right] + \varphi_r,$$

substituting $g'_{th} - g_{th}$ (*Equation 3.7*) and φ_r (*Equation 3.6*):

$$\Delta\varphi = \frac{2L}{c}\left[n_g\Delta\omega - \frac{c\alpha}{2}\left(-\frac{\kappa_{ext}}{L}cos(\omega\tau_{ext})\right)\right] - \kappa_{ext}sin(\omega\tau_{ext}),$$

finally:

$$\Delta\varphi = \frac{2n_gL}{c}(\omega - \omega_{th}) + \kappa_{ext}[\alpha cos(\omega\tau_{ext}) - sin(\omega\tau_{ext})].$$

Equation 3.14

The term $\frac{2n_gL}{c}$ in *Equation 3.14* represents the round-trip time in the diode cavity, denoted as τ_d. Additionally, let's leverage trigonometric relations to consolidate these two trigonometric functions into a single expression.

$$Asin(x + \theta) = \alpha cos(x) - sin(x),$$

expanding the sine of the sum:

$$A[sin(x)cos(\theta) + \cos(x)sin(\theta)] = \alpha cos(x) - sin(x),$$

by orthogonality:

$$Acos(\theta) = -1,$$

$$Asin(\theta) = \alpha,$$

taking the squared on both sides and equations:

$$A^2cos^2(\theta) = 1,$$

$$A^2sin^2(\theta) = \alpha^2,$$

summing:

$$A^2[cos^2(\theta) + sin^2(\theta)] = 1 + \alpha^2 \rightarrow A = \sqrt{1+\alpha^2},$$

for the θ we use:

$$\frac{Asin(\theta)}{Acos(\theta)} = \frac{\alpha}{-1},$$

$$tan(\theta) = -\alpha,$$

then:

$$\theta = arctan(-\alpha) = -arctan(\alpha),$$

for $x = \omega\tau_{ext}$, we have:

$$\alpha cos(x) - sin(x) = \sqrt{1+\alpha^2}sin\big(\omega\tau_{ext} - arctan(\alpha)\big),$$

the phase change turns into:

$$\Delta\varphi = \tau_d(\omega - \omega_{th}) + \kappa_{ext}\sqrt{1+\alpha^2}sin\big(\omega\tau_{ext} - arctan(\alpha)\big).$$

Now, it is useful to define another coupling parameter, related to the oscillations of the difference between the round-trip phase and 2π:

$$C \equiv \frac{\tau_{ext}}{\tau_d}\kappa_{ext}\sqrt{1+\alpha^2},$$

Equation 3.15

then, the equation for $\Delta\varphi$ becomes:

$$\Delta\varphi = \tau_d(\omega - \omega_{th}) + C\frac{\tau_d}{\tau_{ext}}sin\big(\omega\tau_{ext} - arctan(\alpha)\big).$$

Equation 3.16

By graphing Equation 3.16, we can underscore the significance of coupling the diode to an external cavity. The figure below illustrates a series of plots for this function, encompassing various values of the coupling parameter, C. These plots provide insights into the diode's behavior under varying degrees of feedback. Notably, as the feedback increases, $\Delta\varphi$ exhibits more pronounced oscillations.

Figure 15: Difference between the round-trip phase and 2π for various values of the coupling parameter, C. For C equals zero (blue), C equals 1 (orange), C equals 5 (green) and C equals 10 (red). Values Normalized by $\tau_d = 1$.

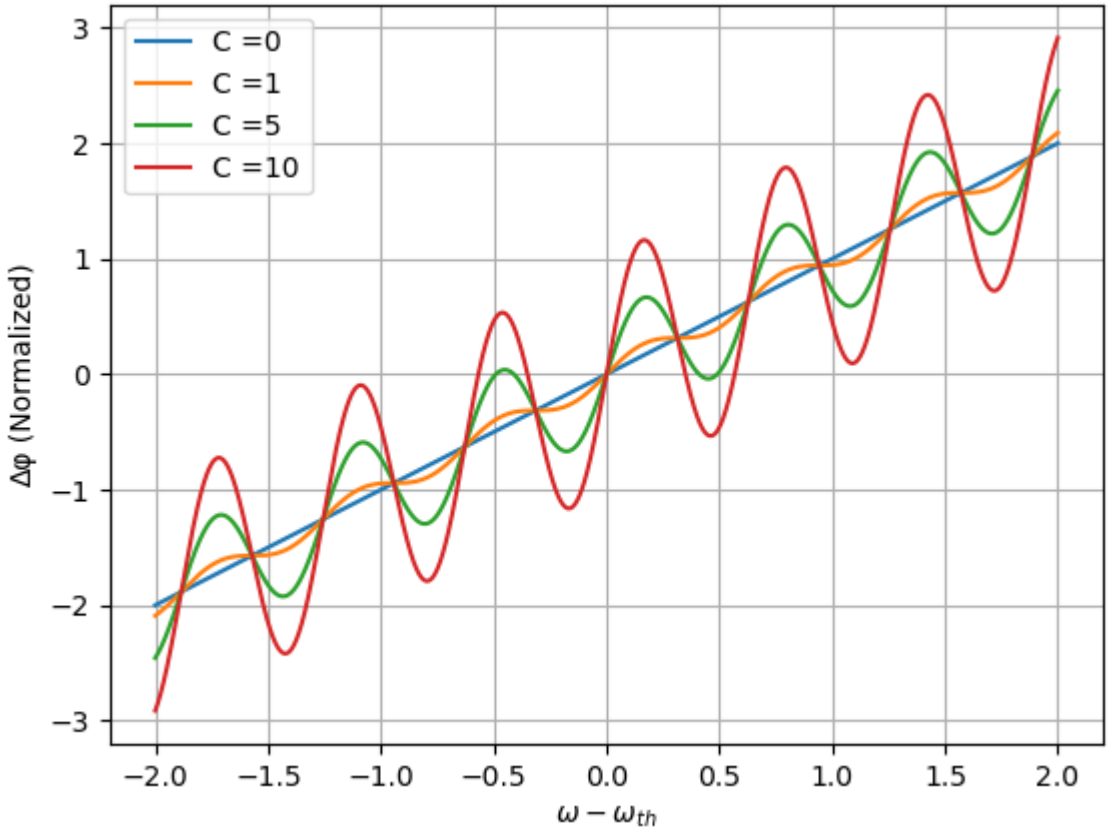

Source: Author, 2024.

In the absence of feedback, $\Delta\varphi$ and $\omega - \omega_{th}$ exhibit a linear relationship, affirming that the laser operates solely at the threshold frequency, ω_{th}. An intriguing scenario arises when C < 1, wherein $\Delta\varphi$ remains strictly monotonic. In this weak feedback regime, the laser would still oscillate at a single frequency, but not at the threshold frequency, ω_{th}. Instead, the frequency undergoes a shift by $\Delta\omega$. It's noteworthy that this frequency shift is contingent on τ_{ext}, implying that a slight modification in the external cavity's length, on the order of the laser's wavelength, can influence the laser's frequency. In this manner, the maximum frequency shift can be determined by satisfying the laser oscillation condition for phase ($\Delta\varphi = 0$):

$$0 = \tau_d \Delta\omega + C\frac{\tau_d}{\tau_{ext}} sin\big(\omega\tau_{ext} - arctan(\alpha)\big),$$

then:

$$\Delta\omega = -\frac{C}{\tau_{ext}} sin\big(\omega\tau_{ext} - arctan(\alpha)\big),$$

Equation 3.17

the maximum value for the frequency shift is given when $sin\big(\omega\tau_{ext} - arctan(\alpha)\big) = -1$, then:

$$\Delta\omega_{max} = \frac{C}{\tau_{ext}} = \frac{\frac{\tau_{ext}}{\tau_d}\kappa_{ext}\sqrt{1+\alpha^2}}{\tau_{ext}} = \frac{\kappa_{ext}}{\tau_d}\sqrt{1+\alpha^2}.$$

As an example, considering *Equation 3.17*, a variation in the external cavity length of approximately $\lambda/4$, a laser cavity with a length of 300μm, and an external field reflectivity on the order of 10^{-4}, the frequency shift would be approximately 18MHz ($\alpha = 5$). Hence, if maintaining laser frequency stability is crucial for your experiment, incorporating an optical isolator could prove beneficial.

Moreover, there are three primary methods for providing feedback: (a) utilizing the first-order light reflected from a diffraction grating, known as the Littrow Configuration, (b) using the light reflected from a combination of a grating and a mirror, where the first-order light reflected from the grating reaches a mirror before returning to the diode, referred to as the Littman-Metcalf Configuration, or (c) replacing the mirror of the Littman-Metcalf Configuration with another grating, forming the double-grating configuration. Starting with the Littrow configuration, the simplest. The linewidth of the laser is given by the modified Schawlow-Townes formula[19][20]:

$$\Delta\nu_{laser} = \Delta\nu_0\left(1 + \frac{\tau_{ext}}{\tau_d'}\right)^{-2},$$

Equation 3.18

here, $\Delta\nu_0$ is the linewidth of the laser without the external cavity and τ_d' is the round-trip time of the diode using the group velocity. Then:

$$\Delta\nu_{laser} = \Delta\nu_0\left(\frac{\tau_d' + \tau_{ext}}{\tau_d'}\right)^{-2} = \Delta\nu_0\left(\frac{\tau_d'}{\tau_d' + \tau_{ext}}\right)^{2} = \Delta\nu_0\left(\frac{\tau_d'}{\tau_{eff}}\right)^{2},$$

where τ_{eff} is the effective round-trip time. Moreover, the effective round-trip time can be found using the round trip phase by[17]:

$$\tau_{eff} = \frac{d(\Delta\varphi)}{d\omega},$$

then, from *Equation 3.16*:

$$\frac{d(\Delta\varphi)}{d\omega} = \tau_d' + C\frac{\tau_d'}{\tau_{ext}}\tau_{ext}cos\big(\omega\tau_{ext} - arctan(\alpha)\big) = \tau_d' + C\tau_d'cos\big(\omega\tau_{ext} - arctan(\alpha)\big),$$

consequently:

$$\Delta\nu_{laser} = \Delta\nu_0\left(\frac{\tau_d'}{\tau_{eff}}\right)^2 = \Delta\nu_0\left(\frac{\tau_d'}{\tau_d' + C\tau_d'cos\big(\omega\tau_{ext} - arctan(\alpha)\big)}\right)^2,$$

finally:

$$\Delta\nu_{laser} = \frac{\Delta\nu_0}{\Big(1 + C\cdot cos\big(\omega\tau_{ext} - arctan(\alpha)\big)\Big)^2},$$

Equation 3.19

in the regime of strong feedback, $C \gg 1$, the laser oscillation occurs when $sin\big(\omega\tau_{ext} - arctan(\alpha)\big) \approx 0$, then $cos\big(\omega\tau_{ext} - arctan(\alpha)\big) \approx 1$ and we get:

$$\Delta\nu_{laser} \approx \frac{\Delta\nu_0}{(1+C)^2}.$$

Equation 3.20

The addition of an external cavity can significantly reduce the linewidth of a diode laser. For instance, in the case of large coupling (C), for an uncoated diode with $r_2 = 0.6$ and an external reflector with r_3 of about 0.5, the coupling parameter κ_{ext} is 0.6. With a diode length of 0.3 mm, an external cavity of 10 mm, and a loss coefficient $\alpha = 2$, the C parameter is approximately 39.75. Consequently, the modified linewidth experiences a reduction of about 1660 compared to the solitary diode linewidth. This reduction can be even more significant for external reflectors with higher reflectivity or increased external cavity length. In the strong feedback regime, the frequency modulation sensitivity is reduced by a factor of 1+C in relation to the no feedback regime[17]:

$$\left(\frac{\partial\nu_{laser}}{\partial I}\right)_{feedback} = \frac{1}{1+C}\left(\frac{\partial\nu_0}{\partial I}\right)_{no\ feedback}.$$

Equation 3.21

Up to this point, our analysis has been general, irrespective of the chosen configuration. Now, we will examine specific configurations in more detail, starting with the Littrow mount.

3.1 THE LITTROW CONFIGURATION

In the Littrow configuration, a grating serves as the reflecting surface, and the first-order diffracted light is back-reflected back to the laser along the same path as the incident light. To enhance frequency selectivity and avoid beam divergence, a collimating lens is employed, allowing the light incident on the grating to cover as many lines as possible. Additionally, an antireflection coating is applied to the lens to minimize the feedback sensitivity of the diode laser. To better illustrate it, Figure 16 brings a scheme.

Figure 16: Littrow configuration for an ECDL, where the groove spacing is given by a, and with an incident angle of θ with respect to the normal. Where we can see the position of the pivot point in relation to the origin, set to be at the first mirror of the diode cavity. We use point A just to express the z coordinate of the pivot point.

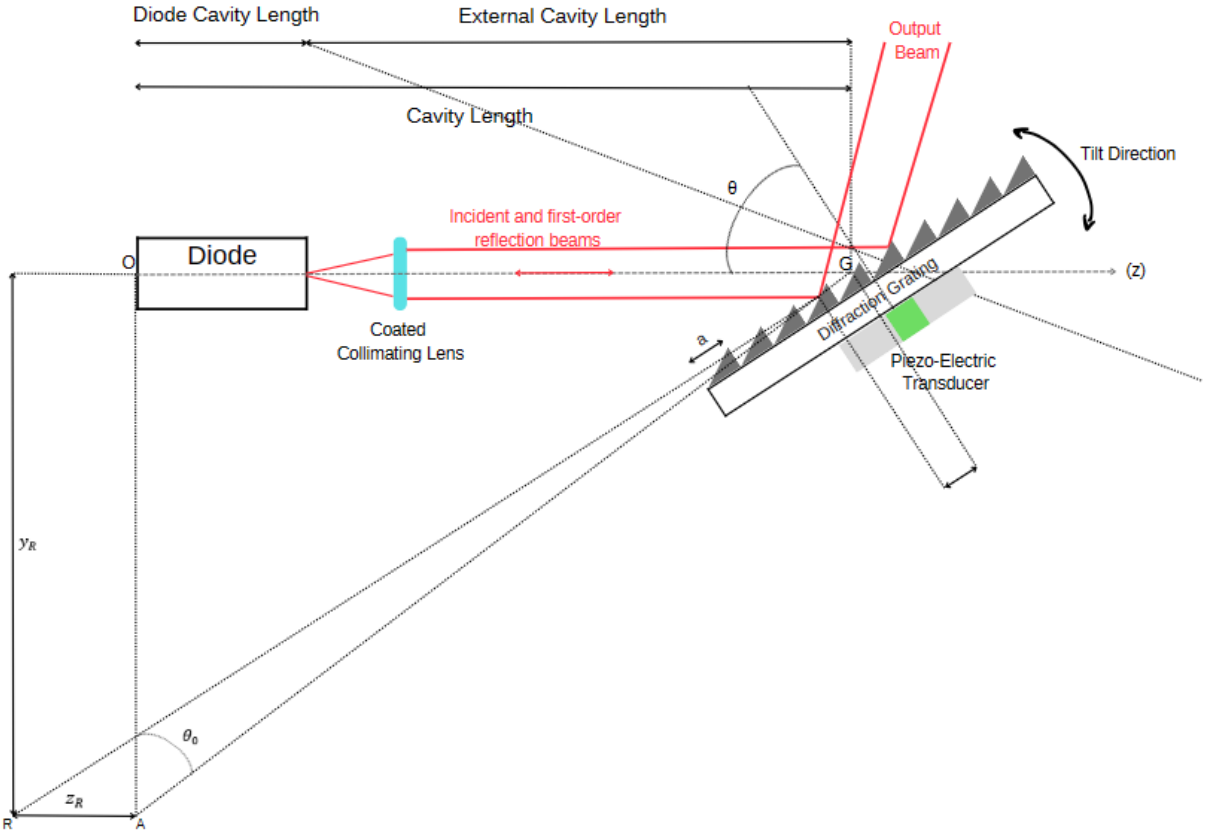

Source: Author, 2024.

In this setup, coarse tuning is achieved by tilting the grating, whereas fine adjustments require the translation of the grating along the z-axis. This fine adjustment

can be performed by using a Piezoelectric Transducer (PZT), indicated in green in the figure. Additionally, the output beam corresponds to the zeroth order diffraction. To prevent mode hops during tuning the laser with the grating, it's essential to tilt the grating around an axis that maintains the relationship between the grating center frequency and the cavity resonance frequency. To achieve this, we begin by determining the location of the pivot point that accomplishes this. For the grating wavelength, λ_r, we have:

$$\lambda_r = 2asin(\theta).$$

Equation 3.22

Where a is the groove spacing and θ the angle of incidence. Considering that the diode cavity is much smaller than the external cavity, the diode becomes part of a larger cavity of length given by L, the cavity resonances will occur whenever the following condition is satisfied:

$$L = m\frac{\lambda_m}{2}.$$

Equation 3.23

Here, we are disregarding the refractive index of the grating. "m" is an integer, and λ_m is the resonance wavelength of the grating. Adjusting the laser geometry so for an initial angle of incidence (θ_0) and a cavity length (L_0) these two wavelengths, λ_m and λ_r, are equal, ensuring the resonance cavity wavelength matches the grating wavelength.

$$\lambda_m(L_0) = \lambda_r(\theta_0).$$

Equation 3.24

We want to find the pivot point, that is, the point where the rotation axis of the grating is, which is at the coordinates y_R and z_R with respect to the origin. We need to find the pivot point that preserves the equality in *Equation 3.24* over the largest possible range of wavelengths.

The wavelength difference can be defined as:

$$\Lambda(\theta) = \lambda_m(\theta) - \lambda_r(\theta).$$

We will find the location of the pivot point where the second derivative of $\Lambda(\theta)$ with respect to θ is zero. Before we proceed, we must consider the translations of the grating due to the PZT. A translation of the grating by an amount of t_0 generates a phase shift, due to the decrease of the external cavity length. For a variation of length equal to the grating period, a, the phase shifts by -2π. Then, the round-trip phase change turns to:

$$\Delta\varphi_{RT} = \frac{4\pi L}{\lambda} - \frac{2\pi t_0}{a},$$

Equation 3.25

considering the condition for resonance, that the round-trip beam phase must be in phase with the initial beam, then the resonance wavelength is:

$$2\pi m = \frac{4\pi L}{\lambda_m} - \frac{2\pi t_0}{a},$$

$$m = \frac{2L}{\lambda_m} - \frac{t_0}{a},$$

$$\frac{2L}{\lambda_m} = m + \frac{t_0}{a} \rightarrow \lambda_m = \frac{2L}{m + \frac{t_0}{a}},$$

now, the wavelength resonance condition englobes the translations of the grating. Therefore, $\Lambda(\theta)$ becomes:

$$\Lambda(\theta) = \frac{2L(\theta)}{m + \frac{t_0(\theta)}{a}} - 2asin(\theta),$$

Equation 3.26

from *Equation 3.24*, and assuming that in the initial conditions the grating isn't translated, $t_0(\theta_0) = 0$, we have:

$$\frac{2L_0}{m} = 2asin(\theta_0),$$

then:

$$m = \frac{L_0}{asin(\theta_0)},$$

putting it into *Equation 3.26*:

$$\Lambda(\theta) = \frac{2L(\theta)}{\frac{L_0}{asin(\theta_0)} + \frac{t_0(\theta)}{a}} - 2asin(\theta),$$

finally:

$$\Lambda(\theta) = 2a\left[\frac{L(\theta)sin(\theta_0)}{L_0 + t_0(\theta)sin(\theta_0)} - sin(\theta)\right].$$

Equation 3.27

Using Figure 16 and some geometry, the cavity length can be expressed as[17]:

$$L(\theta) = -y_R\left(\frac{sin(\theta_0)}{cos(\theta)} - tan(\theta)\right) - z_R\left(\frac{cos(\theta_0)}{cos(\theta)} - 1\right) + \frac{cos(\theta_0)}{cos(\theta)}L_0,$$

Equation 3.28

Here we have $L(\theta)$ in terms of the initial values for angle and cavity length. Furthermore, the cavity length satisfies $\Lambda(\theta_0) = 0$. Therefore, by Figure 16, using geometry we can infer that:

$$tan(\theta_0) = \frac{L_0}{y_R},$$

then:

$$y_R = \frac{L_0}{tan(\theta_0)},$$

Equation 3.29

substituting in $L(\theta)$:

$$L(\theta) = -L_0\left(\frac{cos(\theta_0)}{cos(\theta)} - \frac{tan(\theta)}{tan(\theta_0)}\right) - z_R\left(\frac{cos(\theta_0)}{cos(\theta)} - 1\right) + \frac{cos(\theta_0)}{cos(\theta)}L_0,$$

$$L(\theta) = L_0\frac{tan(\theta)}{tan(\theta_0)} - z_R\left(\frac{cos(\theta_0)}{cos(\theta)} - 1\right),$$

then for the first derivative of $\Lambda(\theta)$ with respect to θ:

$$\frac{d\Lambda(\theta)}{d\theta} = 0 = \frac{\frac{dL(\theta)}{d\theta}sin(\theta_0)}{L_0 + t_0(\theta)sin(\theta_0)} - \frac{L(\theta)sin^2(\theta_0)\frac{dt_0(\theta)}{d\theta}}{\left(L_0 + t_0(\theta)sin(\theta_0)\right)^2} - cos(\theta),$$

the derivative vanishes when:

$$\frac{dt_0(\theta)}{d\theta} = \frac{L_0 - z_R}{cos(\theta)}.$$

To calculate the translation, let's assume that the translated lengths are small variations around the initial position. Then, we can expand $t_0(\theta)$ up to the first order:

$$t_0(\theta) = t_0(\theta_0) + \left.\frac{dt_0(\theta)}{d\theta}\right|_{\theta=\theta_0}(\theta - \theta_0),$$

as said before, $t_0(\theta_0) = 0$, then:

$$t_0(\theta) = \frac{L_0 - z_R}{cos(\theta_0)}(\theta - \theta_0).$$

Equation 3.30

To determine the z-coordinate of the pivot point, we evaluate the second derivative and make it equal to zero. Consequently, we find that $z_R = -L_0$. This implies that the pivot point is situated behind the rear facet of the diode by a distance of L_0. Optimal position of the pivot point in this manner ensures the broadest possible range of wavelengths where the resonance wavelength and grating wavelength remain equal.

The Littrow configuration offers advantages in terms of simplicity and efficiency, with lower losses compared to the Littman configuration. However, a notable drawback is the variation in the output beam angle during wavelength tuning. This challenge can be addressed by attaching a mirror parallel to the grating on the grating assembly, as illustrated in Figure 17. The inclusion of this mirror retains the angle of the output beam,

as now the grating mount is what we going to tilt, so the mirror gets adjusted equivalently. Consequently, during the tuning process, the output beam maintains its angle, although there is a limited parallel displacement determined by $\approx 2L_{GM}\Delta\theta$ for an angular change in the grating mount of $\Delta\theta$, where L_{GM} represents the distance between the grating and the mirror.

Figure 17: Littrow configuration with the addition of a mirror aligned with the grating. This arrangement eliminates angle changes with wavelength tuning.

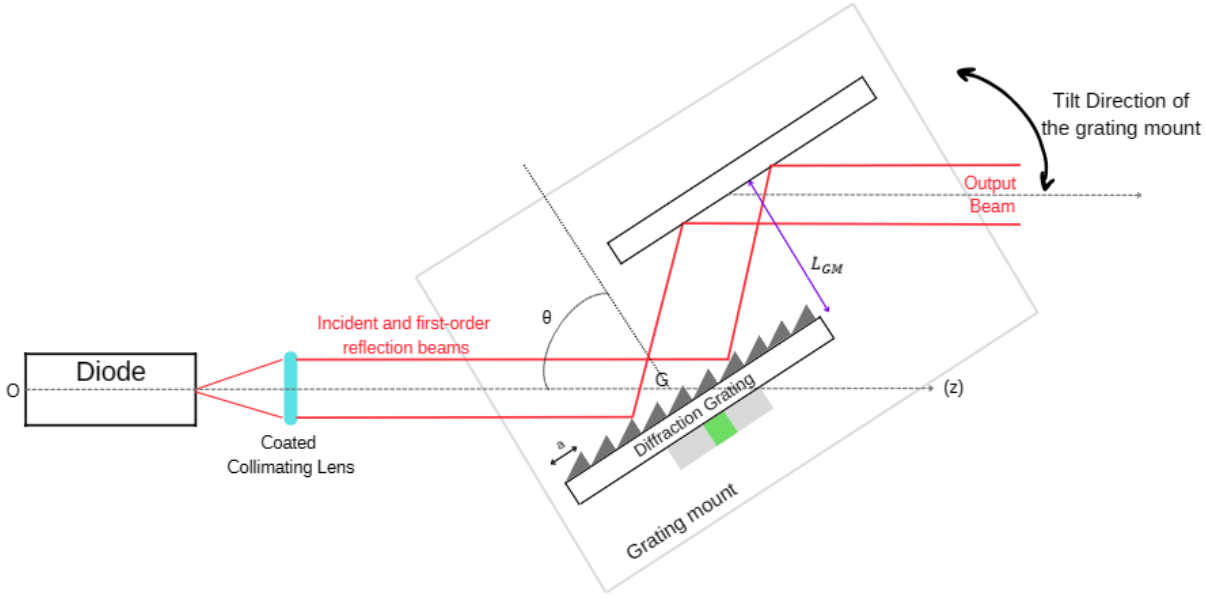

Source: Author, 2024.

Nevertheless, while the Littrow configuration is simpler than the Littman configuration, it suffers from poor cavity dispersion. In practice, achieving good mode stability often requires the use of additional elements such as prism beam expanders or wavelength-selective components like etalons[24]. This drawback is effectively addressed in the Littman mount without the need for supplementary elements. This improvement is achieved by employing a grazing incident angle of the grating along with a mirror to reflect the first-order diffraction.

3.2 THE LITTMAN CONFIGURATION

In the Littman configuration, coarse frequency tuning is accomplished by adjusting the grating at near grazing incidence, and a rotating mirror reflects the first-order diffracted beam back into the laser. The grazing incidence is used to illuminate the whole diffraction grating (Figure 18), which is crucial for a narrowband operation[22]. Like the Littrow configuration, the output beam is formed by the zeroth diffraction order,

and its orientation remains fixed. In this setup, tuning is achieved by rotating the mirror, leading to changes in the cavity length. The pivot point is strategically chosen to maintain a connection between the cavity modes and the grating frequency. In this configuration, the tracking in the Littman configuration is precise across the entire tuning range of the grating. Similarly to the Littrow case, we assume that the optical length of the diode matches its physical length.

In the Littman configuration, we adhere to the same conditions as in the Littrow configuration, aiming to match the grating wavelength with the cavity resonance wavelength. The Littman mount provides an alternative approach to satisfy these conditions. To avoid mode hops during the tuning process, it is crucial to design the geometry such that Equation 3.24 is satisfied. Figure 18 illustrates the geometry required to meet the wavelength condition.

Figure 18: Littman configuration for accomplishing self-tracking. PZT now is placed behind the mirror instead of the grating and the grating is placed with a grazing incidence angle, $\theta_0 \approx 90°$.

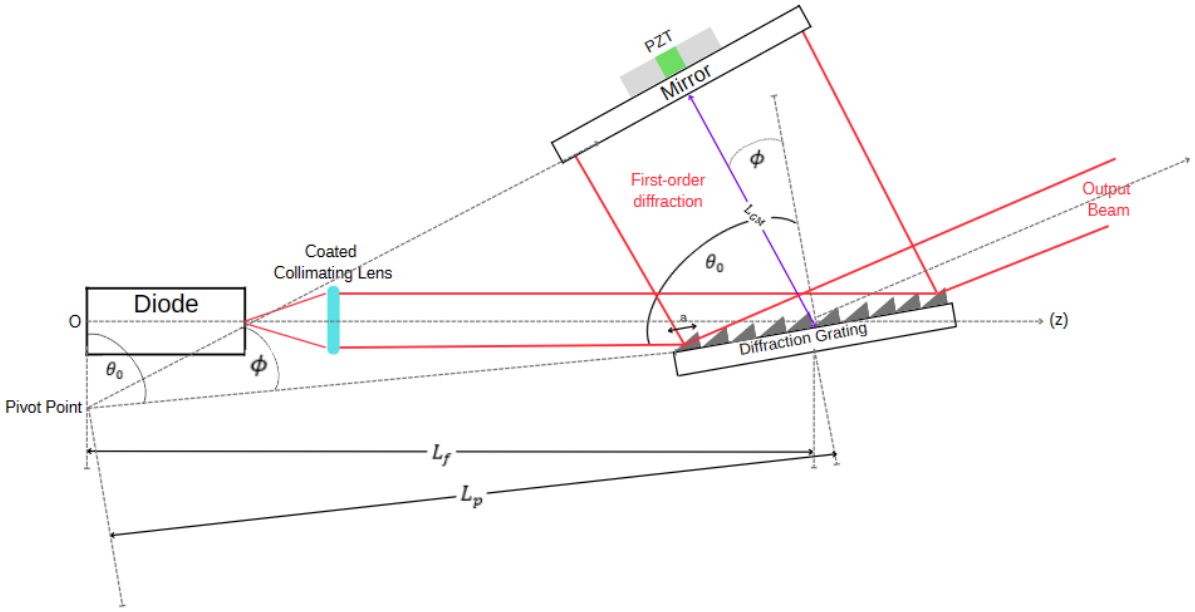

Source: Author, 2024.

Figure 18 highlights significant distinctions between the Littrow and Littman approaches. In the Littman approach, an additional element is introduced into the cavity — a mirror responsible for reflecting the first-order diffraction. This mirror is crucial for utilizing the first-order diffraction as feedback. In contrast, the Littrow approach concludes at the grating, where the inclusion of a mirror is primarily to maintain the output angle without directly influencing the laser tuning process.

In the Littman configuration, the mirrors play a pivotal role in the tuning process. The cavity extends beyond the grating, ending at the mirror. Consequently, the placement of the PZT, which facilitates changes in cavity length, is positioned behind the last cavity component, i.e., behind the mirror. Additionally, as the grating angle is fixed, the analysis stands by other angle, the mirror angulation with respect to the grating normal. The cavity modes, or resonances, follow *Equation 3.31*:

$$L(\phi) = m\frac{\lambda_m}{2} = L_f + L_{GM}(\phi).$$

Equation 3.31

This condition remains consistent with the previous analysis, with the only modification being the inclusion of an additional path in the cavity length, represented by the distance between the grating and the mirror, $L_{GM}(\phi)$. The variables m and ϕ represent the cavity axial order (cavity resonances) and the angle between the mirror and grating normal, respectively.

For the grating wavelength, the standard grating master relationship is utilized, considering the angles of incidence and reflection of the grating. The incoming beam has an angle of incidence θ_0 and reflects to the mirror at an angle ϕ. The condition is expressed as:

$$\lambda_r = \frac{a}{p}\big(sin(\theta_0) + sin(\phi)\big),$$

Equation 3.32

where a is the grating period, p is an integer representing the propagation-mode of interest called the diffraction order. We are using p to avoid confusion with the cavity axial order, m. Moreover, the wavelength difference of the Littman configuration is:

$$\Lambda_{Littman}(\phi) = \lambda_m(\phi) - \lambda_r(\phi),$$

Equation 3.33

we have then:

$$\Lambda_{Littman}(\phi) = \frac{2L(\phi)}{m} - \frac{a}{p}\big(sin(\theta_0) + sin(\phi)\big),$$

note that with some geometry we can express $L(\phi)$ as:

$$L(\phi) = L_f + L_p sin(\phi),$$

therefore:

$$\Lambda_{Littman}(\phi) = \frac{2\left(L_f + L_p sin(\phi)\right)}{m} - \frac{a}{p}\left(sin(\theta_0) + sin(\phi)\right).$$

The wavelength, as in Littrow configuration must be equal to match the modes of the cavity and the grating. Then:

$$\Lambda_{Littman}(\phi) = 0 = \frac{2\left(L_f + L_p sin(\phi)\right)}{m} - \frac{a}{p}\left(sin(\theta_0) + sin(\phi)\right),$$

$$\frac{2L_f}{m} + \frac{2L_p sin(\phi)}{m} = \frac{a}{p} sin(\theta_0) + \frac{a}{p} sin(\phi),$$

by orthogonality, we must have, for the tracking to occur:

$$\frac{2L_f}{m} = \frac{a}{p} sin(\theta_0).$$

Equation 3.34

$$\frac{2L_p}{m} = \frac{a}{p}.$$

Equation 3.35

Dividing one equation by the other:

$$\frac{L_f}{L_p} = sin(\theta_0).$$

The location of the pivot point is consistent with Figure 18. As implied by the figure, the pivot point is situated at the intersection of the mirror and grating planes. Additionally, we can deduce that the pivot point is directly below the rear facet of the diode, i.e., at $z_R = 0$, and according to Figure 18, $y_R = L_p cos(\theta_0)$. Thus, this configuration provides the necessary pivot point to construct a Littman-Metcalf type ECDL, offering a narrower lasing linewidth and improved wavelength selectivity compared to the Littrow type[21].

The bandwidth of the Littman-Metcalf configuration (Full Width at Half Maximum) has a minimum value when the active medium and the grating are spaced by the Rayleigh length, which is a parameter that describes the distance over which

the cross-sectional area of a focused laser beam remains relatively small, that is, the distance that the beam doesn't diverge. Where this parameter is given by:

$$L_R = \frac{\pi w^2}{\lambda},$$

Equation 3.36

in that case, the linewidth for the Littman configuration is expressed as:

$$\frac{(\Delta\lambda)_{linewidth}^{Littman}}{\lambda} = \frac{2\sqrt{2}\lambda}{\pi l\big(sin(\theta_0) + sin(\phi)\big)},$$

as we're using a grazing incidence angle ($\theta_0 \approx \pi/2$), we can approximate the last equation to:

$$\left(\frac{\Delta\lambda}{\lambda}\right)_{Linewidth}^{Littman} = \frac{2\sqrt{2}\lambda}{\pi l\big(1 + sin(\phi)\big)}.$$

Equation 3.37

In this equation, l represents the illuminated width of the grating. A larger illuminated portion of the grating corresponds to a smaller linewidth for the laser. This is the most significant achievement of the Littman configuration, as it enables a narrow linewidth without the need for additional high-quality intracavity optical elements[24], such as beam expander[23], which are required in a conventional Hänsch dye laser[22][23].

3.3 THE DOUBLE-GRATING CONFIGURATION

Now, let's investigate a more advanced configuration based on the Littman-Metcalf design. Initially theorized by Littman[22] and experimentally tested by Oppenheim and Shoshan[23], this modification replaces the mirror in the Littman-Metcalf configuration with another grating. This enhancement brings notable improvements to mode stability and provides a broader, continuous tuning range for the laser system. Moreover, this refined design ensures reliable operation in a single longitudinal cavity mode. Additionally, this configuration offers enhanced conversion efficiency when operated in multimode[22].

The crucial distinction in this configuration lies in the use of a Littrow grating instead of the tuning mirror. A Littrow grating is a standard grating positioned at an

angle such that the first-order diffraction reflects and overlaps with the incident beam, known as the Littrow condition or Littrow angle. There are two potential scenarios for the second grating to meet the Littrow condition, as illustrated by solid and dashed lines in Figure 19. Improved operation requires the dispersion of the grazing-incidence grating and the dispersion of the Littrow grating to combine. This condition is satisfied only in one of the two possible orientations of the Littrow grating, represented by the solid lines in Figure 19. However, the dashed configuration offers a reduction in net dispersion due to the dispersions of the gratings having opposite signs.

Figure 19: Double-grating configuration for an ECDL. The laser beam has a grazing Incident angle. The period spacing of each grating is a for the incident grating and b for the Littrow grating. The tuning is done by rotating the Littrow grating.

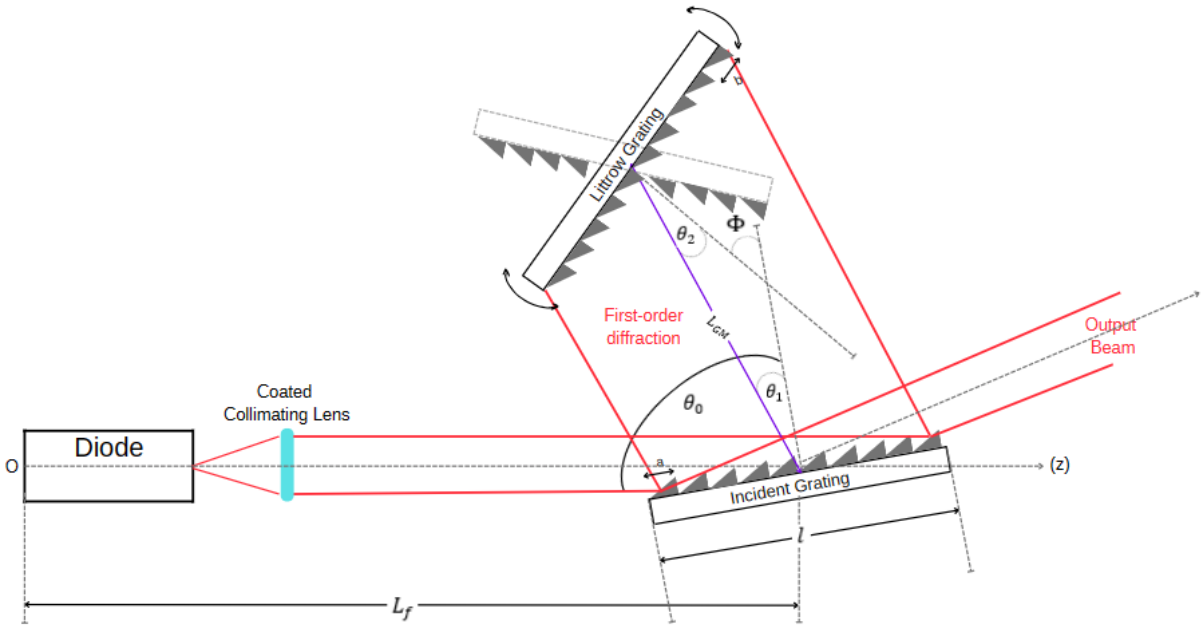

Source: Author, 2024.

To find the tunning curve of the double-grating case, we will use the basic equations for the diffraction on both gratings:

$$m\lambda = a(\sin(\theta_0) + sin(\theta_1)),$$

Equation 3.38

$$m'\lambda = 2bsin(\theta_2).$$

Equation 3.39

Equation 3.38 gives the condition for the incident grating, and *Equation 3.39* for the Littrow grating. Here, θ_0 is the angle of incidence, θ_1 is the angle of the diffracted ray and θ_2 is the Littrow angle. From now on, we're assuming that the Littrow grating

is in fact at the Littrow angle. Note that we can extract from Figure 19 that $\theta_1 + \theta_2 = \Phi$, where Φ is the angle between the gratings normals. Then, we can eliminate θ_2 from *Equation 3.39* and substitute the result in Equation 3.38, we can eliminate θ_1 as well. Therefore, by solving the system we get a quadratic equation in λ which has as solution two possibilities:

$$\lambda_+ = \frac{\big(4\alpha + 2\beta cos(\Phi)\big)\sin(\theta_0) + 2sin(\Phi)\sqrt{\beta^2 cos^2(\theta_0) + 4\alpha\big(\alpha + \beta cos(\Phi)\big)}}{4\alpha^2 + \beta^2 + 4\alpha\beta cos(\Phi)},$$

$$\lambda_- = \frac{\big(4\alpha + 2\beta cos(\Phi)\big)\sin(\theta_0) - 2sin(\Phi)\sqrt{\beta^2 cos^2(\theta_0) + 4\alpha\big(\alpha + \beta cos(\Phi)\big)}}{4\alpha^2 + \beta^2 + 4\alpha\beta cos(\Phi)}.$$

However, only the λ_+ solution returns to *Equation 3.32* in the case that $m' = 0$, that is, if the Littrow grating was acting as a mirror (using its zero-order diffraction). Here, $\alpha = m/a$ and $\beta = m'/b$. Then our tunning curve is given by:

$$\lambda = \frac{\big(4\alpha + 2\beta cos(\Phi)\big)\sin(\theta_0) + 2sin(\Phi)\sqrt{\beta^2 cos^2(\theta_0) + 4\alpha\big(\alpha + \beta cos(\Phi)\big)}}{4\alpha^2 + \beta^2 + 4\alpha\beta cos(\Phi)},$$

to simplify our calculations, let us consider the case that the diffraction orders and the period of the grooves of both gratings are equal, $m = m'$ and $a = b$, respectively. Also, for the grazing incidence angle case, $\theta_0 \approx \pi/2$, then:

$$\lambda = \frac{\big(4\alpha + 2\alpha cos(\Phi)\big) + 2sin(\Phi)\sqrt{4\alpha\big(\alpha + \alpha cos(\Phi)\big)}}{4\alpha^2 + \alpha^2 + 4\alpha\alpha cos(\Phi)},$$

$$\lambda = \frac{2\alpha\big(2 + 1cos(\Phi)\big) + 2sin(\Phi)\sqrt{4\alpha^2\big(1 + cos(\Phi)\big)}}{5\alpha^2 + 4\alpha^2 cos(\Phi)},$$

$$\lambda = \frac{2\alpha\big(2 + 1cos(\Phi)\big) + 4\alpha sin(\Phi)\sqrt{\big(1 + cos(\Phi)\big)}}{\alpha^2\big(5 + 4cos(\Phi)\big)},$$

$$\lambda = \frac{4 + 2cos(\Phi) + 4sin(\Phi)\sqrt{\big(1 + cos(\Phi)\big)}}{\alpha\big(5 + 4cos(\Phi)\big)},$$

finally:

$$\lambda_{DG} = \frac{a}{m}\left[\frac{4 + 2cos(\Phi) + 4sin(\Phi)\sqrt{\left(1 + cos(\Phi)\right)}}{\left(5 + 4cos(\Phi)\right)}\right].$$

Equation 3.40

Where in λ_{DG}, DG stands for Double Grating. For a grazing incident grating, the single-grating configuration yields the tuning curve:

$$\lambda_{SG} = \frac{a}{m}[1 + sin(\Phi)].$$

Where in λ_{SG} stands for Single Grating. Plotting both curves, double and single grating, we have: (10^{-6})

Figure 20: Tuning curve for single and double grating laser using 2400 lines/mm gratings. The blue curve corresponds to double-grating design and the golden curve, the single-grating design. Plot has been done in the domain of $-\frac{\pi}{2} \leq \Phi \leq \pi$.

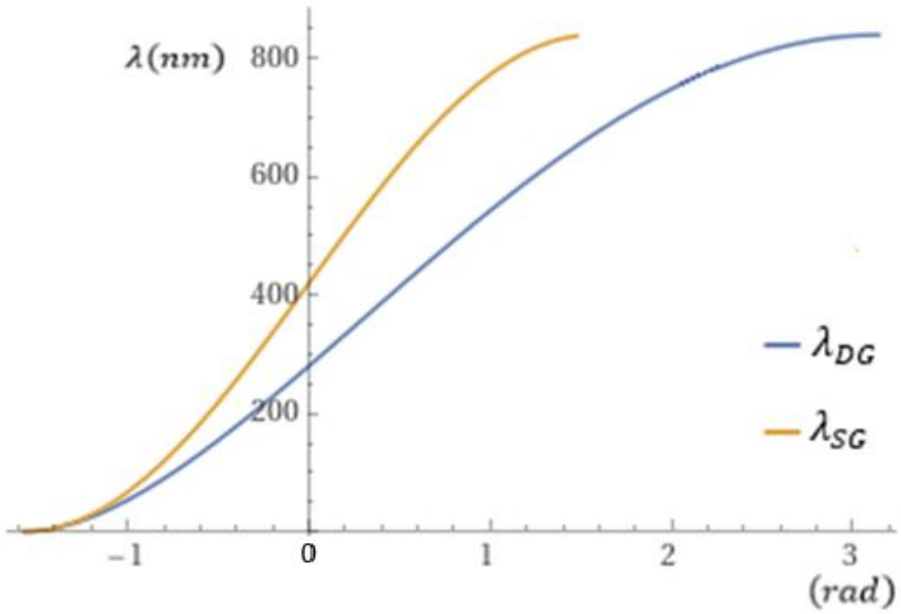

Source: Author, 2024.

In both tuning curves, the original single-grating design and the double-grating design are shown for the case of 2400 lines/mm gratings used in first order. From this figure, we can infer that the double-grating configuration has the advantages of a less-steep turning curve and a broad, nearly linear region. An expression for the single-pass linewidth (bandwidth) of the double-grating laser can be obtained from *Equations 3.38* and *3.39*. For the case when $a = b$ and $m = m'$, we have:

$$m\lambda = a(\sin(\theta_0) + sin(\theta_1)),$$

$$m\lambda = 2asin(\theta_2),$$

using the equation for the bandwidth[25]:

$$\Delta\lambda = \sqrt{\left(\Delta\lambda_{input\ angle}\right)^2 + \left(\Delta\lambda_{exit\ angle}\right)^2},$$

the input angle is given by θ_0 and exit angle is given by θ_2:

$$\Delta\lambda = \sqrt{\left(\frac{\partial\lambda}{\partial\theta_0}\Delta\theta_{input}\right)^2 + \left(\frac{\partial\lambda}{\partial\theta_0}\Delta\theta_{exit}\right)^2},$$

where $\Delta\theta_{input}$ and $\Delta\theta_{exit}$ are the beam spread during the travel from the first grating to the second. It is possible to show that[22]:

$$\left(\frac{\Delta\lambda}{\lambda}\right)_{Linewidth}^{Double-grating} = \frac{4\sqrt{2}}{\pi l}\left[\frac{2\alpha + \beta cos(\Phi) - \frac{\beta^2 sin(\Phi)sin(\theta_0)}{\sqrt{\beta^2 cos^2(\theta_0) + 4\alpha\left(\alpha + \beta cos(\Phi)\right)}}}{\beta^2 + 4\alpha^2 + 4\alpha\beta cos(\Phi)}\right].$$

Equation 3.41

Equation 3.41 is valid in the limit that the distance between the active medium and the grazing-incidence grating is equal to the Rayleigh length. In the special case when $m = m'$, $a = b$, and $\theta_0 \approx \pi/2$, the equation simplifies to:

$$\left(\frac{\Delta\lambda}{\lambda}\right)_{Linewidth}^{Double-grating} = \frac{4a\sqrt{2}}{m\pi l}\left[\frac{2 + cos(\Phi) - \frac{sin(\Phi)}{2\sqrt{\left(1 + cos(\Phi)\right)}}}{5 + 4cos(\Phi)}\right].$$

Equation 3.42

Having the expression for the linewidth in both cases, single and double grating, in hand, we can compare them in a graph of $\Delta\lambda/\lambda$ versus the rotation angle.

Figure 21: Graph of $\Delta\lambda/\lambda$ versus rotation angle, Φ, for single and double-grating laser using $l = 4$ cm wide 2400-lines/mm gratings. Blue curve corresponds to double-grating design, and the golden curve represents the single-grating laser, $m' = 0$.

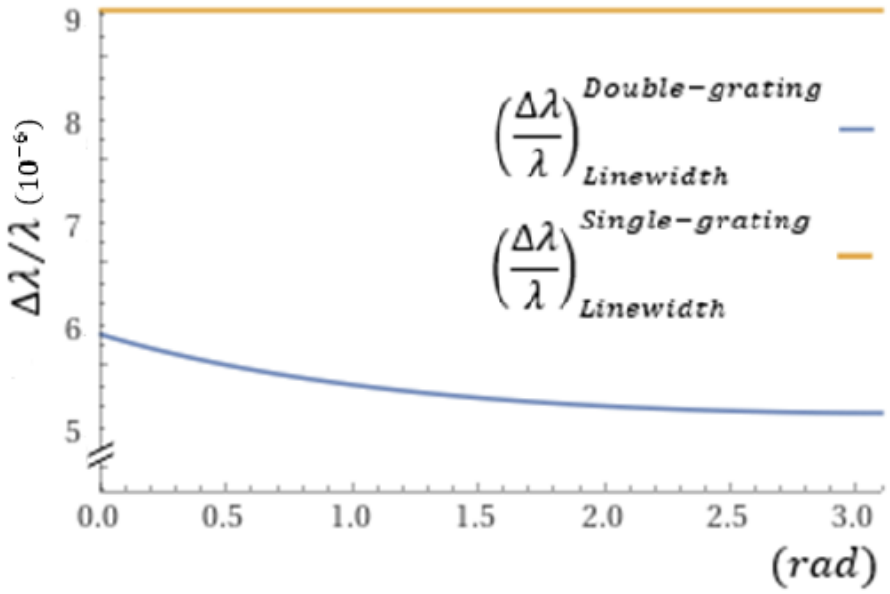

Source: Author, 2024.

We note that the double-grating arrangement provides a single-pass linewidth that can be almost twice as narrower than that of the single-grating design. Other way to interpret this result is that for operation with a given linewidth, the new design requires a smaller value of θ_0. By decreasing θ_0 we can effectively decrease the illuminated length of the incident grating, l, which results in an increased spectral width. This last point is significant regarding conversion efficiency for multimode operation, since the off-Littrow grating losses increase dramatically as θ_0 approaches $\pi/2$.

For single-mode operation of the double-grating laser, several parameters must be carefully determined. First, it is necessary to shrink the cavity length (diode till incident grating) as much as possible so that the free spectral range (FSR) between adjacent cavity modes is large. A consequence of reducing the spacing between the output mirror and the diode is increased background fluorescence.

4 RESULTS AND DISCUSSION

In this chapter, I will present the construction of an External Cavity Diode Laser (ECDL) and the characterization of a Fabry-Perot Cavity using a commercial diode laser.

4.1 ECDL

As an ECDL is sensible as to current and temperature, its construction must have strict control over them. For that, it was done by two controllers from Thorlabs, the LDC240C for current and the TED200C for temperature. To accomplish the construction it was used, a tunable diode laser (M9-A64-0200), an adjustable collimation tube (LTN330-C), a 12.7mm squared diffraction grating (GR13-1210), a PZT (PA3JEW), two 12.7mm mirrors (BB05-E03), two mirror mounts, a temperature sensor (AD592ANZ To-92), a 10 $k\Omega$ thermistor, a Peltier tablet (TEC1-12706). Besides these components, there were some homemade pieces, such as the copper case for the diode, the aluminum platforms, two 1D translators, and the acrylic box where the system was mounted.

The construction started with an 8mm thick acrylic box without the bottom and was replaced by a 19mm thick aluminum plate to serve as the thermal reservoir for temperature stabilization. See figure 22.

Figure 22: acrylic box and thermal reservoir. The acrylic box is made with 8 mm thick acrylic with dimensions of 131mm by 131 mm and 80 mm in height, all external measures. The thermal reservoir is made of a high-density aluminum block with dimensions of 115 mm by 115mm and 19 mm in height. The box is made of independent acrylic plates, which are put together by M3 millimetric screws, and the box is also fixed to the aluminum block by these screws.

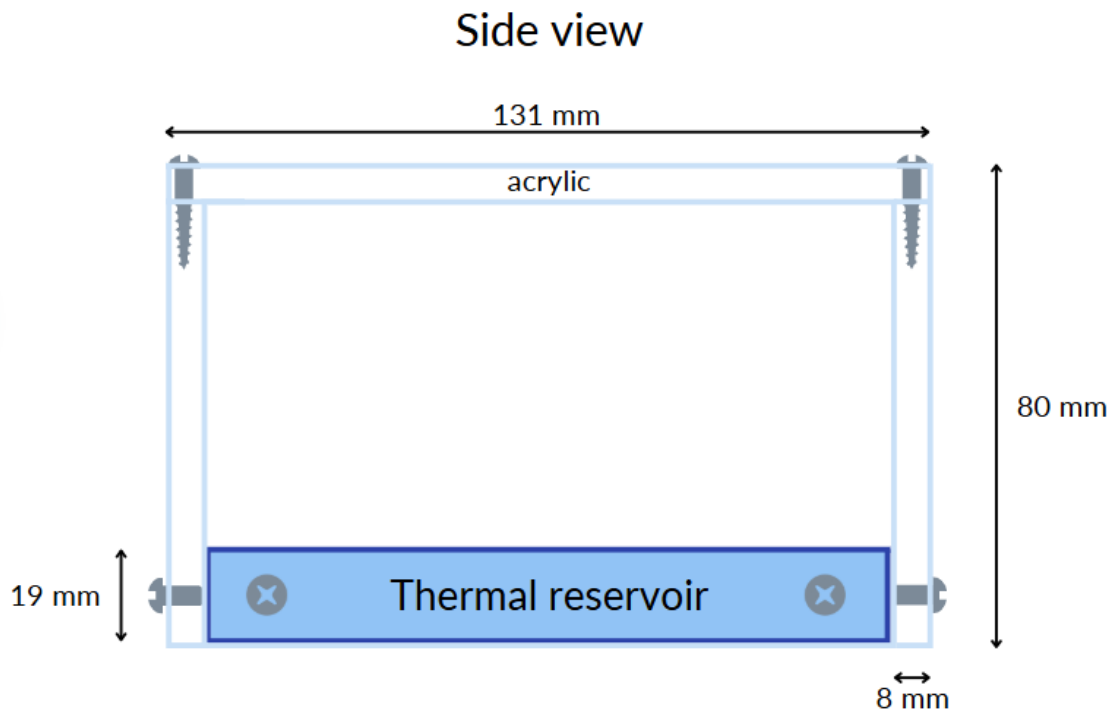

Source: Author, 2025.

After that, the Peltier should be put on the thermalization platform with the cooling side up, which can be found by simply giving tension and checking which side heats or cools. Above the Peltier, we put the copper structure that will hold the diode, the thermistor, and the temperature sensor. Let's define this structure as the diode thermalization housing (DTH). As the DTH should stabilize the diode temperature, copper was chosen over aluminum because of its better heat conductivity. Furthermore, stabilization would work more efficiently as the diode thermalization housing weighs less, then instead of a block of copper, it had as many extremities removed as possible. In doing so, the volume is reduced by 5.6%. The scheme of the diode thermalization housing is in figure 23.

Figure 23: Scheme with the structure of the thermalization housing and its dimensions with front, back and up views. The four M4 screw holes are designed to securely fasten the structure to the aluminum block, ensuring precise horizontal and vertical alignment. The two holes in the upper side of the case are used to fasten tightly the collimation tube to the structure.

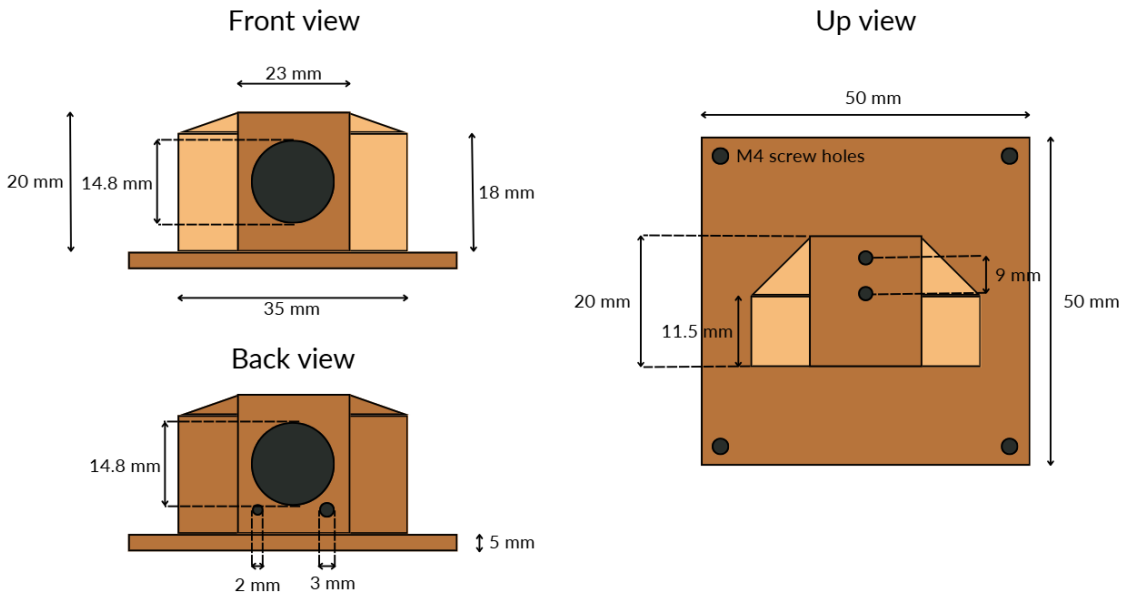

Source: Author, 2025.

The DTH, is placed above the Peltier and it is placed on an aluminum block, which is placed over the thermal reservoir, as shown in the next figure.

Figure 24: side view of the DTH, Peltier and Fixating aluminum block put together and fastened to the thermal reservoir.

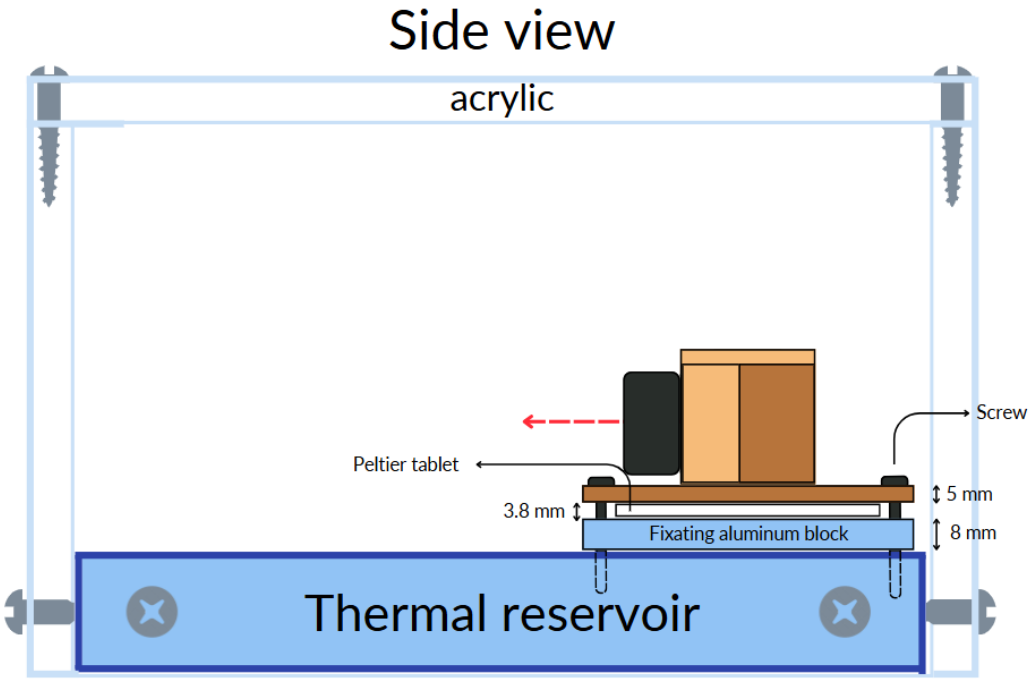

Source: Author, 2025.

With the DTH placed as shown in figure 24, the temperature control must be tested. The temperature sensor and the thermistor are placed inside the DTH and have their terminals soldered to the Db9 female connector through wires as indicated by the temperature controller manual. Using the controller, the first thing to do is adjust the controller's PID so the actual temperature oscillates around the set temperature no more than twice. The whole process of thermalization, after PID adjustment, took around 2 minutes. After the temperature control, the laser current control must be set as well. After that, we soldered the terminals of the diode and the LED to the Db9 male connector as the current controller indicates in its manual. Next, a small current is given to the diode, and a NIR card is used to check if the diode is operating correctly. Then, the PID of the temperature controller should be re-adjusted because there is a temperature rise, as the diode operates.

The laser's collimation must be adjusted as well. Then, the next step is to plot the curve of power versus current before the introduction of the grating. The results are in the figure below.

Figure 25: Power x current graph for the ECDL without introducing the grating (blue solid line). The threshold current found by plotting the data with a Python code was 22.50 mA. The maximum current applied to the laser was 325 mA, which gave a power of 266 mW.

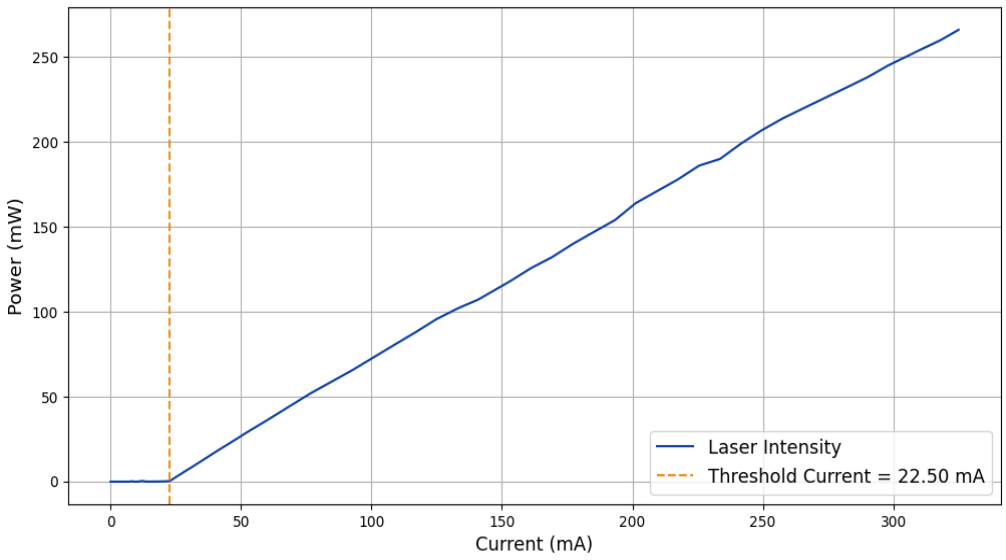

Source: Author, 2025.

This first characterization revealed some differences between some of the measured parameters and the corresponding values in the datasheet. From datasheet information, the typical threshold current should be around 50 mA, a minimum threshold value was not informed. However, the measured value was 22.5 mA,

considerably smaller. Also, although the maximum current is 350 mA, to avoid damaging the laser, the maximum current was set in 325 mA. At this value, the maximum power measured was 266 mW, exceeding the expected maximum power of 200 mW, from the datasheet.

The laser's spectrum should be the second parameter to be measured before the grating introduction. A spectrometer (HR4000) from Ocean Optics, with an optical resolution of 0.03nm, was used. By using a Python code, the central spectrum wavelength was found by simply determining the wavelength that corresponds to the maximum spectrum intensity. Moreover, the laser presented additional peaks in the spectrum for current values near the current threshold, 30.3 mA, and near the maximum current, 300.8 mA. The additional peaks were not static, they appeared and disappeared constantly. For current values around 150.2 mA, the spectrum did not show additional peaks and had a smaller laser linewidth. For current values greater than 230 mA, secondary and tertiary peaks started to appear again. The spectrum for each current value is plotted in the figure below.

Figure 26: Laser's spectrum (blue solid line) throughout four values of applied current. For each graph, there are colored dashed lines indicating the central peak wavelength. The spectrum for 30.3 and 300.8 mA presented peaks for multiple wavelengths, indicating that at these currents the laser emitted laser beams with more than one principal wavelength value. The peaks are organized from left to right. These spectra are for the laser at 20.04ºC.

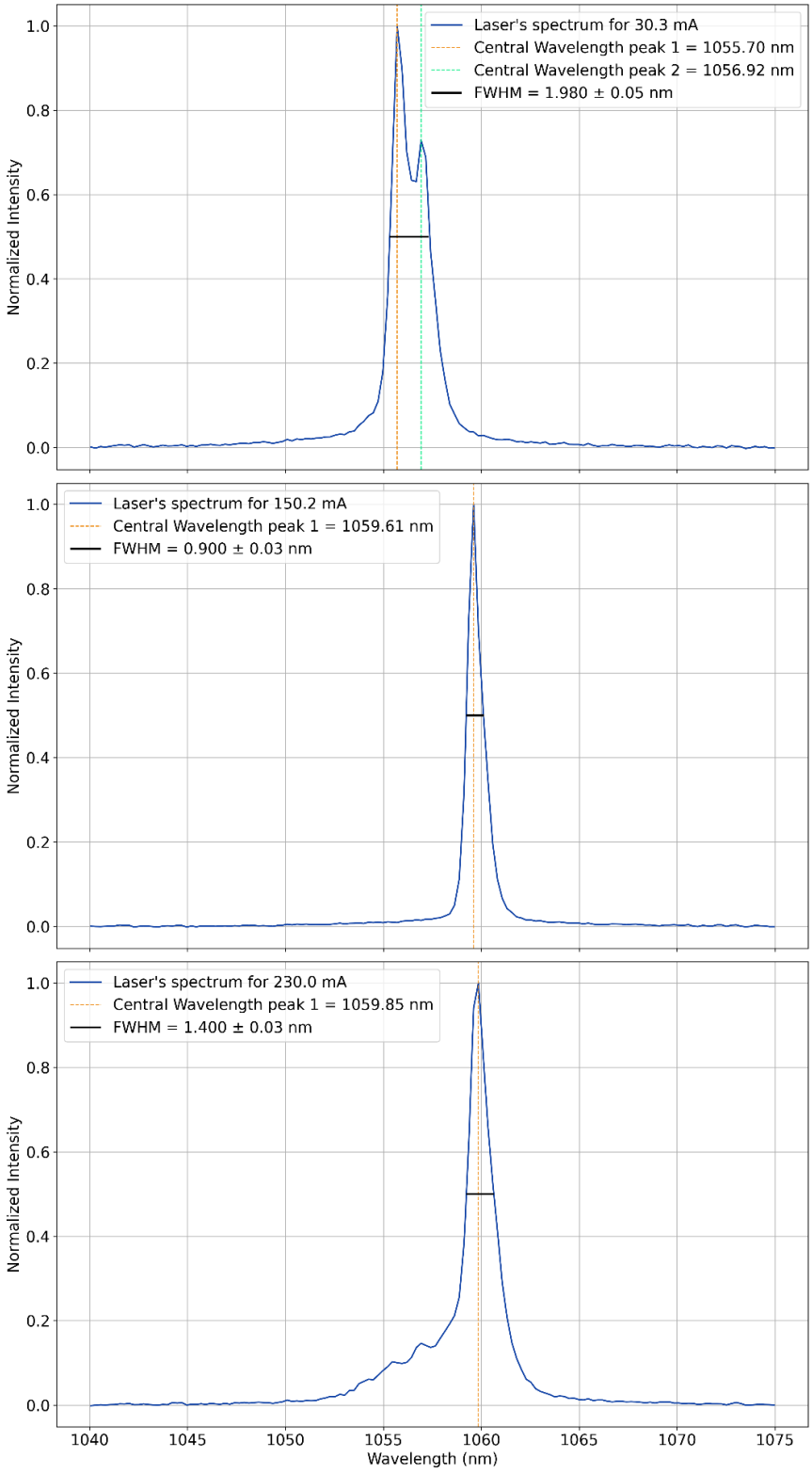

Source: Author, 2025.

The Laser linewidth was only calculated for the first three graphs, due to the last spectrum having more than one distinct peak. The error values are the standard error of the mean. The laser presented a big variation in its linewidth with the current change. From the datasheet, the laser has a spectral bandwidth of 0.5 nm to 2 nm, and the FWHM for the first three spectrum are inside this range.

Progressing with the ECDL construction, we will add the grating. The grating coupling type chosen was the Littman-Metcalf configuration due to its theoretically better wavelength selectivity and smaller linewidth. The scheme used is given in Figure 27.

Figure 27: Littman-Metcalf ECDL configuration scheme. The laser output is represented by the solid red arrow, the external cavity is composed of Path 1, Path 2 and the length the laser travels inside the collimation tube till the diode. The grating is placed with its normal vector pointing 74º to the incident laser path. The laser beam leaves the grating at a tilted angle, that is corrected by the second mirror.

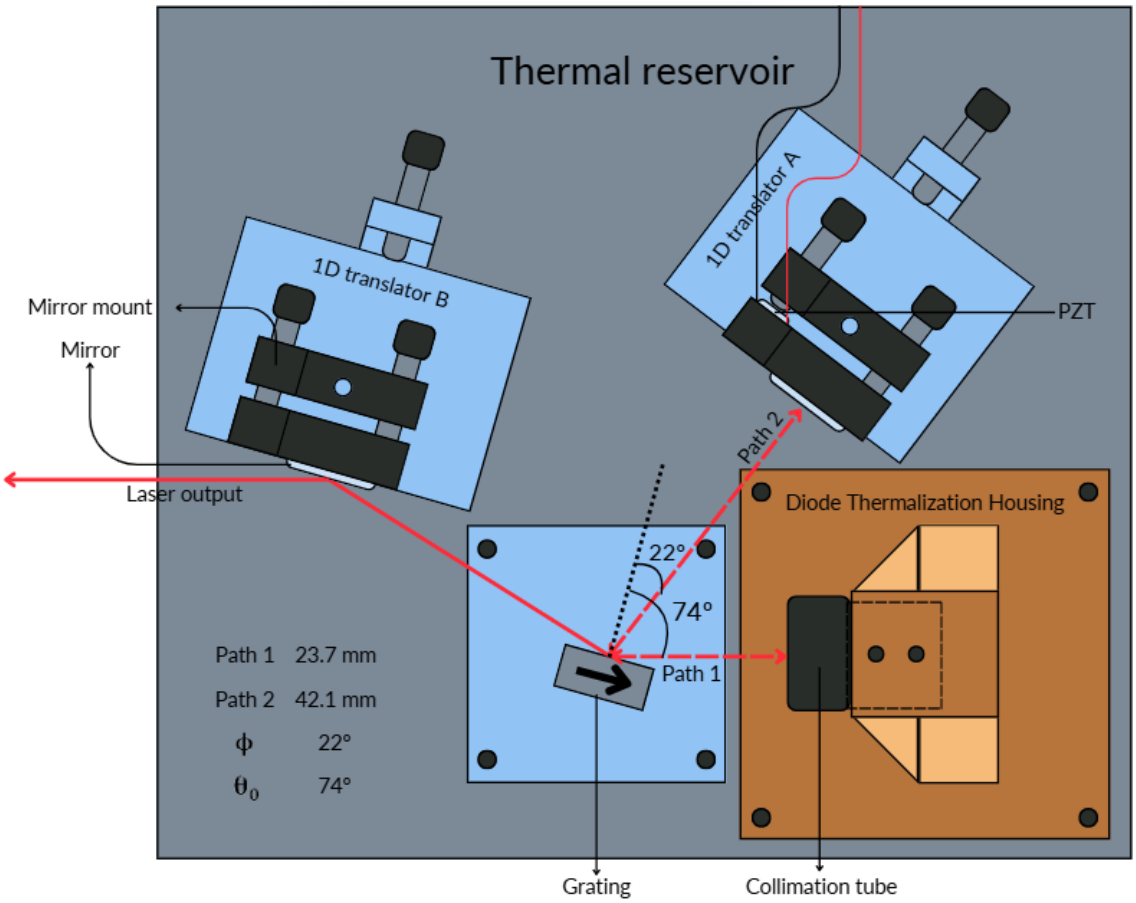

Source: Author, 2025.

The beam leaves the collimation tube with an elliptical shape with a waist of 1 mm horizontally and 0.5 mm vertically. From *Equation 3.36* the Rayleigh length, that

is, the distance between the grating and diode that gives the smaller linewidth of the Littman configuration, is $L_R \approx 3$ mm. The distance between the grating and diode is about 32.7 mm. The actual distance is approximately 10.9 times the Rayleigh length. This was the smallest distance possible considering that the laser's beam should not be partially blocked in Path 2.

With the setup mounted, the first data to be acquired is the power versus current curve, to verify if the laser is functioning properly.

Figure 28: Power x current graph for the ECDL with introducing the grating (blue solid line) at 74º to the laser incident axis. The threshold current found by plotting the data with a Python code was 17.50 mA. The maximum current applied to the laser was 325 mA, which gave a power of 157 mW.

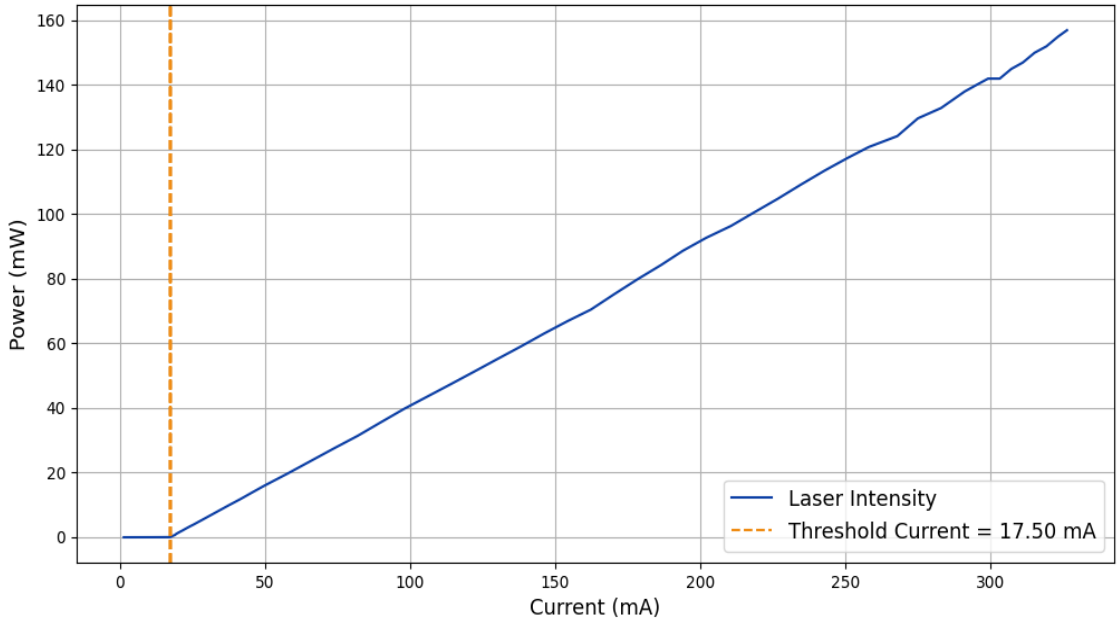

Source: Author, 2025.

From figures 25 and 28, there are differences between the curves with and without grating, the first one to analyze is the laser's power. After grating, the laser power was reduced to 54.04% of the value without the grating, as seen in Figure 29.

Figure 29: Comparison of the output power of the laser with grating (ochre solid line) and the laser without grating (blue solid line) and its respective threshold current.

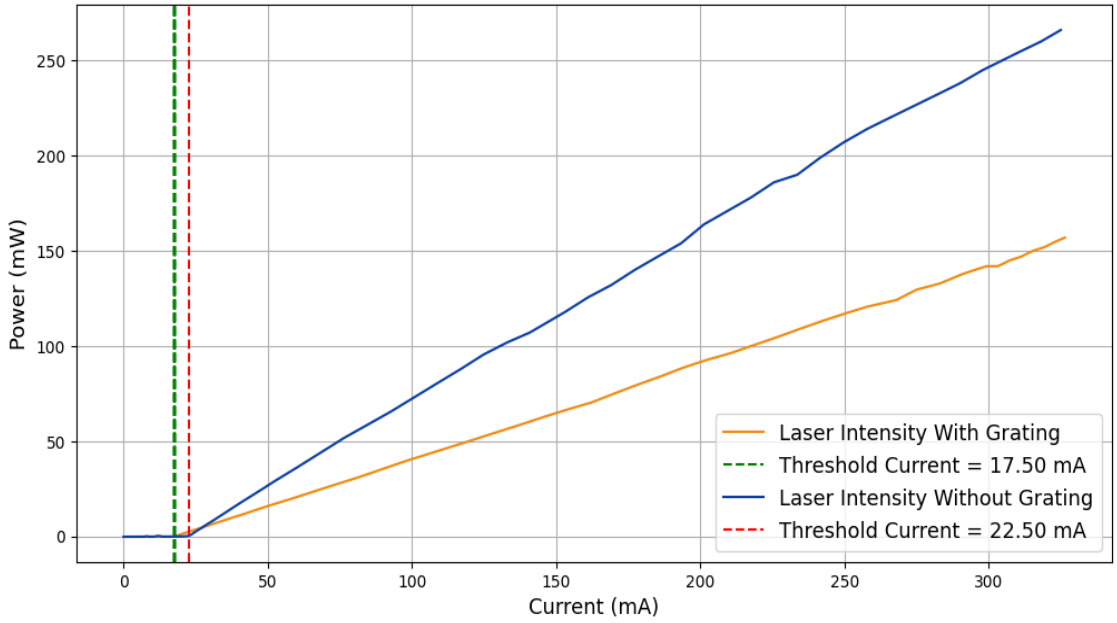

Source: Author, 2025.

Another of the changes induced by the grating presence is the threshold current modification for a smaller value. It was measured to be a reduction of 5 mA in the threshold current, as seen in Figure 30.

Figure 30: Reduction of the laser's threshold current from 22.50 mA (red dashed line) for the laser without grating (blue solid line) to 17.50 mA (green dashed line) for the laser with grating (ochre solid line).

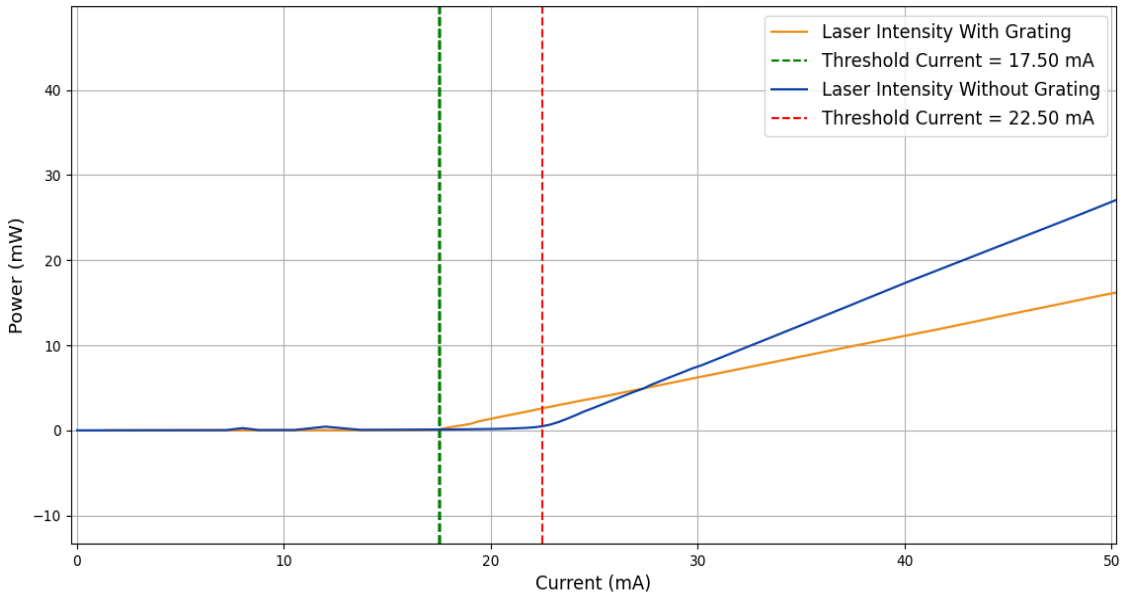

Source: Author, 2025.

The last parameter to compare was the laser linewidth. The data was collected for 3 currents for the spectrum: 24.8 mA (above threshold), 150.2 mA, and 300.8 mA (below maximum current). The system was kept at the same temperature, 20.04ºC. With the grating, the central wavelength stayed at 1057.17 nm.

From *Equation 3.37* we can estimate the linewidth of the Littman configuration. The l parameter in *Equation 3.37* is the illuminated length of the grating, with an angle of 74º. The grating had its horizontal axis fully illuminated by the incoming laser beam. The angle between the first diffraction order and the grating normal vector was 22º. Then the predicted Littman linewidth would be 0.0059 nm, which the spectrometer does not have resolution to measure.

The best configuration we got was with the spectrometer data. Making an average over the data spectrum for 150.2 mA, the linewidth with grating found was 1.03 ± 0.03 nm, where the error is the standard error of the mean. This value is approximately 14% greater than the value without grating.

Figure 31: FWHM of the ECDL with grating at 20.04ºC and applied current of 150.2 mA.

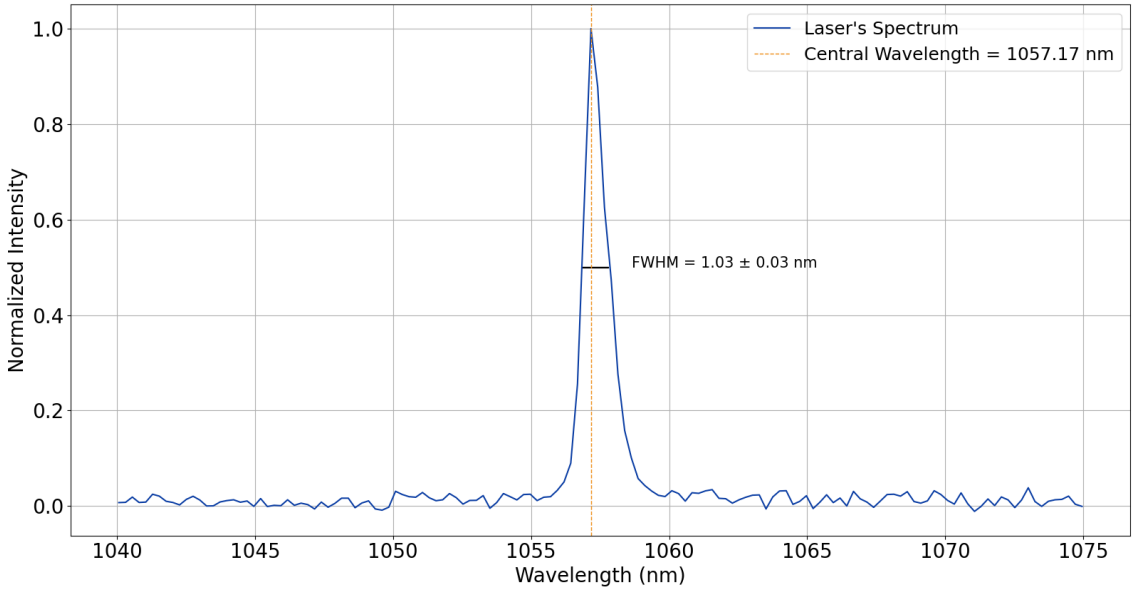

Source: Author, 2025.

This value in frequency can be found through the equation $\Delta\nu_{FWHM} = (c/\lambda_0^2)\Delta\lambda_{FWHM}$, that yields to a frequency of 276 GHz, which is very high. This measurement is limited by the spectrometer resolution. The best way to measure this parameter is to build a beat signal between this laser and another more stable, with similar wavelength and a

known linewidth. However, there was not a laser with these characteristics available, and the correct value could not be found.

The last step in this initial characterization is to measure how the wavelength behaves to changes in the system temperature. To do so, it was used a wavemeter, the Bristol 621 Wavelength Meter. The results are discussed below.

Figure 32: Relation of the current to the wavelength at 20.04ºC. The graph is divided into two regimens to ease the understanding. The graph presents plateaus where the laser mode is kept constant and slopes that represent regions of instability, where mode hops occur.

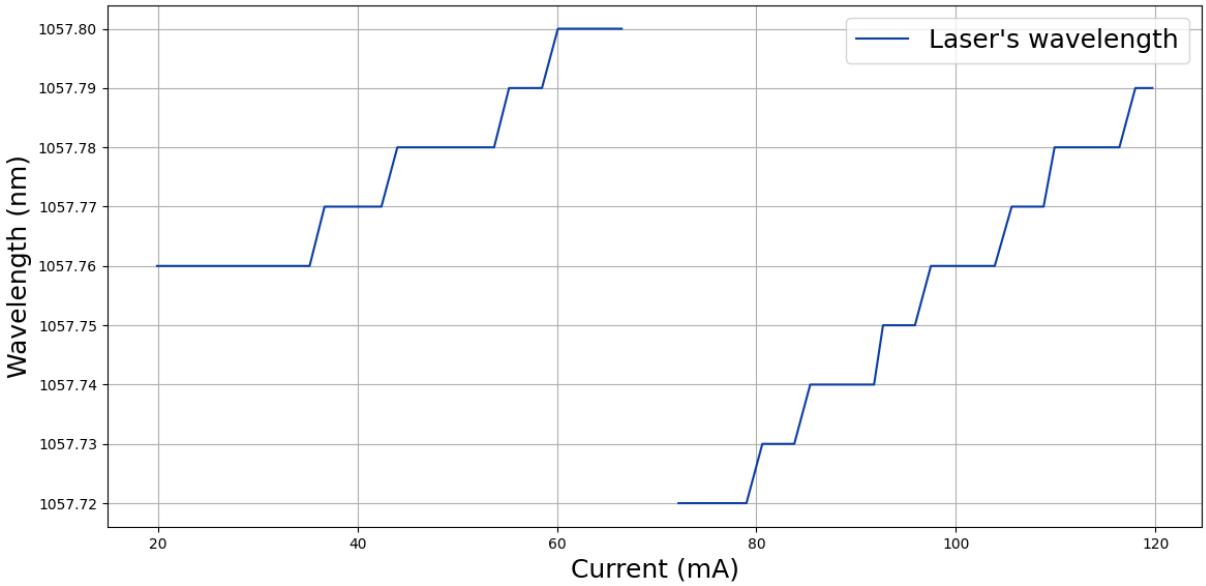

Source: Author, 2025.

First, it is possible to recognize regions of stability in the laser's wavelength, the plateaus, which do not have mode hops, which means the laser's wavelength is approximately constant. The slopes represent regions with laser's wavelength (and its frequency) instabilities, which do occur mode hops, which means changes in the wavelength, discontinuously and abruptly, and cannot be controlled.

It is worth mentioning that the laser works till the current of 325 mA, but the graph only goes to 120 mA. That occurs because for currents above 120 mA, it presents only unstable wavelength regions. After this instability, the laser could not be stabilized, even after months of tries, the stability accomplished was brief and smaller than needed. This graph should be repeated more times at different temperatures to keep track of the wavelength variation it produces. However, it was not possible to keep the laser's wavelength stable for any value of temperature from 18ºC to 30ºC.

The wavelength (frequency) stability is mandatory to couple the laser to a Fabry-Perot cavity. The experiment could not be continued with this laser, and an alternative should be presented to continue the experiment. The only suitable solution, with little time left to complete the master's degree, was to use a commercial single-frequency laser, which the process is described in the next subchapter.

4.2 COMMERCIAL SINGLE FREQUENCY LASER

Let's begin with the description of the laser. The chip used was the QFBGLD-1060-40 from QPHOTONICS, with a 14-pin butterfly case. The laser was set to work at 25ºC and controlled by the Benchtop Laser Controller EM595 from Gooch & Housego. The laser fiber is connected to a collimation mount composed of one FC/APC Fiber Adapter Plate (SM1FCA), which is inserted in a cage plate (CP02T/M) and connected to a Z-Axis Translation Mount with millimetric adjust (SM1ZA) and inside it a collimation lens (A260TM-C) is put using a Lens Cell Adapter (S1TM09). This entire structure is mounted over a Kinematic Prism Mount (KM100PM/M). After collimating the laser beam, the first step is to verify if the laser behaves properly by plotting the curve of Power versus Current.

Figure 33: Plot of the laser power by the applied current. From the plotting it was possible to determine the threshold current of the laser to be $I_{threshold} = 20.00$ mA, indicated by the ochre dashed line. after a certain current value of $I_{maximum} = 140.00$ mA, the laser does not behave properly anymore, that will be the maximum current limit for the laser.

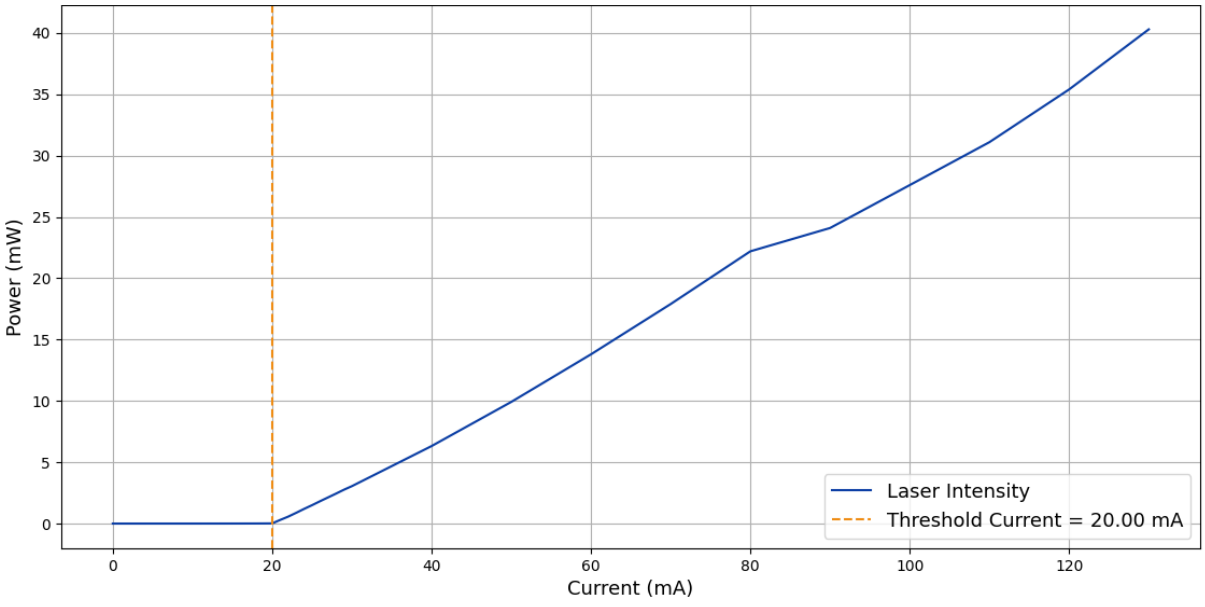

Source: Author, 2024.

From this data, there was some information that differed from what was in the laser's datasheet. First, from the datasheet, the threshold current should be 70 mA, which is 50 mA above the threshold current measured. Besides that, the datasheet brings an operating current up to 245 mA, but there is an unstable regime after 140 mA, and the current shall not pass this limit. The next step is measuring the laser's spectrum. For that, the Ocean Optics spectrometer HR4000 was used. By using Python code, it was possible to find the central spectrum wavelength by simply determining the wavelength that corresponds to the maximum spectrum intensity. Then, making an average, the average central wavelength found was $\lambda_0 = 1063.27 \pm 0.01$ nm, where the error is the standard error of the mean. The spectrum plot is given in Figure 34.

Figure 34: plot of the laser spectrum for a current of 50 mA, blue solid line, so that the spectrometer is not saturated and does not need an intensity filter. Central wavelength is given by the ochre dashed line.

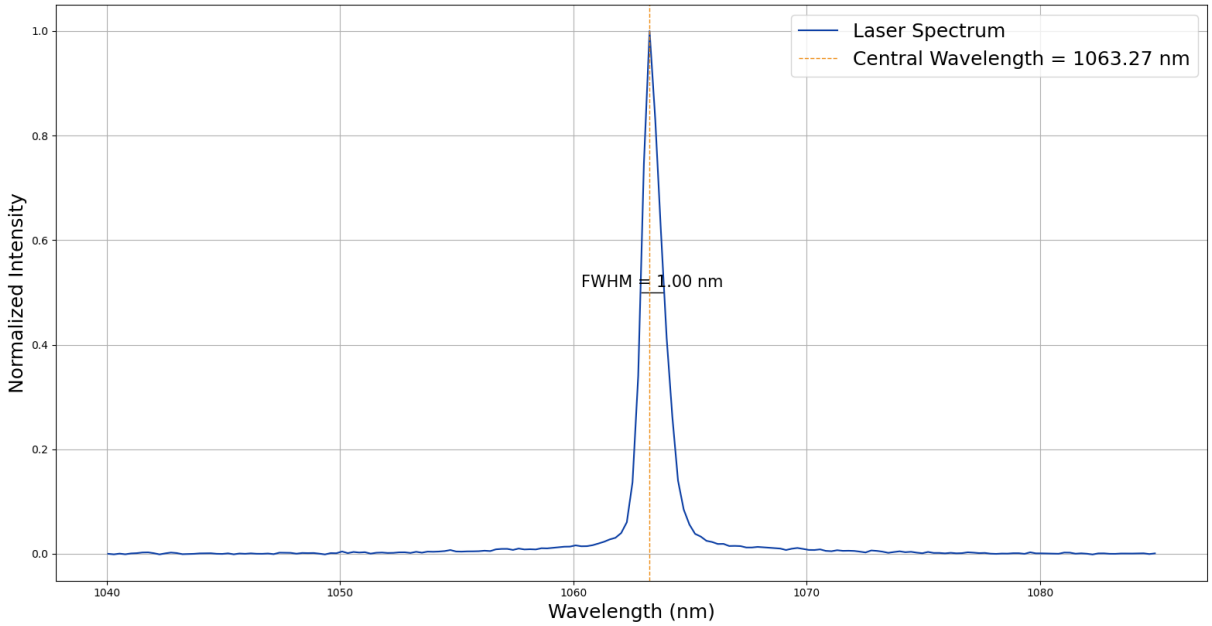

Source: Author, 2025.

Furthermore, by zooming in the graph, it was possible to find the FWHM of the laser spectrum. Once again, making an average over the values, the average FWHM found was $\Delta\lambda_{FWHM} = 1.00$ nm, as indicated by the black horizontal line. We can transform the FWHM from wavelength to frequency by a derivative on $\nu = (c/\lambda)$ and getting $\Delta\nu_{FWHM} = (c/\lambda_0^2)\Delta\lambda_{FWHM}$. It yields a FWHM in frequency of over 265 GHz. From the datasheet, the FWHM in frequency should be typically 1 MHz up to 10 MHz at maximum. These values correspond to a FWHM in wavelength of about 0.377

femtometer to 3.77 femtometer, which the spectrometer does not have resolution to measure. That explains the difference between the values expected and found.

4.2.1 FABRY-PEROT CAVITY COUPLING AND CHARACTERIZATION

The characterization of a Fabry-Perot cavity is done by measuring some properties, such as cavity finesse, cavity FSR, the mirrors reflectivities, the photon lifetime, and its quality factor. These properties can be measured, directly or indirectly, by the transmission signal of the cavity.

First, we want to construct an ECDL and use an ultra-high finesse Fabry-Perot ULE to characterize it. As seen in topic 4.1 (ECDL) from the RESULTS AND DISCUSSION, the ECDL presented instability due to the quality of the diode used, making the laser not suitable for locking it at the ultra-finesse cavity. The solution to this problem was to use the commercial single-frequency laser, QFBGLD-1060-40 from QPHOTONICS. This laser, even though it was single frequency, was capable of modulating its frequency for a few kilohertzs. However, the ultra-stable cavity had a FSR of 1.5GHz and the modulation was not enough for the coupling. The solution was to use a low-finesse homemade Fabry-Perot interferometer.

The homemade cavity has a PZT behind one of its mirrors, allowing it to change the cavity length and, therefore, change its FSR. As we scam the PZT, we can measure the fundamental transmission in the oscilloscope. The laser frequency does not change. If the laser frequency peak is originally close enough to one of the fundamental cavity resonance peaks, the modulation of the cavity will force a superposition between the bandwidths, which gives the same result as modulating the laser frequency.

This superposition will allow a transmitted signal that can be analyzed, however, it will not approach the same intensity as the incident beam, as expected by coupling the cavity with a tunable laser. The cavity scheme is illustrated in Figure 35.

Figure 35: Scheme of the Fabry-Perot interferometer. The mirrors used were the CM254P-025-E03 from Thorlabs, with a 12mm diameter and 50mm curvature radii. The mirror center was 1.6mm deeper than its borders. There was no information about the PZT used, but its dimensions were 8mm in height and 16mm in external diameter, it was a ring PZT. The separation cylinder was 68mm in height. The distance between the mirrors was 50.2mm.

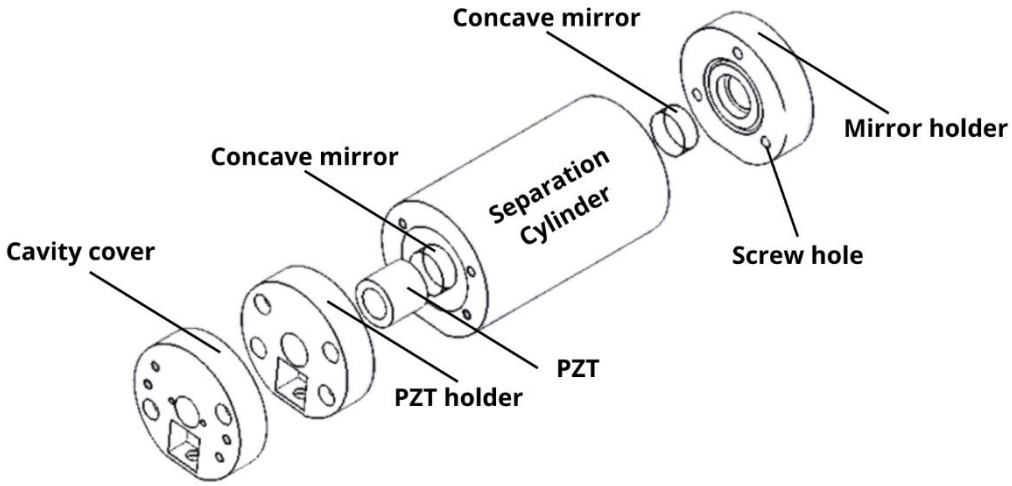

Source: João Guilherme, 2024.

We can estimate some parameters of the cavity to compare to the measured ones. The first parameter is the FSR, FSR = 2985.98 MHz, by using *Equation 2.11*. The reflectivity used was found in the datasheet. The fabricant gives the raw data for plotting the reflectance versus the laser wavelength. With a Python code it was possible to locate in the curve the value of the reflectance for the wavelength found for the laser, as shown in Figure 36.

Figure 36: reflectance of the concave mirror used to build up the Fabry-Perot interferometer (blue solid line). The vertical ochre dashed line marks the wavelength value. Finding the corresponding value at the reflectance curve showed a value of 99.750% reflectance.

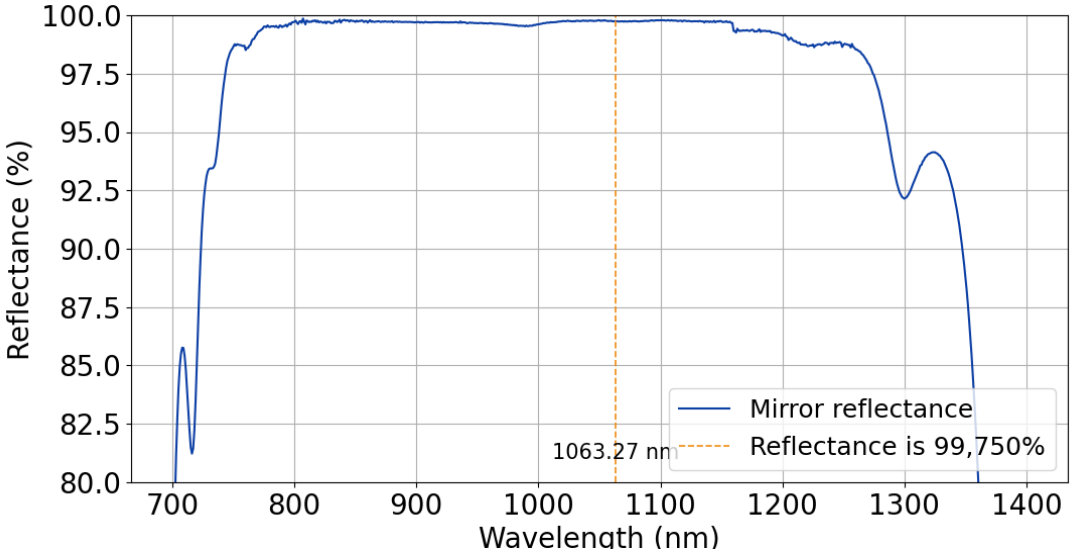

Source: Author, 2025.

With the extracted reflectance of $\mathbb{R} = 0.9975$ and using *Equation 2.12,* the finesse value of $\mathcal{F} = 1255$. The photon lifetime can be found using *Equation 2.22* for a lossless case, then:

$$\frac{1}{\tau_c} = -\frac{\ln(\mathbb{R}_1\mathbb{R}_2)}{t_{RT}}.$$

Since the mirrors used to build the cavity are identical, $\mathbb{R}_1 = \mathbb{R}_2 = \mathbb{R}$. The round-trip time, t_{RT}, can be found by dividing twice the cavity length by the speed of light, then:

$$\frac{1}{\tau_c} = -\frac{299792458 \cdot \ln(0.9975^2)}{2 \cdot 50.2 \cdot 10^{-3}} = 1.4948 \cdot 10^7\ s^{-1}.$$

Then $\tau_c = 66.9$ nanoseconds. The quality factor for this value τ_c can be found using *Equation 2.17*, where $Q = 1.18 \cdot 10^8$. Also, it is possible to estimate the linewidth of the cavity by using *Equation 2.13*, which yields $\Delta\nu_{FWHM} = 2.38$ MHz. We show these parameters at Table 4.1.

Table 4.1: Theoretical Fabry-Perot Interferometer Parameters.

Parameter	Value
Cavity Length (L)	50.2 mm
Free Spectral Range (FSR)	2985.98 MHz
Reflectance ($\mathcal{R}$)	0.9975
Finesse ($\mathcal{F}$)	1255
Photon Lifetime (τ_c)	66.9 ns
Quality Factor ($\mathcal{Q}$)	$1.18 \cdot 10^8$
Linewidth ($\Delta\nu_{FWHM}$)	2.38 MHz

Source: Author, 2025.

With these theoretical values, the next step is to measure the actual data to compare. We are going to start with the experimental setup used. With the same collimation mount described on the first paragraph of section 4.2 (COMMERCIAL SINGLE FREQUENCY LASER). A Free Space Optical Isolator (IO-D-1064-VLP) was placed before any other equipment, to prevent any reflected light from entering the fiber and causing instability to the laser. Then there was a polymer halfwave plate (WPH05ME-1064), a Polarizing Beam Splitter and a PBS (PBS125) mounted on a kinematic prims mount (KM100PM). The halfwave plate and the PBS control the laser's polarization and helps to align the cavity reflected beam. The PBS output was the p-polarized beam and the halfwave plate maximized this component.

A telescope was introduced after the PBS to reduce the beam diameter. The telescope was made with two lenses, one of 50 mm (the objective) and a 30 mm (the ocular) spaced 80 mm apart from each other. The diameter of the beam was reduced from approximately 1.5 mm to approximately 1 mm. Then, a polymer zero-order quarter-wave plate (WPQ10E-1064) is placed to control the reflected beam polarization. The polarization was cleaned by the PBS, so the quarter-wave plate placed at the entrance of the cavity works as a half-wave plate (the beam passes through it twice), then it is possible to make the polarization of the reflected beam change from p-polarized to s-polarized and be reflected at the PSB. After the laser passes the quarter-wave plate, the beam finally enters the cavity. The experimental setup is illustrated in Figure 37.

Figure 37: Experimental setup to couple the commercial laser to the homemade Fabry-Perot interferometer.

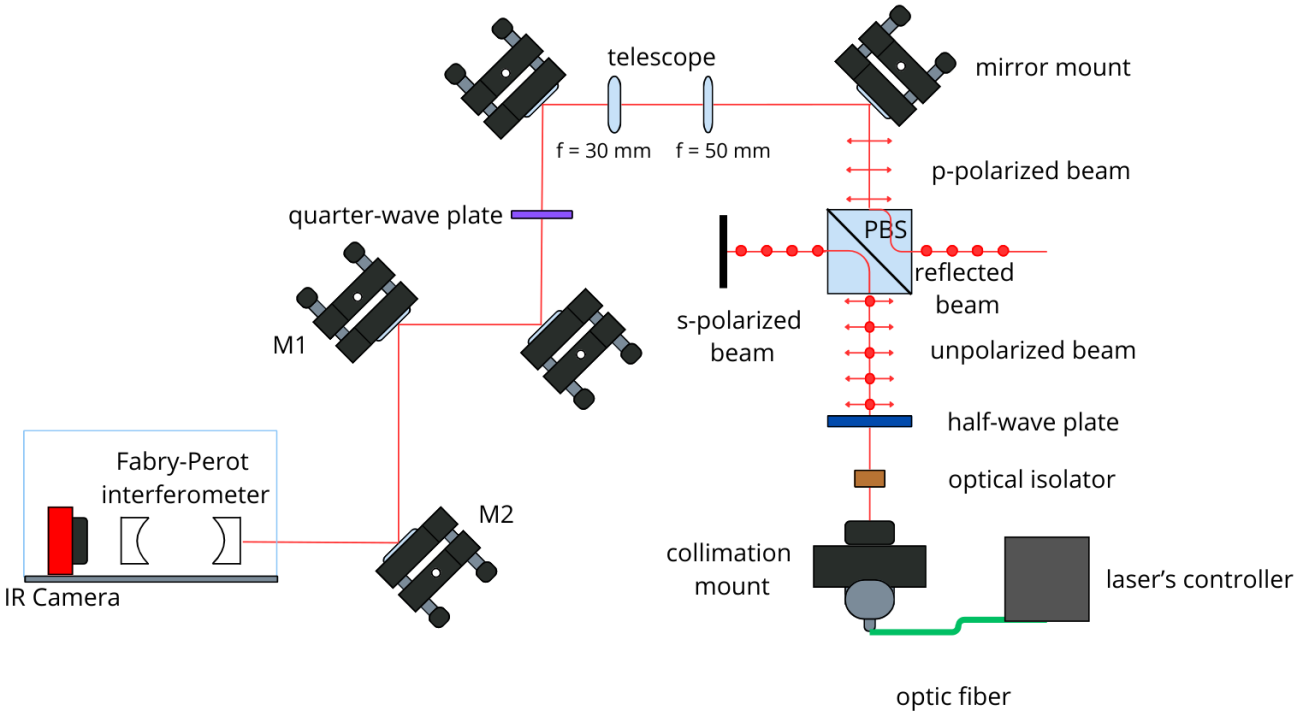

Source: Author, 2025.

Before continuing with the experiment, it is necessary to stabilize the cavity by reducing mechanical vibrations. To do so, it was ordered another acrylic box, but now with an apparatus to absorb the mechanical vibration as well to keep the cavity aligned horizontally and vertically since it is crucial for coupling. The next figure contains the scheme for it.

Figure 38: apparatus to absorb mechanical vibrations and keep cavity alignment. There are two layers of rubber sheet, the first layer is placed between the lab table and the fixed platform, which absorbs the vibrations. The second layer is placed between the platforms and absorbs the remaining vibrations from the first layer. The sliding stem is used to adjust the cavity height and keep it aligned vertically, helped by the millimetric marks in both arms. There is an acrylic box with its walls covered inside by black styrofoam and outside with yellow Ethylene Vinyl Acetate (EVA), to block light from entering and vibrations from air. There is a slit in the acrylic box for the laser and on the box lid for the camera (or detector) wires and on one of the sides for the PZT wires.

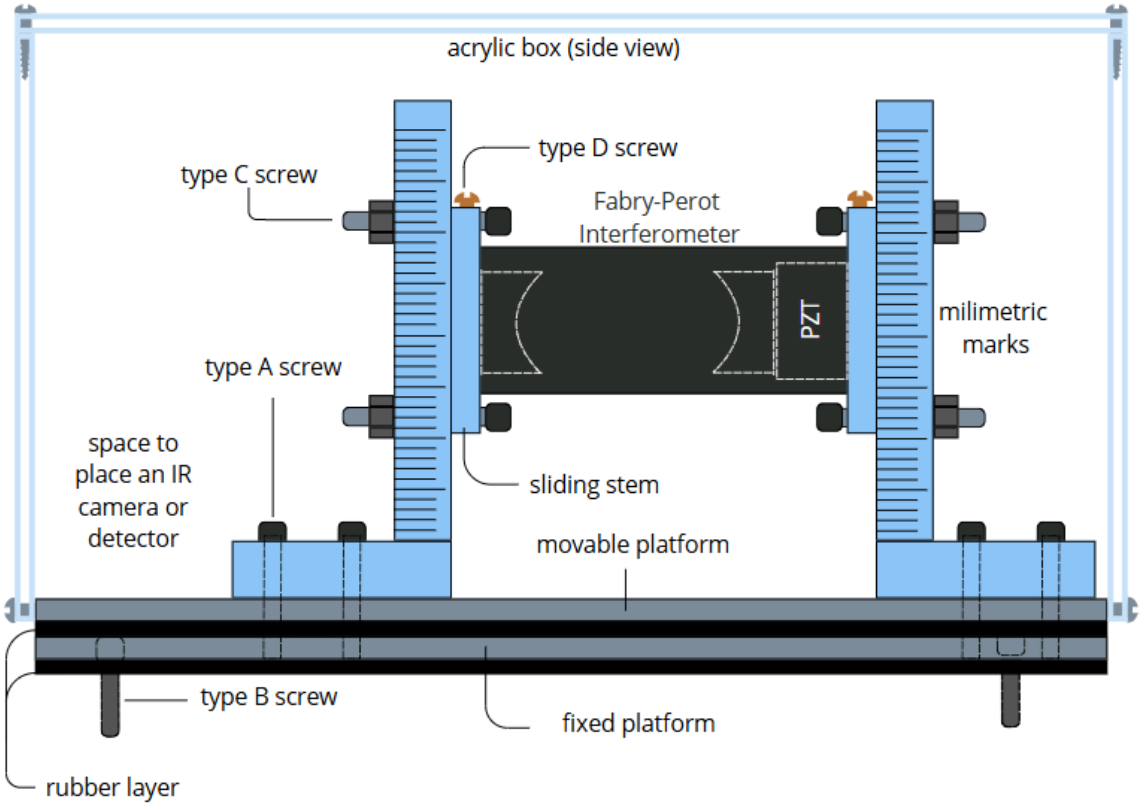

Source: Author, 2025.

We must mode-match the laser beam to the cavity in order to couple light into it. That can be accomplished by introducing a lens before the cavity entrance. However, this lens must have its focus and distance from the cavity center calculated. To do so, first we shall find the cavity ABCD matrix. To do so, the laser's path gives us the interactions relevant to the resultant matrix. Since the ABCD transfer matrix is given by the smallest reproducible cell and the mirrors are identical, the matrix is made of the interaction with one mirror and the propagation to the next one.

Figure 39: smallest reproducible cell for the ABCD transfer matrix. The concave mirror acts the same way as a lens to the ABCD matrix.

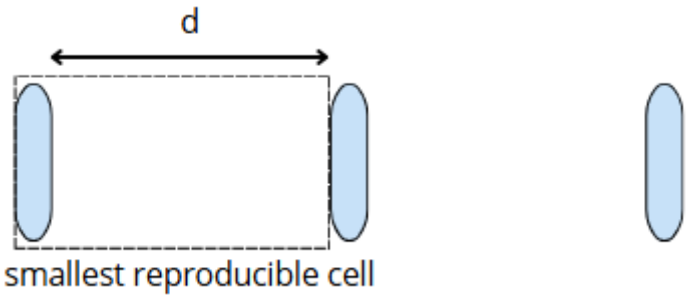

Source: Author, 2025.

$$\begin{bmatrix} A & B \\ C & D \end{bmatrix} = \begin{bmatrix} 1 & 0 \\ -1/f & 1 \end{bmatrix} \begin{bmatrix} 1 & d \\ 0 & 1 \end{bmatrix}$$

$$\begin{bmatrix} A & B \\ C & D \end{bmatrix} = \begin{bmatrix} 1 & d \\ -1/f & 1 - d/f \end{bmatrix}$$

Knowing that[29]:

$$\frac{\pi\omega_0^2}{\lambda_0} = \frac{B}{\sqrt{1-\left(\frac{A+D}{2}\right)^2}} = \frac{d}{\sqrt{1-\left(\frac{2f-d}{2f}\right)^2}}$$

Equation 4.1

and[16][29]:

$$R = \frac{2B}{D-A} = -2f.$$

Equation 4.2

Where ω_0 is the beam waist at the cavity focus (at its center) and R is the radius of curvature of the wavefronts to couple with the cavity. With the cavity properties, we have $\omega_0 \approx 0.130$ mm of waist at focus and $R = -50$ mm. These values correspond to the cavity, to find the focus of the lens that will reproduce this behavior we can use[30]:

$$2\omega_0 = \frac{1.22\lambda_0 f}{2\omega},$$

where ω is the beam waist at the lens. This yields value for the focus of $f = 201.5$ mm. As displayed in Figure 40.

Figure 40: scheme of the correct lens to mode-match the cavity with the laser wavefronts. The lens gives the laser a wavefront of R = 50 mm, which matches the curvature of the cavity mirrors and provides the laser waist required. The values f and r are the focus and mirror curvature.

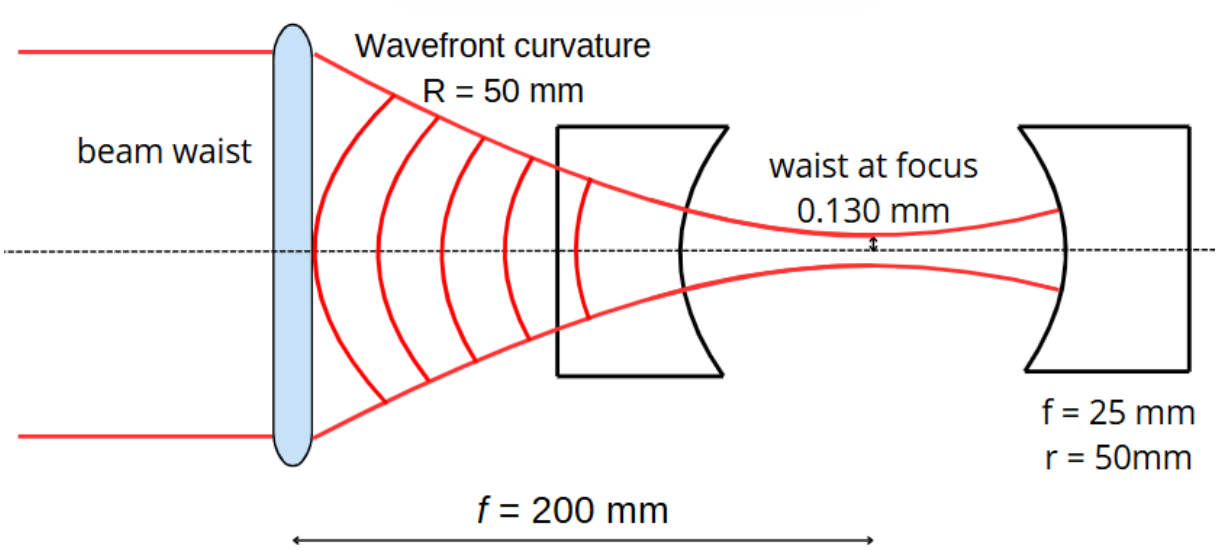

Source: Author, 2025.

Besides that, by calculating the Rayleigh length, we would have an acceptable range, where the focus can deviate without compromising the desired behavior. For this focus, the length is $z_R = \pi\omega_0^2/\lambda_0 = 50.2$ mm. Then using a lens with a focus from 150 mm to 250 mm should be fine. Before continuing, we must check the general condition for stability for the cavity, given by[29]:

$$0 \leq \frac{A + D + 2}{4} \leq 1.$$

Substituting the values we get a value of 0.498, which is inside the region for stability, confirming that the cavity is stable. The lens used had a focus of 200 mm. It is important to notice that the focus of the lens must coincide with the focus of the cavity, so the distance of 200 mm is to the center of the cavity, not to its entrance. It is useful to put this lens on a translator to have better control over the distance it is placed.

Settled the experimental setup, the next step is the alignment. Setting every optical component to have its middle at the same height should guarantee that the laser beam hits the mirror cavity at its center. The laser's wavelength was in the Near Infrared (NIR) spectrum, so an IR viewer was needed. The reflected beam must be antiparallel to the incident beam, superposed. Hence, it is impossible to distinguish between them, so the quarter-wave plate is essential here because, with the s-

polarized and proper alignment, the output of the PBS should show the reflected beam, which must be collimated.

With this pre-alignment, a camera (CS165MU1/M) was put on the back of the cavity. Here the layers on the inside and outside walls were essential to block any external light. The output signal on the oscilloscope was on a scale of 2 mV per division. To see it with the camera, we needed to use it with maximum gain. If the pre-alignment is well done, with modulating the cavity's PZT it would be possible to already see higher cavity modes on the camera. The PZT modulation was done using a waveform generator from SIGLENT Technologies (SDG1032X) connected to an amplifier (HVA200). With this modulation, it was possible to see higher Gaussian modes without changing the alignment. The alignment was done with mirrors M1 and M2.

Figure 41: some of the Gaussian cavity modes. The first line is closer to a rectangular symmetry (Hermite-Gauss modes) and the second line is closer to a cylindrical symmetry (Laguerre-Gauss modes).

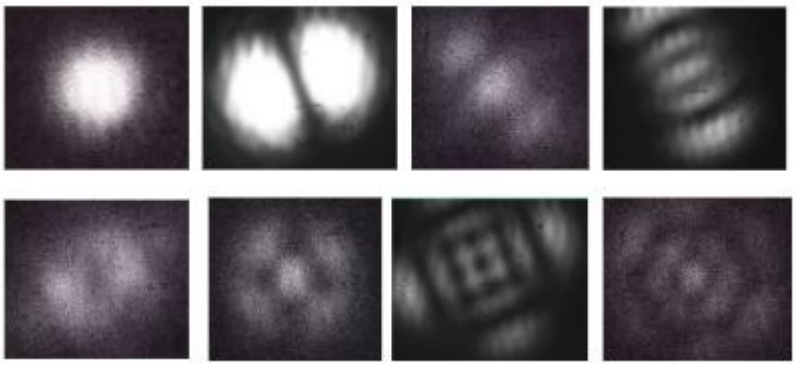

Source: Author, 2025.

From Figure 41, we can distinguish two kinds of cavity modes. These changes in the symmetry are due to some little imperfections on the mirror and misalignment along the procedure. Besides that, generally, the modes are not pure, and usually, they are the result of the sum of more than one mode. As the Gaussian mode approaches the fundamental mode, the intensity the camera captures grows and the need for the camera gain decreases. We changed the camera by a detector when the fundamental mode is achieved.

Since the expected signal should be weak, the detector used was the Si avalanche photodetector (APD130A/M) from Thorlabs. The oscilloscope (DSO7104B) read the photodetector signal. By modulating the PZT, the transmitted signal should

display two peaks for each upward or downward part of the modulation ramp. The presence of smaller peaks indicates that the laser coupling is not purely at the fundamental mode, but there are also higher modes with a weaker coupling. The goal is to reduce these higher modes as much as possible. If the oscilloscope read shows only one peak per upward (downward) ramp, changing the parameter of the modulation such as a DC offset and amplitude can help solve this problem.

The coupling achieved was not purely at the fundamental mode, instead, the acquired one had some higher mode that could not be extinguished. This may happen because the modulation was done by the cavity's PZT and not at the laser frequency. The transmitted signal is displayed in Figure 42.

Figure 42: cavity's transmitted signal (blue solid line) for a modulation ramp (ochre solid line) of amplitude of 100 volts and repeat frequency of 1 Hz applied to the PZT. Alongside the fundamental mode (bigger peaks), there are two other higher modes (smaller peaks).

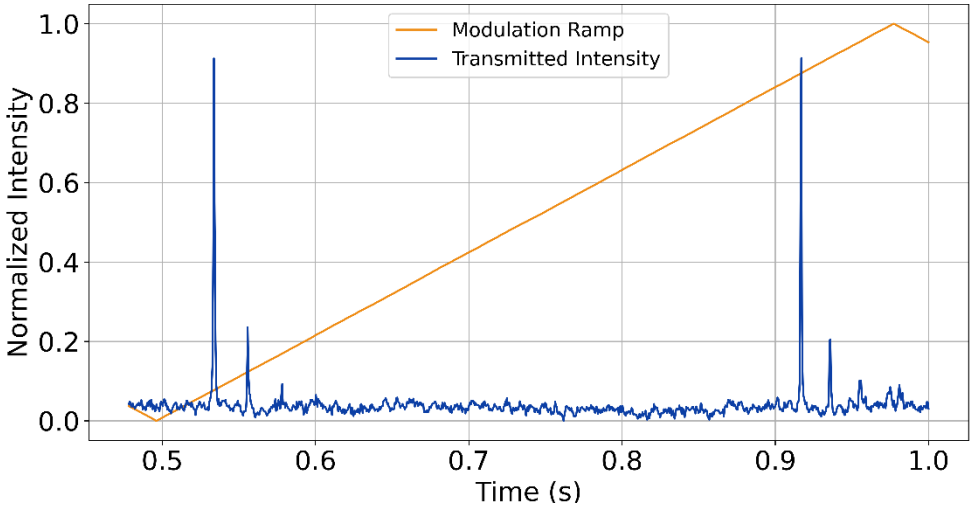

Source: Author, 2025.

Although it was possible to see the fundamental mode peaks, its power was weak. From the photodetector datasheet, we can estimate the power of the fundamental mode peak, for a set of data the average power found was around 15.8 nW, in comparison to 30 mW of cavity incident laser intensity. The output intensity of the cavity was $2 \cdot 10^6$ smaller than the input. That could indicate that even though the cavity is being modulated, the modulation is not enough to make the cavity resonance come near the laser peak. Another signal's characteristic was that the peaks were not static, they changed positions, including concerning each other, and height, this can also indicate an instability in the cavity, due to the cavity not being locked.

To find the cavity's finesse, we used its definition of FSR divided by FWHM. The FSR is the separation between two consecutive fundamental modes at the same upward (downward) ramp, and it was easy to find by Python code. The FWHM was obtained by a curve fit. As seen in section 2.1.1.1 (Lossless Fabry-Perot Cavity), near the resonance, the transmitted signal follows a Lorentzian. Then a Lorentzian fit makes it possible to find the FWHM, where:

$$L(t) = \frac{A \cdot wid^2}{(t-b)^2 + wid^2} + DC_{offset},$$

here, the parameter *b* gives the *t* value for the peak, *A* is the amplitude, the *wid* is the Half Width at Half Maximum and the DC_{offset} is usually given by the natural DC that comes from the detector. Then the FWHM is given by $FWHM = 2 \cdot wid$. To find the finesse, we used more than 400 collected peaks and made an average over them. The higher modes can create problems when fitting the data, then they need to be out of the *t* range for the fitting.

Figure 43: A peak to represent the value of the average finesse and the Lorentzian fit. For this figure we used the second fundamental peak (ochre solid line) from Figure 42 as an example. The blue points represent the data that were used to make the fitting. The finesse displayed is an average of over 434 peaks, the error is the standard error.

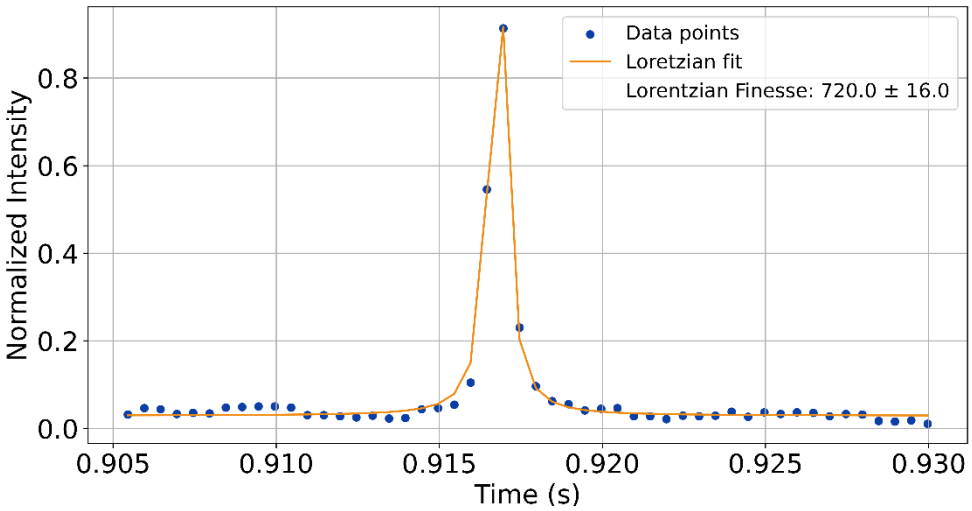

Source: Author, 2025.

The finesse value found was 720 ± 16, approximately 0.57 of the theoretical value. This difference can be explained by cavity losses not accounted by the initial theoretical prediction. Another way to measure the cavity's finesse is through the photon lifetime. To find the photon lifetime, the cavity should be locked to the laser,

however, due to short time and lack of equipment, the locking was not possible. Instead, a DC offset was chosen by hand to maximize the cavity's output. Nevertheless, the output did not hold continuously and had a noisy pattern, which sometimes showed peaks.

To determine the photon lifetime, we can find an exponential decay time from the photodetector, to see how long it naturally takes to diminish the signal. To do so, we used a chopper (SR540) from Stanford Research Systems set to work at a frequency of 50Hz. To find the photodetector parameter we put the proper filter so it did not saturate. We plotted a monolog scale graph to find the time constant and did a linear fit at the exponential part with a form of $y = a \cdot x + b$. The time constant was given be the inverse of the slope. The average time constant for the photodetector was 145.25 $\pm$ 0.01 μs, where the error is given by the standard error.

For the cavity's photon lifetime, a monolog-scaled graph would not give any useful information due to noise. Therefore, a different fit was done, using the following curve:

$$y = \begin{cases} a \; for \; t < c \\ b + (a - b) \cdot exp\left(-\dfrac{(t - c)}{\tau}\right) \; for \; t \geq c \end{cases}'$$

Equation 4.3

where "*a*" is the average value of the higher plateau, "*b*" is the average value of the lower plateau, "*c*" is the transitional time when the curve changes from a constant to an exponential and τ is the time decay constant. A Python code adjusted the parameters to better fit the data. The average value for the time constant with the cavity was 145.30 $\pm$ 0.1 μs. Where the error is given by the standard error of the mean. The curve and the fit are in Figure 44.

Figure 44: Curve fit to find the exponential decay time with the laser passing through the cavity. The data is given by the solid blue line and the curve fit by the dashed ochre line.

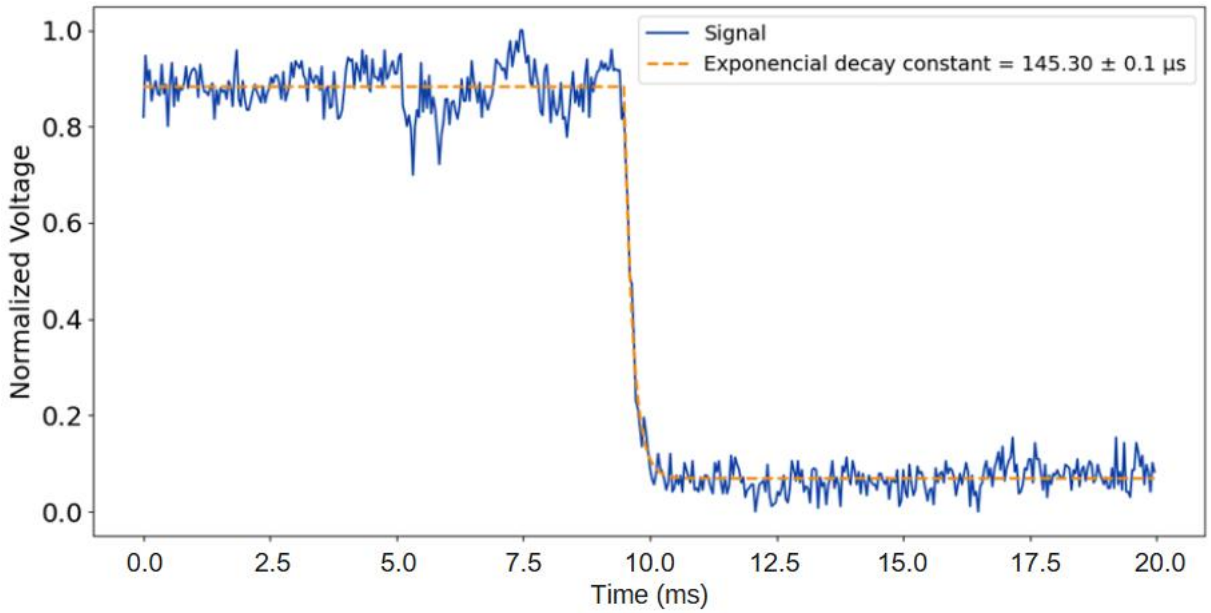

Source: Author, 2025.

With both values in hand, to find the photon lifetime we must compare the value for the time decay constant with and without the cavity. The decay constant for the photodetector alone is the detector's response. Then subtracting the detector's response from the value found with the cavity, the extra time is the photon lifetime. Then, $\tau_c = 50 \pm 0.03$ ns. Where the error is given by the error propagation between the individual errors. The value is smaller than the predicted value of 66.9 ns. Since the finesse was also lower than expected, a smaller value for the photon lifetime is consistent.

With the value for the photon lifetime is possible to find the quality factor. Using *Equation 2.17*, the quality factor found was $8.86 \cdot 10^7$. Since these differences between the predicted and measured values can come from the losses at the cavity, we can use Equations 2.22 and 2.26 to estimate the propagation-loss coefficient α_{prop}. From *Equation 2.22*:

$$\frac{1}{\tau_c} = -\frac{\ln(\mathbb{R}_1\mathbb{R}_2)}{t_{RT}} + c\alpha_{prop}$$

Since the mirrors are identical $\mathbb{R}_1 = \mathbb{R}_2 \equiv \mathbb{R}$. And from *Equation 2.26*:

$$\mathcal{F}^{loss} = \frac{\pi\sqrt{\mathbb{R}e^{-\frac{c\alpha_{prop}}{FSR}}}}{1-\mathbb{R}e^{-\frac{c\alpha_{prop}}{FSR}}},$$

By the photon lifetime, the coefficient value is $\alpha = 0.0168 \pm 0.0004\, m^{-1}$ and by the finesse value the coefficient is $\alpha = 0.018 \pm 0.003\, m^{-1}$. Making an average between these values we get $\alpha_{prop} = 0.017 \pm 0.003\, m^{-1}$. Where the error is given by the error propagation. At last, we can estimate the mirror reflectance by using[14]:

$$\frac{1}{\tau_c} = -\frac{\ln(\mathbb{R}_1\mathbb{R}_2)}{t_{RT}}$$

$$\mathbb{R}^2 = e^{-\frac{t_{RT}}{\tau_c}}$$

Then for a 50 ns photon lifetime, we get a reflectance of $\mathbb{R} \approx 0.9966 \pm 0.0006$, the error is given by error propagation. The measured value deviates from the estimated value by about 0.09%. Equation 2.27 gives the value for the cavity's linewidth as 4.0 ± 0.7 MHz, where the uncertainty propagation provides the error. The estimated and measured values of the parameters are in Table 4.2.

Table 4.2: Values predicted and measured for the cavity's parameters.

Parameter	Predicted Value	Measured Value
Reflectance ($\mathbb{R}$)	0.9975	0.9966 ± 0.0006
Finesse ($\mathcal{F}$)	1255	720 ± 16
Photon Lifetime (τ_c)	66.9 ns	50 ± 0.03 ns
Quality Factor ($\mathcal{Q}$)	$1.18 \cdot 10^8$	$8.86 \cdot 10^7$
Linewidth ($\Delta\nu_{FWHM}$)	2.38 MHz	4.0 ± 0.7 MHz

Source: Author, 2025.

5 CONCLUSIONS

The research presented in this dissertation has explored the construction of an ECDL and the characterization of a homemade Fabry-Perot cavity. For the ECDL, the goal was to lock it to an ultra-high finesse Fabry-Perot through the Pound-Drever Hall (PDH) technique. The ECDL could not be stabilized, so the PDH technique was not implemented, and the ECDL was unused. For future steps, we aim to acquire a better diode to remake the characterization. An ECDL locked to an ultra-high finesse Fabry-Perot cavity provides a laser suited for metrologic purposes, such as high-precision spectroscopy.

Despite that, it was possible to measure the optical parameters of the cavity. Table 4.2 has measured parameters for the finesse, photon lifetime, mirror reflectance and quality factor. Also, we were able to estimate the cavity's loss coefficient. With the cavity characterized it can be used for a laser to work as a reference. However, as the laser was not coupled into the cavity with its central wavelength, it could not be characterized as well, and its properties were not measured. In summary, this dissertation has successfully characterized a homemade Fabry-Perot interferometer

REFERÊNCIAS

[1] SORRENTINO, F et al. **LASER COOLING AND TRAPPING OF ATOMIC STRONTIUM FOR ULTRACOLD ATOMS PHYSICS, HIGH-PRECISION SPECTROSCOPY AND QUANTUM SENSORS.** Vol. 20, pag 1287–1320. Modern Physics Letters B, No. 21, 2006.

[2] SANJUAN, Josep; ABICH, Klaus et al. **Long-term stable optical cavity for special relativity tests in space.** Vol. 27, Issue 25, pag. 36206-36220. Optics Express, 2019.

[3] HOND, Julius de *et al.* **Medium-finesse optical cavity for the stabilization of Rydberg lasers**. Vol. 56. Applied Optics, 2017.

[4] FERNÁNDEZ, D. Rodríguez *et al.* **Low-cost medium-finesse optical cavity for diode laser stabilization**. São Paulo: USP, 2023.

[5] LÖW, Robert *et al*. **An experimental and theoretical guide to strongly interacting Rydberg gases**. Vol. 45. Journal of Physics B: Atomic, Molecular and Optical Physics, 2012.

[6] KESSLER, T. *et al*. **A sub-40-mHz-linewidth laser based on a silicon single-crystal optical cavity**. Vol 6. Nature Photonics, 2012.

[7] BLACK, Eric D. **An introduction to Pound–Drever–Hall laser frequency stabilization**. California Institute of Technology, 2001.

[8] DREVER, Ronald W. P; HALL, John L. *et al.* **Laser Phase and Frequency Stabilization Using an Optical Resonator**. Applied Physics B: Photophysics and Laser Chemistry. Vol 31, pag.97–105, 1983.

[9] BJORKLUND, Gary C. et al. **Frequency Modulation (FM) Spectroscopy: Theory of Line shapes and Signal-to-Noise Analysis**. Applied Physics B: Photophysics and Laser Chemistry. Vol 32, pag.145–152, 1983.

[10] BJORKLUND Gary C. **Frequency-modulation spectroscopy: A new method for measuring weak absorptions and dispersions**. Optics Letters. Vol.5, pag.15–17, 1980.

[11] FERNÁNDEZ, D. Rodríguez. **Cavidades ópticas para experimentos em Física Atômica**. São Paulo: UPS São Carlos, 2023.

[12] SINGH, Siddhant. **Stabilization of 866 nm laser with Pound-Drever-Hall (PDH) technique for quantum manipulation of Ca^+ ion in Paul trap**. Universität Basel, 2019.

[13] POULSEN, Gregers. **Sideband Cooling of Atomic and Molecular Ions**. Denmark: University of Aarhus, 2011.

[14] ISMAIL, Nur et al. **Fabry-Pérot resonator: spectral line shapes, generic and related Airy distributions, linewidths, finesses, and performance at low or**

frequency-dependent reflectivity. Optics express. Vol.24, pag. 16366 – 16389, 2016.

[15] POLLNAU, Markus; EICHHORN, Marc. **Spectral coherence, Part I: Passive-resonator linewidth, fundamental laser linewidth, and Schawlow-Townes approximation**. Elsevier, Progress in Quantum Electronics, 2020.

[16] YARIV, Amnon; YEH, Pochi. **Photonics: Optical Electronics in Modern Communications**. 6th Ed. New York: Oxford University Press, 2007.

[17] NAGOURNEY, Warren. **Quantum Electronics for Atomic Physics**. New York: Oxford University Press, 2010.

[18] HANAMURA, Eiichi; KAWABE, Yutaka; YAMANAKA, Akio. **Quantum Nonlinear Optics**. 1st ed. pag. 75 – 99. Springer, 2007

[19] HARVEY; K. C.; MYATT, Christopher J. **External-cavity diode laser using grazing-incidence diffraction grating**. Vol. 16, Nº 12. Optical Society of America, 1991.

[20] PATZAK, E. *et al*. **SEMICONDUCTOR LASER LINEWIDTH IN OPTICAL FEEDBACK CONFIGURATIONS**. Vol. 19, Nº 24. Electronics Letters, 1983.

[21] BREGUET, Jean-Marc et al. **Tunable Extended-cavity Diode Laser based on a novel flexure-mechanism**. International Journal of Optomechatronics, 2013.

[22] LITTMAN, Michael G. **Single-mode operation of grazing-incidence pulsed dye laser**. OPTICS LETTERS. Vol. 3, Nº 4, 1978.

[23] SHOSHAN, I; OPPENHEIM, Uri P. **THE USE OF A DIFFRACTION GRATING AS A BEAM EXPANDER IN A DYE LASER CAVITY**. OPTICS COMMUNICATION. Vol 25, Nº 3, 1978.

[24] WANDT, D; LASCHEK, M. et al. **Continuously tunable external-cavity diode laser with a double-grating arrangement**. OPTICS LETTERS. Vol. 22, Nº 6, 1997.

[25] LITTMAN, Michael G; METCALF, Harold J. **Spectrally narrow pulsed dye laser without beam expander**. APPLIED OPTICS. Vol. 17, Nº 14, 1978.

[26] AZUMA, Hironobu *et al*. **Propagation loss in polyfluorene waveguides due to nanometer-roughness at their interfaces, studied by amplified spontaneous emission measurements**. Jpn. J. Appl. Phys. ***63*** 02SP02, 2024.

[27] NEWELL, T. C; BOSSERT, D. J. et al. **Gain and Linewidth Enhancement Factor in InAs Quantum-Dot Laser Diodes.** IEEE PHOTONICS TECHNOLOGY LETTERS. VOL. 11, Nº 12, December, 1999.

[28] VAHALA, K; CHIU, L. C; MARGALIT, S; YARIV, A. **On the linewidth enhancement factor α in semiconductor injection lasers.** Appl. Phys. Lett. Vol. 42, Issue 8, pag. 631 – 633. April 1983.

[29] VERDEYEN, J. Thomas. **Laser Electronics**. 3rd Ed. Prentice Hall, 1995.

[30] PEDROTTI, Leno. **Fundamentals of Photonics - Basic Physical Optics.** pag. 117 – 168. SPIE, 2008.

[31] Advanced information. NobelPrize.org. Nobel Prize Outreach 2025. Wed. 26 Feb 2025. <https://www.nobelprize.org/prizes/physics/2022/advanced-information/>

[32] Advanced information. NobelPrize.org. Nobel Prize Outreach 2025. Wed. 26 Feb 2025. <https://www.nobelprize.org/prizes/physics/2023/advanced-information/>

[33] BAI, Zhenxu; ZHAO, Zhongan. et al. **Narrow-Linewidth Laser Linewidth Measurement Technology**. Frontiers in Physics. Vol. 9, 2021.

[34] ZHANG, W; STERN, L. et al. **Ultranarrow Linewidth Photonic-Atomic Laser**. Laser & Photonics Reviews. Vol. *14, Issue* 4. March 2020.

[35] THERON, F; CARRAZ, O; RENON, G. et al. **Narrow linewidth single laser source system for onboard atom interferometry**. Appl. Phys. B. **118**, 1–5 (2015).

APPENDIX A – PYTHON CODE TO THE SIMULATION OF THE INTERNAL RESONANCE ENHANCEMENT FACTOR

```
@author: João L. R. Daré

# Simulation of the Internal Resonance Enhancement Factor

import numpy as np

import matplotlib.pyplot as plt

# Function ʊ(ω, r)

def ʊ(ω, r):

    return 1/((1 - r**2*np.exp(-(α*c)/FSR))**2 + 4 *np.exp(-(α*c)/FSR)* r**2 * (np.sin(ω*np.pi))**2)

# Values of importants constants and r

α = 0.1

c = 299792458

FSR = c/(2*0.1)

r = 0.9

# Values de ω_c

ω_c_values = np.linspace(-1.5, 1.5, 100000)

# Calculate ʊ values of ω_c

ʊ_values = ʊ(ω_c_values, r)

# Create a graph of the Enhancement Factor

plt.plot(ω_c_values, ʊ_values, linewidth=0.9)

plt.xlabel(r'$\frac{ω - ω_{RESONANCE}}{FSR}$', fontsize=12)

plt.ylabel('Intensity', fontsize=12)

plt.title(r'Internal Resonance Enhancement Factor',fontsize=12)

plt.grid(False)  # Disable the grids of the graph
```

```
plt.xticks([-1.5,-1,-0.5, 0.0,0.5,1,1.5])  # Define the values to mark in the x-axis
#plt.axhline(y=1, color='red', linestyle='--', label='y = 1', linewidth=0.9)
#plt.ylim(0, 10)
plt.show()
```

APPENDIX B – PYTHON CODE TO THE SIMULATION OF THE TRANSMITTANCE, REFLECTTANCE AND INTRINSIC PROPAGATION-LOSS INTENSITY

```
@author: João L. R. Daré

# Simulation of the Transmittance, Reflectance and Intrinsic Propagation-loss Intensity

import numpy as np

import matplotlib.pyplot as plt

def L(ω, r):

    return ((1-r**2*np.exp(-(α*c)/FSR))**2-(1-r**2)**2*np.exp(-(α*c)/FSR))/((1-r**2*np.exp(-(α*c)/FSR))**2 + 16*r**4*np.exp(-(α*c)/FSR)*(np.sin(ω*np.pi))**4 + ((4*r**2*(1+np.exp(-(α*c)/FSR))*(1+r**4*np.exp(-(α*c)/FSR))-4*r**3*np.exp(-(α*c)/FSR)*(1+2*r))*(np.sin(ω*np.pi))**2)/((1-r**2)**2))

def T(ω, r):

    return  (1-r**2)**2*np.exp(-(α*c)/FSR)/((1 - r**2*np.exp(-(α*c)/FSR))**2 + 4 *np.exp(-(α*c)/FSR)* r**2 * (np.sin(ω*np.pi))**2)

def R(ω, r):

    return (r**2*(1-np.exp(-(α*c)/FSR))**2 + 4*r**2*np.exp(-(α*c)/FSR)*(np.sin(ω*np.pi))**2)/((1 - r**2*np.exp(-(α*c)/FSR))**2 + 4 *np.exp(-(α*c)/FSR)* r**2 * (np.sin(ω*np.pi))**2)

# Values of the importants constants and r

α = 0.1

c = 299792458

FSR = c/(2*0.1)

r = 0.9

# Values of ω_c

ω_c_values = np.linspace(-1.5, 1.5, 100000)

# Calculate the values of T, R, L and S for different values of ω_c

T_values = T(ω_c_values, r)
```

```
R_values = R(ω_c_values, r)

L_values = 1 - T_values - R_values

S_values =  + T_values + R_values + L_values

# Creating a graph of the imaginary part with respect to ω_c

plt.plot(ω_c_values, T_values, linewidth=0.9, label = 'Transmittance')

plt.plot(ω_c_values, R_values, linewidth=0.9, label = 'Reflectance')

plt.plot(ω_c_values, S_values, linewidth=0.9, label = 'Sum')

plt.plot(ω_c_values, L_values, linewidth=0.9, label = 'Intrinsic Losses')

plt.xlabel(r'$\frac{ω - ω_{RESONANCE}}{FSR}$', fontsize=16)

plt.ylabel('Intensity', fontsize=12)

plt.title(r'Transmittance, Reflectance and Intrinsic Intensity Loss of a Fabry-Perot Cavity',fontsize=12)

plt.grid(False)  # Disable the grids in the graph

plt.xticks([-1.5,-1,-0.5, 0.0,0.5,1,1.5])  # Define the values to mark in the x-axis

#plt.axhline(y=1, color='red', linestyle='--', label='y = 1', linewidth=0.9)

#plt.ylim(0, 10)

plt.legend(fontsize=10)

plt.show()
```

APPENDIX C – PYTHON CODE TO THE SIMULATION OF THE POUND-DREVER-HALL ERROR SIGNAL FOR LOW-FREQUENCY MODULATION

```
@author: João L. R. Daré

# Simulation of the Pound-Drever-Hall Error Signal for Low-Frequency Modulation

import numpy as np

import matplotlib.pyplot as plt

# Function of R(ω, r)

def R(ω, r):

    return (r * (np.exp(1j *1*(ω)-1)))/(1-r**2*np.exp(1j*1*(ω)))

# Derivative of the squared modulus of R(ω_c) with respect to ω_c

def derivative_mod_squared_R(ω, r):

    R_val = R(ω, r)

    return 2 * np.abs(R_val)**2 * np.imag(np.conj(R_val) * np.exp(1j*1*(ω)))

# Values of the constants Ω and r

Ω = 0.00001  # Valor constante de Ω

r = 0.9999 # Valor constante de r

# Values of ω_c

ω_c_values = np.linspace(-0.002,0.002, 500)

# Calculate the expression for |d|R(ω_c)|^2/dω_c| * Ω

expression_values = [-derivative_mod_squared_R(ω_c, r) * Ω * np.sin(2*Ω) for ω_c in
ω_c_values]

# Creating a graph of the expression part with respect to ω_c

plt.plot(ω_c_values, expression_values,linewidth=0.9)

plt.xlabel('ω - ω$_{RESONANCE}$')

plt.ylabel(r'$\frac{\varepsilon_r}{2J_0(\beta)J_1(\beta)P_0}$', fontsize = 16)
```

```
plt.title('Normalized Error Signal for Low-Frequency Modulation')
plt.grid(False)  # Aqui, definimos grid como False para remover as grades
plt.show()
xticks = [-0.002,-0.001, 0.0,0.001, 0.002]
plt.xticks(xticks)
```

APPENDIX D – PYTHON CODE TO THE SIMULATION OF THE POUND-DREVER-HALL ERROR SIGNAL FOR HIGH-FREQUENCY MODULATION

```
# Simulation of the Pound-Drever-Hall Error Signal for High-Frequency Modulation

@author: João L. R. Daré

import numpy as np

import matplotlib.pyplot as plt

# Function R(ω, r)

def R(ω, r):

    return (r * (np.exp(1j * 1*(ω) )- 1)) / (1 - r**2 * np.exp(1j * 1*ω))

# Values of the constants Ω and r

Ω = 0.001 # Valor constante de Ω

r = 0.99999  # Valor constante de r

# Values of ω_c

ω_c_values = np.linspace(-0.002, 0.002, 100000)

# Calculate the imaginary part of the expression for various values of ω_c

imaginary_part_values = []

for ω_c in ω_c_values:

    term1 = R(ω_c, r) * np.conj(R(ω_c + Ω, r))

    term2 = np.conj(R(ω_c, r)) * R(ω_c - Ω, r)

    expression = (term1 - term2)*np.cos(2*Ω)

    imaginary_part_values.append(expression.imag)

# Creating a graph of the imaginary part with respect to ω_c

plt.plot(ω_c_values, imaginary_part_values, linewidth=0.9, color='#dc9c34')

plt.xlabel('ω - ω$_{RESONANCE}$')

plt.ylabel(r'$\frac{\varepsilon_r}{2J_0(\beta)J_1(\beta)P_0}$', fontsize = 16)
```

```
plt.title('Normalized Error Signal for Low abd High Frequency Modulation')
plt.grid(False)  # Here, we have defined the grid as False to remove the grids
xticks = [-0.002, 0.0, 0.002]
plt.xticks(xticks)
plt.show()
```

APPENDIX E – PYTHON CODE TO AUTOMATIZE OSCILLOSCOPE DATA COLLECTION

```
import pyvisa

import time

import pygame

from pygame import mixer

import pandas as pd

import numpy as np

from datetime import date

from pathlib import Path

import time

import os


# Definition of the oscilloscope data parameters, they can be found on the manual of your oscilloscope

def channel_data(instrument, channel, n_points_mode, n_points):


    instrument.write(f':DIGitize [CHANnel{channel}:]')

    instrument.write(f':WAVeform:SOURce CHANnel{channel}')

    instrument.write(f':WAVeform:FORMat ASCii')

    instrument.write(f':WAVeform:POINts:MODE {n_points_mode}')

    instrument.write(f':WAVeform:POINts {n_points}')

    instrument.write(':WAVeform:DATA?')


    values = [n for n in instrument.read().replace(' ', ',').split(',')]

    data_list = list(map(float,filter(None,values[1:])))
```

```
    return data_list

def time_vector(instrument, channel, n_points_mode, n_points):

    instrument.write(f':DIGitize [CHANnel{channel}:]')
    instrument.write(f':WAVeform:SOURce CHANnel{channel}')
    instrument.write(f':WAVeform:FORMat ASCii')
    instrument.write(f':WAVeform:POINts:MODE {n_points_mode}')
    instrument.write(f':WAVeform:POINts {n_points}')

    instrument.write(':WAVeform:XORigin?')
    x_0 = float(instrument.read())

    instrument.write(':WAVeform:XINCrement?')
    dx= float(instrument.read())

    array = np.linspace(x_0, x_0 + n_points * dx, n_points)

    return array

rm = pyvisa.ResourceManager()
inst_addr_list = rm.list_resources()
osc_addr = "USB0::0x0957::0x175D::MY50340840::INSTR" #USB port, can be found
at the back of the oscilloscope or by the lines below, just uncomment them:
```

```
####################

# # Initiate o resource generator

# rm = pyvisa.ResourceManager()


# # List all the resources available

# resources = rm.list_resources()


# # Filter only the address of the UBS ports

# usb_resources = [resource for resource in resources if 'USB' in resource]


# # exhibit the addresses of the UBS ports

# print("Endereços das portas USB disponíveis:")

# for resource in usb_resources:

#     print(resource)

####################

# lab LMO: "USB0::0x0957::0x175D::MY50340840::INSTR"

# lab FELINTO: "USB0::0x0957::0x1798::MY51138309::INSTR"


# Definition of the Path to save the data

path = r'C:\Users\deskl\OneDrive\Documentos\Daré\Cavidades\Pequena\Dados Coletados\Janeiro 2025\Laser Comercial'

# channels used: to add one, for example, just add channel_3 = 3

channel_1 = 1

channel_2 = 2

# total points collected in each round
```

```
total_points = 10000

# number of files that will be collected

rounds = 500

# frequency, voltage and offset of the signal to put at the name of the file, it does not influence the data collection and can be removed

frequency = 1

voltage = 20

offset = 10


today = date.today().strftime('%d_%m_%Y')

hour = time.strftime("%H_%M", time.localtime())

output_dir = rf'{path}\{today}\{hour}'

output_avg_dir = rf'{path}\{today}\Médias\{hour}'

Path(output_dir).mkdir(parents=True, exist_ok=True)

Path(output_avg_dir).mkdir(parents=True, exist_ok=True)


if inst_addr_list.count(osc_addr) >= 1:

    pass

else:

    ValueError(f'Error: Oscilloscope address "{osc_addr}" does not exist')


osc_inst = rm.open_resource(osc_addr)


file_paths = []
```

```
for i in range(rounds):

    osc_inst.write(':STOP')

    x_vector = time_vector(osc_inst, channel_1, 'MAXimum', total_points)

    data_1 = channel_data(osc_inst, channel_1, 'MAXimum', total_points)
    data_2 = channel_data(osc_inst, channel_2, 'MAXimum', total_points)
    # if more channels are used, just uncomment the line below and add the channel number
    # data_3 = channel_data(osc_inst, channel_3, 'MAXimum', total_points)

    osc_inst.write(':RUN')

    if len(x_vector) != len(data_1) or len(x_vector) != len(data_2):
        minimum = min([len(x_vector), len(data_1), len(data_2)])
        x_vector = x_vector[:minimum]
        data_1 = data_1[:minimum]
        data_2 = data_2[:minimum]
        # if more channels are used, just uncomment the line below and add the channel number
        # data_3 = data_3[:minimum]

    print(len(x_vector), len(data_1), len(data_2))
    f_data = pd.DataFrame({'second': x_vector, 'Volt': data_1, 'Volt.1': data_2})
```

```
    file_name = rf'{frequency}hz_{voltage}v_{offset}of_coleta_{i+1}.csv'
    file_path = os.path.join(output_dir, file_name)
    f_data.to_csv(file_path, sep=';', index=False, header=True)
    file_paths.append(file_path)

    print(f'Coleta feita: {i+1} de {rounds}')

    time.sleep(2)

# Calculate the mean of the total collection
all_data = []
for file_path in file_paths:
    df = pd.read_csv(file_path, sep=';')
    all_data.append(df)

# Calculate the average point by point
mean_data = pd.concat(all_data).groupby(level=0).mean()

# save the average data
mean_file_path = os.path.join(output_avg_dir,
f'{frequency}_{voltage}v_{offset}of__media.csv')
mean_data.to_csv(mean_file_path, sep=';', index=False, header=True)

print(f'Arquivo com valores médios salvo em: {mean_file_path}')
```

```
print("COLETA FINALIZADA!")


# Play a sound when the collection is finished, does not influence the collection and can be removed

mixer.init()

mixer.music.load(r"C:\Users\deskl\OneDrive\Documentos\Daré\Cavidades\musica\Coleta FINALIZADA.mp3") # path to the sound file

pygame.mixer.music.set_volume(0.1)

mixer.music.play()

while mixer.music.get_busy():  # wait for music to finish playing

    time.sleep(1)
```

APPENDIX F – PYTHON CODE TO NORMALIZE THE OSCILLOSCOPE DATA

```
# Import the libraries


import pandas as pd

import os

import numpy as np


# PATH TO THE ORIGINAL OSCILLOSCOPE FILE, DATA SOURCE

path_1 = r'C:\Users\deskl\OneDrive\Documents\Daré\Cavities\Small\Collected Data\January 2025\Commercial Laser\16_01_2025'


# PATH TO SAVE THE FILE TO BE USED TO CREATE THE FREQUENCY RULER

path_2 = r'C:\Users\deskl\OneDrive\Documents\Daré\Cavities\Small\Collected Data\January 2025\Commercial Laser\16_01_2025\08_24'


# Name of the new destination folder

path_day = r'C:\Users\deskl\OneDrive\Documents\Daré\Cavities\Small\Processed Data\Normalized Data\Finesse\January 2025'


# Names of the new destination folders

folder_day_name = os.path.basename(path_1)

folder_destiny_name = os.path.basename(path_2) + " Normalized"


folder_day = os.path.join(path_day, folder_day_name)

folder_destiny = os.path.join(folder_day, folder_destiny_name)


os.makedirs(folder_day, exist_ok=True)

os.makedirs(folder_destiny, exist_ok=True)


#### CODE TO CREATE A FILE WITH NORMALIZED DATA OF THE TRANSMISSION SIGNAL ####
```

```
# Select the background noise
noise = [i for i in os.listdir(path_2) if i.endswith('_noise.csv')]

noise_file = os.path.join(path_2, noise[0])

noise_data = pd.read_csv(noise_file, header=0, sep=';')

# Iterate over all files in the directory
for file in os.listdir(path_2):

    # Check if the file is a CSV
    if file.endswith('.csv') and not file.endswith("_noise.csv"):
        # Full file path

        file_path = os.path.join(path_2, file)

        # Load data from the files
        data = pd.read_csv(file_path, header=0, sep=';')

        # Remove spaces from column names
        data.columns = data.columns.str.strip()
        noise_data.columns = noise_data.columns.str.strip()

        # Variables (only the first y column)
        x = data['second']
        y = data['Volt']  # First y column of the data
        y_noise = noise_data['Volt']  # First y column of the corresponding noise, MUST BE THE SAME COLUMN AS THE DATA
        y1 = data['Volt.1']

        # Subtract the noise signal
```

```
y = y - y_noise

# Normalize the data
x = x - x.min()
x = x / (x.max() - x.min())

y = y - y.min()
y = y / (y.max() - y.min())

y1 = y1 - y1.min()
y1 = y1 / (y1.max() - y1.min())

# Save only the first normalized column in a new CSV file
normalized_file_name = os.path.splitext(file)[0] + '_normalized.csv'
output_path = os.path.join(folder_destiny, normalized_file_name)
df_normalized = pd.DataFrame({'x': x, 'signal': y, 'ramp': y1})
df_normalized.to_csv(output_path, index=False)
print("File saved at:", output_path)
```

APPENDIX G – PYTHON CODE TO PLOT THE CURVE OF CURRENT VERSUS POWER

```
import numpy as np
import pandas as pd
import matplotlib.pyplot as plt
import os
import ruptures as rpt

# Defining the path
path = r'C:\Users\deskl\OneDrive\Documents\Daré\Dissertation\Data\New folder'
# Creating the folder to save the graphs
folder_name = 'Current vs Power Graphs for ECDL'
folder_destiny = os.path.join(path, folder_name)

os.makedirs(folder_destiny, exist_ok=True)
plt.figure(figsize=(12, 6))
# Accessing the files in the folder
for file in os.listdir(path):
    if file.endswith('Commercial Laser_.csv'):
        file_path = os.path.join(path, file)
        data = pd.read_csv(file_path, header=0, sep=';')
        data.columns = data.columns.str.strip()

        Current = data['Current - mA']
        Power = data['Power - mW']
```

```
# If there is an unstable regime, you can use this mask to remove it. If not, you can just use the original datasets

mask = Current < 140  # stable regime


Current_stable = Current[mask]

Power_stable = Power[mask]


# Finding the threshold current, by detecting the point where the slope changes from a constant value to a linear curve

signal = Power.values

algo = rpt.Pelt(model="rbf").fit(signal)

result = algo.predict(pen=30)


# Plotting the figure

plt.plot(Current_stable, Power_stable, label='Laser Intensity', color='#0c3fa5')

for cp in result:

    # You can adjust Current.iloc[20] to the point of your threshold current

    plt.axvline(x=Current.iloc[20], color='#ef8c14', linestyle='--', label=f'Threshold Current = {Current.iloc[20]:.2f} mA' if cp == result[0] else "")

plt.xlabel('Current (mA)', fontsize=13)

plt.ylabel('Power (mW)', fontsize=13)

plt.legend(fontsize=13)

plt.title(f'Power x Current Curve for the {file.split("_")[2]} {file.split("_")[3]}', fontsize=14)

plt.grid(True)
```

```
        graph_name = f'Graph of Power x Current for {file.split("_")[2]} {file.split("_")[3]}.png'

        # Save the graph

        output_graph = os.path.join(folder_destiny, graph_name)

        plt.savefig(os.path.join(output_graph))

        plt.show()
```

APPENDIX H – PYTHON CODE TO PLOT THE LASER'S SPECTRUM

```
import numpy as np

import pandas as pd

import matplotlib.pyplot as plt

from scipy.signal import find_peaks

from scipy.interpolate import interp1d

import os


# Path to directories

path_1 = r'C:\Users\deskl\OneDrive\Documents\Daré\Dissertation\Raw Data\07-02-2025'

path_2 = r'C:\Users\deskl\OneDrive\Documents\Daré\Ocean\Littman\20.04ºC\Without Grating\230 mA'

# PATH TO SAVE THE FILE TO BE USED FOR MAKING THE FREQUENCY SCALE

path_graph = r'C:\Users\deskl\OneDrive\Documents\Daré\Dissertation\Processed Data\Graphs'

# Create destination directories to save the graphs

folder_day_name_graphs = os.path.basename(path_1)

folder_destiny_name_graphs = os.path.basename(path_2) + " Spectrum Graph"


folder_day_graphs = os.path.join(path_graph, folder_day_name_graphs)

folder_destiny_graphs=os.path.join(folder_day_graphs,folder_destiny_name_graphs)


os.makedirs(folder_day_graphs, exist_ok=True)

os.makedirs(folder_destiny_graphs, exist_ok=True)
```

```
# Process files in the folder
for file in os.listdir(path_2):
    # Full path to the normalized file
    file_path = os.path.join(path_2, file)

    # Load normalized data
    data = pd.read_csv(file_path, sep=';', header=0)

    data.columns = data.columns.str.strip()

    Wavelength = data['Wavelength - nm']
    Intensity = data['Intensity']

    # Filter data within the desired wavelength range
    mask = (Wavelength > 1040) & (Wavelength < 1075)
    Wavelength_zoom = Wavelength[mask]
    Intensity_zoom = Intensity[mask]

    # Normalize intensity
    Intensity_normalized = Intensity_zoom / Intensity_zoom.max()

    # Limits for peak detection
    lower_limit = 0.9  # replace with the desired lower limit
```

```
upper_limit = 1.1 # replace with the desired upper limit


# Find peaks within the y range
peak_indices, _ = find_peaks(Intensity_normalized, height=(lower_limit, upper_limit))


Peak_wavelength = Wavelength_zoom.iloc[peak_indices]


# Create the graph
plt.figure(figsize=(12, 24))
plt.title(f"ECDL Laser's Spectrum without Grating for 30.3 mA and at 20.04ºC", fontsize=20)
plt.plot(Wavelength_zoom, Intensity_normalized, label="Laser's Spectrum", color='#0c3fa5')
plt.axvline(x = Peak_wavelength.iloc[0], color='#ef8c14', linestyle='--', label = f'Central Wavelength of the main peak = {Peak_wavelength.iloc[0]:.2f} nm', linewidth=1.0)
# If there are more peaks, just uncomment the lines below and adjust the values
# plt.axvline(x = Peak_wavelength.iloc[1], color='green', linestyle='--', label = f'Central Wavelength of the secondary peak = {Peak_wavelength.iloc[1]:.2f} nm', linewidth=1.0)
# plt.axvline(x = Peak_wavelength.iloc[2], color='red', linestyle='--', label = f'Central Wavelength of the secondary peak = {Peak_wavelength.iloc[2]:.2f} nm', linewidth=1.0)
plt.xticks(fontsize=20)
plt.yticks(fontsize=20)
plt.xlabel('Wavelength (nm)', fontsize=20)
plt.ylabel('Normalized Intensity', fontsize=20)
```

```
    plt.legend(fontsize=18)
    plt.grid('true')


    # Save the graph
    spectrum_graph_name = f'Spectrum of the {file.split('_')[0]} for a Current of {file.split('_')[1]}.png'
    output_graph_lifetime=os.path.join(folder_destiny_graphs, spectrum_graph_name)
    plt.savefig(output_graph_lifetime)
    plt.show()
    plt.close()
```

APPENDIX I – PYTHON CODE TO FIND THE CAVITY FINISSE

```
import pandas as pd

import numpy as np

import matplotlib.pyplot as plt

import os

from scipy.signal import find_peaks

from scipy.optimize import curve_fit


                                    #### Caminho dos arquivos ####


# CAMINHO PARA O ARQUIVO ORIGINAL DO OSCILOSCÓPIO, FONTE DOS DADOS

path_1 = r'C:\Users\deskl\OneDrive\Documentos\Daré\Cavidades\Pequena\Dados Tratados\Dados normalizados\Finesse\Janeiro 2025\16_01_2025'


# CAMINHO PARA O ARQUIVO NORMALIZADO UTILIZADO

path_2 = r'C:\Users\deskl\OneDrive\Documentos\Daré\Cavidades\Pequena\Dados Tratados\Dados normalizados\Finesse\Janeiro 2025\16_01_2025\08_24 Normalizado'


# Caminho para salvar os gráficos da FINESSE

path_dia = r'C:\Users\deskl\OneDrive\Documentos\Daré\Cavidades\Pequena\Dados Tratados\Gráficos com a Finesse\Cavidade Pequena\Janeiro 2025'


# Certifique-se de que o diretório para os gráficos exista
```

```
folder_day_name_graficos = os.path.basename(path_1)

folder_destiny_name_graficos = os.path.basename(path_2) + " Finesse"


folder_day_graficos = os.path.join(path_dia, folder_day_name_graficos)

folder_destiny_graficos = os.path.join(folder_day_graficos, folder_destiny_name_graficos)


os.makedirs(folder_day_graficos, exist_ok=True)

os.makedirs(folder_destiny_graficos, exist_ok=True)


frequencias_modulacao = {}  # Dicionário para armazenar frequências


larguras_fwhm = []  # Lista para armazenar as larguras a meia altura

erro_larguras_fwhm = []  # Lista para armazenar os erros das larguras a meia altura

erro_centro_picos_ajustados = []  # Lista para armazenar os erros dos centros dos picos ajustados


erro_Finesse_coleta = []  # Lista para armazenar os erros das Finesses de todos os picos do arquivo


finesse_coleta = []  # Lista para armazenar as Finesses de todos os arquivos

amp_coleta = []  # Lista para armazenar as amplitudes de todos os arquivos

wid_coleta = []  # Lista para armazenar as larguras de todos os arquivos

arquivos_utilizados = []  # Lista para armazenar os arquivos utilizados

picos_usados = []
```

```
# Percorrer todos os arquivos no diretório de arquivos normalizados
for arquivo in os.listdir(path_2):
    # Verificar se o arquivo é um CSV
    if arquivo.endswith('_normalizado.csv'):
        # Caminho completo do arquivo normalizado
        caminho_arquivo = os.path.join(path_2, arquivo)

        # Extração de valores de voltagem e frequência do nome do arquivo
        frequencia = arquivo.split('_')[0]  # Frequência (ex: '1hz')
        voltagem = arquivo.split('_')[1][:-1]  # Voltagem (ex: '110v', removendo o 'v')

       # Extração da frequência de modulação do nome do arquivo (por exemplo, '1hz')
        frequencia_modulacao = float(frequencia.replace("hz", ""))  # Converter para número float
        # Armazenar a frequência no dicionário com a chave sendo o nome do arquivo
        frequencias_modulacao[arquivo] = frequencia_modulacao

        # Calcular o período da modulação (T = 1 / f)
        periodo_modulacao = 1 / frequencia_modulacao

          print(f"Arquivo da {arquivo.split('_')[3]} {arquivo.split('_')[4]}, Frequência de Modulação: {frequencia_modulacao} Hz, Período de Modulação: {periodo_modulacao} s")

        # Carregar os dados normalizados
```

```
dados = pd.read_csv(caminho_arquivo)


# Criar o título do gráfico
  titulo_grafico = f"Finesse Value for a {voltagem} Volts Modulation Ramp of {frequencia} Repeat Frequency"


# Extrair colunas x e y
x_regua = dados['x']
y_regua = dados['sinal']
y_rampa = dados['rampa']


# Definir o regime de y para localizar picos
limite_inferior = 0.6  # substitua pelo limite inferior desejado
limite_superior = 1.1  # substitua pelo limite superior desejado


limite_inferior_maximos = 0.95
limite_superior_maximos = 1.1


# Localizar picos dentro do regime de y
indices_picos, _ = find_peaks(y_regua, height=(limite_inferior, limite_superior))
  indices_maximos, _ = find_peaks(y_rampa, height=(limite_inferior_maximos, limite_superior))


if len(indices_maximos) > 1:
   # Calcular a distância entre os máximos consecutivos
```

```
            picos_x_rampa = x_regua.iloc[indices_maximos].dropna()  # Remover possíveis NaNs
        distancia_maximos = picos_x_rampa.diff().dropna()      # Calcular a diferença e remover NaNs
        if distancia_maximos.empty:
            print("Erro: Não foi possível calcular a distância entre máximos.")
        else:
            escala_tempo = periodo_modulacao / distancia_maximos.mean()
            print(f"Escala de tempo (usando máximos): {escala_tempo} s")
    else:
        print("Erro: Número insuficiente de picos máximos encontrados.")

    # Verifique se o arquivo tem dois máximos e um mínimo ou dois mínimos e um máximo
    if len(indices_maximos) == 2:
        # Usar apenas os máximos para calcular a distância
        picos_x_rampa = x_regua.iloc[indices_maximos]
        picos_y_rampa = y_rampa.iloc[indices_maximos]
        # Calcular a distância entre os máximos consecutivos
        distancia_maximos = abs(picos_x_rampa.diff().dropna())
        escala_tempo = periodo_modulacao / distancia_maximos.mean()

    # Obter as posições dos picos nos eixos x e y para o SINAL
    picos_x = x_regua.iloc[indices_picos]
    picos_y = y_regua.iloc[indices_picos]
```

```
# Criar lista para preencher com os picos filtrados, que se encontram na janela de modulação
distancia_minima = 0.25
picos_filtrados_x = []
picos_filtrados_y = []

# filtrar os picos que se encontram apenas dentro da janela de modulação
if len(picos_x) > 1:
    for i in range(len(picos_x)):
        # The + 1 (or -1) is given by the modulation frequency, you can adjust it according to your needs
        if picos_x_rampa.iloc[0] <= picos_x.iloc[i] <= picos_x_rampa.iloc[0] + 1 or picos_x_rampa.iloc[1] - 1 <= picos_x.iloc[i] <= picos_x_rampa.iloc[1] and picos_x[1]-picos_x[0] > distancia_minima:
            picos_filtrados_x.append(picos_x.iloc[i])
            picos_filtrados_y.append(picos_y.iloc[i])

# Exibir os picos encontrados
if len(picos_filtrados_x) ==4 and len(picos_filtrados_y) ==4:
    print(f'Arquivo utilizado {arquivo.split('_')[3]} {arquivo.split('_')[4]}:')
for i in range(len(picos_filtrados_x)):
    print(f"Pico {i+1}: x = {picos_filtrados_x[i]}, y = {picos_filtrados_y[i]}")

# Nova escala de tempo para ser utilizada
x_tempo = x_regua * escala_tempo
```

```
# Plotar o gráfico com o eixo x na nova escala de tempo
plt.plot(x_tempo, y_regua, color='green', label='Fabry-Perot Trasmitted Signal')
plt.plot(x_tempo, y_rampa, color='blue', label='Modulation Ramp')
plt.plot([pico * escala_tempo for pico in picos_filtrados_x], picos_filtrados_y, 'ro')

  # Adicionar linhas tracejadas verticais nos picos de y_rampa (maximos ou minimos)
if len(indices_maximos) > 1:
    for pico in picos_x_rampa:  # Picos de y_rampa (máximos)
        delta_tempo_1_2_rampa = (picos_x_rampa.iloc[1] - picos_x_rampa.iloc[0]) * escala_tempo
        plt.arrow(picos_x_rampa.iloc[0] * escala_tempo, 1, (picos_x_rampa.iloc[1] - picos_x_rampa.iloc[0]) * escala_tempo, 0, head_width=0.02, head_length=0.005 * escala_tempo, fc='blue', ec='blue')
        plt.text(((picos_x_rampa.iloc[0] + picos_x_rampa.iloc[1]) / 2) * escala_tempo, 0.95, f'{delta_tempo_1_2_rampa:.3f} segundos', ha='center', color='blue')

# Calcular a diferença de tempo entre os picos 1 e 2, e 3 e 4
if len(picos_filtrados_x) == 4:
  delta_tempo_1_2 = (picos_filtrados_x[1] - picos_filtrados_x[0]) * escala_tempo
  delta_tempo_3_4 = (picos_filtrados_x[3] - picos_filtrados_x[2]) * escala_tempo
else:
    print('Menos de 4 picos encontrados')
```

```
                    ## FUNÇÃO PARA AJUSTE LORENTZIANO (PROXIMO AOS PICOS) ##
    larguras_fwhm = []
    centro_picos_ajustados = []

    def lorentzian(x, amp, cen, wid, offset):
        return amp * (wid**2) / ((x - cen)**2 + wid**2) + offset

    # separar os picos da rampa de descida
    picos_descida_x = picos_filtrados_x[:2]
    picos_descida_y = picos_filtrados_y[:2]

    # separar os picos da rampa de subida
    picos_subida_x = picos_filtrados_x[2:]
    picos_subida_y = picos_filtrados_y[2:]

    # definir os picos que serão utilizaveis para o ajuste, usar somente os picos que tem aproximadamente a mesma altura que o pico imediatamente adjacente
    picos_utilizaveis_x = []
    picos_utilizaveis_y = []

    # Função para verificar se dois picos têm alturas semelhantes
    def alturas_semelhantes(y1, y2, tolerancia=0.85):
        return min(y1, y2) / max(y1, y2) >= tolerancia
```

```
        # Verificar pares na rampa de descida
        if len(picos_descida_x) == 2:  # Garantir que há dois picos na rampa de descida
            if alturas_semelhantes(picos_descida_y[0], picos_descida_y[1]):
                picos_utilizaveis_x.append(picos_descida_x[0])
                picos_utilizaveis_x.append(picos_descida_x[1])
                picos_utilizaveis_y.append(picos_descida_y[0])
                picos_utilizaveis_y.append(picos_descida_y[1])

        # Verificar pares na rampa de subida
        if len(picos_subida_x) == 2:  # Garantir que há dois picos na rampa de subida
            if alturas_semelhantes(picos_subida_y[0], picos_subida_y[1]):
                picos_utilizaveis_x.append(picos_subida_x[0])
                picos_utilizaveis_x.append(picos_subida_x[1])
                picos_utilizaveis_y.append(picos_subida_y[0])
                picos_utilizaveis_y.append(picos_subida_y[1])

        # Exibir a quantidade de pares utilizáveis
        print(f'Quantidade de pares de picos utilizáveis: {len(picos_utilizaveis_x)}')

        if len(picos_utilizaveis_x) >= 1:
                        for i, (pico_x, pico_y) in enumerate(zip(picos_utilizaveis_x,
picos_utilizaveis_y)):

                # Definir o intervalo para o ajuste (por exemplo, 0.1s ao redor do pico)
```

```
limite_inferior = pico_x - 0.02
limite_superior = pico_x + 0.02

# Selecionar os dados no intervalo definido
    indices_intervalo = (x_regua >= limite_inferior) & (x_regua <= limite_superior)
x_intervalo = x_regua[indices_intervalo]
y_intervalo = y_regua[indices_intervalo]

# Estimativas iniciais para os parâmetros: amplitude, centro e largura
amp_inicial = np.max(y_intervalo)
cen_inicial = pico_x
wid_inicial = 0.002  # Valor inicial arbitrário para a largura
offset_inicial = np.min(y_intervalo)

try:

  # Realizar o ajuste de curva usando curve_fit
    parametros_ajuste, parametros_covariancia = curve_fit(lorentzian, x_intervalo, y_intervalo, p0=[amp_inicial, cen_inicial, abs(wid_inicial), offset_inicial], bounds = ([0, -np.inf, 0, 0], [np.inf, np.inf, np.inf, np.inf]), maxfev=50000)

  # Parâmetros ajustados
      amp_ajustado, cen_ajustado, wid_ajustado, offset_ajustado = parametros_ajuste
  print(f"Ajuste para o pico {i+1}:")
```

```
            print(f"Amplitude ajustada: {amp_ajustado}")
            print(f"Centro ajustado: {cen_ajustado}")
            print(f"Largura ajustada: {wid_ajustado}")

                    erro_amp_ajustado, erro_cen_ajustado, erro_wid_ajustado,
erro_offset_ajustado = np.sqrt(np.diag(parametros_covariancia))

            # Calcular o FWHM a partir da largura
            FWHM = 2 * wid_ajustado
            # Calcular o erro estatístico do FWHM
            erro_FWHM_ajustado = 2 * wid_ajustado * erro_wid_ajustado
                print(f"FWHM para o pico {i+1}: {FWHM} ± {erro_FWHM_ajustado}
segundos")
            larguras_fwhm.append(FWHM)
            erro_larguras_fwhm.append(erro_FWHM_ajustado)
            centro_picos_ajustados.append(cen_ajustado)
            erro_centro_picos_ajustados.append(erro_cen_ajustado)

            # Plot do ajuste de Lorentziana
            y_ajustado = lorentzian(x_intervalo, *parametros_ajuste)
            # Plota o ajuste
            if i == 0:  # Adiciona o label somente para o primeiro ajuste
                    plt.plot(x_intervalo*escala_tempo, y_ajustado, 'r--', label=f'Ajuste
Lorentziano', color = 'orange')
            else:
```

```
                plt.plot(x_intervalo*escala_tempo, y_ajustado, 'r--', color = 'orange')


            except RuntimeError as e:

                print(f"Erro ao ajustar o pico {i+1}: {e}")

        else:

                print(f'{arquivo.split('_')[3]} {arquivo.split('_')[4]} apresenta picos com divergencia em altura')

        if len(picos_utilizaveis_x) == 4:

            # Calcular a finesse

                                Finesse_pico_1 = (centro_picos_ajustados[1]-centro_picos_ajustados[0])/larguras_fwhm[0]

                                Finesse_pico_2 = (centro_picos_ajustados[1]-centro_picos_ajustados[0])/larguras_fwhm[1]

                                Finesse_pico_3 = (centro_picos_ajustados[3]-centro_picos_ajustados[2])/larguras_fwhm[2]

                                Finesse_pico_4 = (centro_picos_ajustados[3]-centro_picos_ajustados[2])/larguras_fwhm[3]


                        erro_FSR_1_2 = np.sqrt(erro_centro_picos_ajustados[0]**2 + erro_centro_picos_ajustados[1]**2)

                        erro_FSR_3_4 = np.sqrt(erro_centro_picos_ajustados[2]**2 + erro_centro_picos_ajustados[3]**2)

                                erro_Finesse_pico_1 = Finesse_pico_1 * np.sqrt((erro_FSR_1_2/(centro_picos_ajustados[1]- centro_picos_ajustados[0]))**2 + (erro_larguras_fwhm[0]/larguras_fwhm[0])**2)
```

```
                erro_Finesse_pico_2 = Finesse_pico_2 * np.sqrt((erro_FSR_1_2/(centro_picos_ajustados[1]- centro_picos_ajustados[0]))**2 + (erro_larguras_fwhm[1]/larguras_fwhm[1])**2)

                erro_Finesse_pico_3 = Finesse_pico_3 * np.sqrt((erro_FSR_3_4/(centro_picos_ajustados[3]- centro_picos_ajustados[2]))**2 + (erro_larguras_fwhm[2]/larguras_fwhm[2])**2)

                erro_Finesse_pico_4 = Finesse_pico_4 * np.sqrt((erro_FSR_3_4/(centro_picos_ajustados[3]- centro_picos_ajustados[2]))**2 + (erro_larguras_fwhm[3]/larguras_fwhm[3])**2)

            if Finesse_pico_1 >= 150:
                finesse_coleta.append(Finesse_pico_1)
                erro_Finesse_coleta.append(erro_Finesse_pico_1)
            if Finesse_pico_2 >= 150:
                finesse_coleta.append(Finesse_pico_2)
                erro_Finesse_coleta.append(erro_Finesse_pico_2)
            if Finesse_pico_3 >= 150:
                finesse_coleta.append(Finesse_pico_3)
                erro_Finesse_coleta.append(erro_Finesse_pico_3)
            if Finesse_pico_4 >= 150:
                finesse_coleta.append(Finesse_pico_4)
                erro_Finesse_coleta.append(erro_Finesse_pico_4)
            print(f"Finesse do pico 1: {Finesse_pico_1} ± {erro_Finesse_pico_1}")
            print(f"Finesse do pico 2: {Finesse_pico_2} ± {erro_Finesse_pico_2}")
            print(f"Finesse do pico 3: {Finesse_pico_3} ± {erro_Finesse_pico_3}")
            print(f"Finesse do pico 4: {Finesse_pico_4} ± {erro_Finesse_pico_4}")
```

```
                plt.text(picos_filtrados_x[0] * escala_tempo, picos_filtrados_y[0]/2 , r'$\mathcal{F}$ ' f'= {Finesse_pico_1:.3f} ± {erro_Finesse_pico_1: .3f}', ha='center', color='black')

                plt.text(picos_filtrados_x[1] * escala_tempo, picos_filtrados_y[1]/2 , r'$\mathcal{F}$ ' f'= {Finesse_pico_2:.3f} ± {erro_Finesse_pico_2: .3f}', ha='center', color='black')

                plt.text(picos_filtrados_x[2] * escala_tempo, picos_filtrados_y[2]/2 , r'$\mathcal{F}$ ' f'= {Finesse_pico_3:.3f} ± {erro_Finesse_pico_3: .3f}', ha='center', color='black')

                plt.text(picos_filtrados_x[3] * escala_tempo, picos_filtrados_y[3]/2 , r'$\mathcal{F}$ ' f'= {Finesse_pico_4:.3f} ± {erro_Finesse_pico_4: .3f}', ha='center', color='black')

            else:

                    erro_FSR_1_2 = np.sqrt(erro_centro_picos_ajustados[0]**2 + erro_centro_picos_ajustados[1]**2)


                                Finesse_pico_1 = (centro_picos_ajustados[1]- centro_picos_ajustados[0])/larguras_fwhm[0]

                                Finesse_pico_2 = (centro_picos_ajustados[1]- centro_picos_ajustados[0])/larguras_fwhm[1]

                                    erro_Finesse_pico_1 = Finesse_pico_1 * np.sqrt((erro_FSR_1_2/(centro_picos_ajustados[1]- centro_picos_ajustados[0]))**2 + (erro_larguras_fwhm[0]/larguras_fwhm[0])**2)

                                    erro_Finesse_pico_2 = Finesse_pico_2 * np.sqrt((erro_FSR_1_2/(centro_picos_ajustados[1]- centro_picos_ajustados[0]))**2 + (erro_larguras_fwhm[1]/larguras_fwhm[1])**2)


            if Finesse_pico_1 >= 150:

                finesse_coleta.append(Finesse_pico_1)
```

```
            erro_Finesse_coleta.append(erro_Finesse_pico_1)
        if Finesse_pico_2 >= 150:
            finesse_coleta.append(Finesse_pico_2)
            erro_Finesse_coleta.append(erro_Finesse_pico_2)

        print(f"Finesse do pico 1: {Finesse_pico_1} ± {erro_Finesse_pico_1}")
        print(f"Finesse do pico 2: {Finesse_pico_2} ± {erro_Finesse_pico_2}")

            plt.text(picos_filtrados_x[0] * escala_tempo, picos_filtrados_y[0]/2 , r'$\mathcal{F}$ ' f'= {Finesse_pico_1:.3f} ± {erro_Finesse_pico_1: .3f}', ha='center', color='black')
            plt.text(picos_filtrados_x[1] * escala_tempo, picos_filtrados_y[1]/2 , r'$\mathcal{F}$ ' f'= {Finesse_pico_2:.3f} ± {erro_Finesse_pico_2: .3f}', ha='center', color='black')
        # salvar o gráfico
        nome_grafico_finesse = os.path.splitext(arquivo)[0] + '_FINESSE.png'
            output_grafico_finesse = os.path.join(folder_destiny_graficos, nome_grafico_finesse)

        if len(picos_utilizaveis_x) == 4:
                Finesse_arquivo = (Finesse_pico_1+Finesse_pico_2+Finesse_pico_3+Finesse_pico_4)/4
                erro_Finesse_arquivo = Finesse_arquivo * np.sqrt((erro_Finesse_pico_1/Finesse_pico_1)**2 +
(erro_Finesse_pico_2/Finesse_pico_2)**2 +
(erro_Finesse_pico_3/Finesse_pico_3)**2 +
(erro_Finesse_pico_4/Finesse_pico_4)**2)
```

```
                print(f"Finesse da Coleta com 4 picos utilizaveis: {Finesse_arquivo} ± {erro_Finesse_arquivo}")
                amp_coleta.append(amp_ajustado)
                wid_coleta.append(wid_ajustado)
                picos_usados.append(picos_utilizaveis_x)

            else:
                Finesse_arquivo = (Finesse_pico_1+Finesse_pico_2)/2
                erro_Finesse_arquivo = Finesse_arquivo * np.sqrt((erro_Finesse_pico_1/Finesse_pico_1)**2 + (erro_Finesse_pico_2/Finesse_pico_2)**2)
                print(f"Finesse da Coleta com 2 picos utilizaveis: {Finesse_arquivo} ± {erro_Finesse_arquivo}")
                amp_coleta.append(amp_ajustado)
                wid_coleta.append(wid_ajustado)
                picos_usados.append(picos_utilizaveis_x)


            plt.plot([], [], ' ', label= f"Lorentzian Finesse Average: {Finesse_arquivo:.3f} ± {erro_Finesse_arquivo:.3f}")
            plt.xlabel('Tempo (s)')
            plt.ylabel('Voltagem (normalizada)')
            # Plotar o gráfico com o título
            plt.title(titulo_grafico)
            plt.legend()
            plt.grid(True)
```

```
            plt.savefig(output_grafico_finesse)
            plt.close()
            arquivos_utilizados.append(arquivo)
        # Remover arquivos que não possuem 4 picos utilizáveis
        if arquivo not in arquivos_utilizados:
            os.remove(caminho_arquivo)
                print(f'Arquivo da {arquivo.split('_')[3]} {arquivo.split('_')[4]} removido com sucesso!')
if len(finesse_coleta) > 0:
    pesos = 1/np.array(erro_Finesse_coleta)**2
    finesse_coleta_media = sum(np.array(finesse_coleta)*pesos)/sum(pesos)
    erro_Finesse_coleta_media = np.sqrt(1/sum(pesos))
    largura_media = sum(wid_coleta) / len(wid_coleta)
    amplitude_media = sum(amp_coleta) / len(amp_coleta)
    finesse_coleta_average = sum(finesse_coleta)/len(finesse_coleta)
    erro_average = np.std(finesse_coleta)/np.sqrt(len(finesse_coleta))
    print(f'Quantidade de picos utilizadas: {len(finesse_coleta)} picos')
    print(f"Finesse média da Cavidade Média Ponderada: {finesse_coleta_media:.5f} ± {erro_Finesse_coleta_media:.5f}")
    print(f"Finesse média da Cavidade Média Aritmética: {finesse_coleta_average:.5f} ± {erro_average:.5f}")
    print(f"Largura média da Cavidade: {largura_media:.5f}")
    print(f"Amplitude média da Cavidade: {amplitude_media:.5f}")
```

APPENDIX J – PYTHON CODE TO FIND THE PHOTON LIFETIME INSIDE THE CAVITY

```
import ruptures as rpt

import pandas as pd

import matplotlib.pyplot as plt

import os

import numpy as np

from scipy.optimize import curve_fit

from scipy.stats import norm

from scipy.special import erf


# CAMINHO PARA O ARQUIVO ORIGINAL DO OSCILOSCÓPIO, FONTE DOS DADOS

path_1 = r'C:\Users\deskl\OneDrive\Documentos\Daré\Cavidades\Pequena\Dados Coletados\Janeiro 2025\Laser Comercial\16_01_2025'

path_2 = r'C:\Users\deskl\OneDrive\Documentos\Daré\Cavidades\Pequena\Dados Coletados\Janeiro 2025\Laser Comercial\16_01_2025\16_48 foton'


# CAMINHO PARA SALVAR O ARQUIVO A SER UTILIZADO PARA FAZER A REGUA DE FREQUÊNCIA

path_dia = r'C:\Users\deskl\OneDrive\Documentos\Daré\Cavidades\Pequena\Dados Tratados\Dados normalizados\Tempo de vida do Foton\Janeiro 2025'


path_grafico = r'C:\Users\deskl\OneDrive\Documentos\Daré\Cavidades\Pequena\Dados Tratados\Grafico do Tempo de vida do Fóton\Janeiro 2025'


# Nome das novas pastas de destino
```

```
folder_day_name = os.path.basename(path_1)

folder_destiny_name = os.path.basename(path_2) + " Normalizado"


folder_day_name_graficos = os.path.basename(path_1)

folder_destiny_name_graficos= os.path.basename(path_2) + " Graficos"


folder_day = os.path.join(path_dia, folder_day_name)

folder_destiny = os.path.join(folder_day, folder_destiny_name)


folder_day_graficos = os.path.join(path_grafico, folder_day_name_graficos)

folder_destiny_graficos = os.path.join(folder_day_graficos,
folder_destiny_name_graficos)


os.makedirs(folder_day_graficos, exist_ok=True)

os.makedirs(folder_destiny_graficos, exist_ok=True)


os.makedirs(folder_day, exist_ok=True)

os.makedirs(folder_destiny, exist_ok=True)


Constante_de_tempo_coleta = []

erro_Constante_de_tempo_coleta = []


#### CÓDIGO PARA CRIAR UM ARQUIVO COM OS DADOS NORMALIZADOS
DO TEMPO DE VIDA DO FOTON ####
```

```
# Percorrer todos os arquivos no diretório
for arquivo in os.listdir(path_2):

    # Verificar se o arquivo é um CSV
    if arquivo.endswith('.csv') and not arquivo.endswith("_ruido.csv"):
        plt.clf()

        # Caminho completo do arquivo
        caminho_arquivo = os.path.join(path_2, arquivo)

        # Carregar os dados dos arquivos
        data = pd.read_csv(caminho_arquivo, header=0, sep=';')

        # Remover espaços dos nomes das colunas
        data.columns = data.columns.str.strip()

        # Variáveis
        x = data['second']
        y = data['Volt']  # Primeira coluna de y dos dados

        if max(y) > 0.0050:
         dado_filtrado = data[data['Volt'] < 0.007]

         if not dado_filtrado.empty:
```

```
x_filtrado = dado_filtrado['second']
y_filtrado = dado_filtrado['Volt']

dado_suavizado = dado_filtrado.rolling(window=1).mean()
x_suavizado = dado_suavizado['second']
y_suavizado = dado_suavizado['Volt']

# Detectar mudanças de regime usando ruptures
signal = y_suavizado.dropna().values  # Remover valores NaN
algo = rpt.Pelt(model="rbf").fit(signal)
result = algo.predict(pen=25)

combined_intervals = []
# identificar os regimes
regimes = [(result[i], result[i+1]) for i in range(len(result)-1)]

        # Definição do teste de Chauvenet

def chauvenet_criteria(dado_suavizado, media, desvio_padrao, N,
threshold=1/2):
    media = np.mean(dado_suavizado)  # Média dos pontos  do regime
    desvio_padrao = np.std(dado_suavizado)  # Desvio padrão dos pontos do
regime
    N = len(dado_suavizado)  # Número de pontos do regime
    deviations = np.abs(dado_suavizado - media) / desvio_padrao
```

```
        prob = 1 - (2 * (1 - 0.5 * (1 + erf(deviations / np.sqrt(2)))))
        return prob > threshold / N

    def apply_chauvenet(signal, result):
        filtered_signal = np.copy(signal)
        start = 0

        for end in result:
            sub_regime = signal[start:end]
            mean_chauvenet = np.mean(sub_regime)
            std_dev_chauvenet = np.std(sub_regime)
            N_chauvenet = len(sub_regime)

            if N_chauvenet > 1:  # Evita cálculo com regimes muito curtos
                mask = chauvenet_criteria(sub_regime, mean_chauvenet,
std_dev_chauvenet, N_chauvenet)
                sub_regime_filtered = sub_regime[mask]
                # Substitui os valores fora do critério com a média do regime
                filtered_signal[start:end] = np.where(mask, sub_regime,
np.mean(sub_regime))
            start = end
        return filtered_signal

    filtered_signal = apply_chauvenet(signal, result)
    # fim da definição do teste de Chauvenet
```

```
        # Comparar a média do primeiro regime com o próximo
        if len(regimes) > 1:
            first_start, first_end = regimes[0]
            second_start, second_end = regimes[1]

        mean_first = y_suavizado.iloc[first_start:first_end].mean()
        mean_second = y_suavizado.iloc[second_start:second_end].mean()

        # se a média do primeiro for menor que a do segundo, então descartamos o primeiro regime
        if mean_first < mean_second:
            regimes = regimes[1:] # começa do segundo regime

        if len(regimes) > 1:  # Garantir que há pelo menos dois regimes para comparar
            last_start, last_end = regimes[-1]
            penultimate_start, penultimate_end = regimes[-2]

            mean_last = y_suavizado.iloc[last_start:last_end].mean()
            mean_penultimate = y_suavizado.iloc[penultimate_start:penultimate_end].mean()

            if mean_last > mean_penultimate:
                regimes = regimes[:-1]  # Remover o último regime
```

```
# Agrupar os regimes em pares parte alta + parte baixa
for i in range(0, len(regimes)-1, 2):
   if i + i < len(regimes): # garantir que ha ao menos um par
       start = regimes[i][0]
       end = regimes[i+1][1] # incluir o final do proximo regime
       combined_intervals.append((start, end))

# Função para o ajuste com decaimento exponencial
def transition_model(t, a, b, c, d, tau):
    return np.where(
       t < c, a,
       b + (a - b) * np.exp(-(t - c) / tau)
    ) + d
# Ajustar o modelo em cada intervalo
fitted_params = []
covariances = []
constante_tempo = []
erro_constante_tempo = []

for i, (start, end) in enumerate(combined_intervals):
    plt.clf()
    regime_data = y_suavizado.iloc[start:end].values
```

```
            regime_time = x_suavizado.iloc[start:end].values


              # Aplicar o teste de Chauvenet para remover outliers
            regime_data = apply_chauvenet(regime_data, result)
            regime_time = regime_time[:len(regime_data)]  # Ajustar o tempo para corresponder aos dados filtrados


            # Redefinir o eixo x para começar em zero
            regime_time_zeroed = regime_time - regime_time[0]


            # Normalização do regime
            min_val = regime_data.min()
            max_val = regime_data.max()
            normalized_data = (regime_data - min_val) / (max_val - min_val)


            try:
                # Valores iniciais estimados: [amplitude alta, amplitude baixa, tempo de transição, offset, constante de tempo]
                inicial_guess = [mean_first, mean_second, regime_time_zeroed.mean(), 0.005, 0.0001]
                popt, pcov = curve_fit(transition_model, regime_time_zeroed, normalized_data, p0=inicial_guess, maxfev=30000)


                amp_a_ajustado, amp_b_ajustado, c_ajustado, d_ajustado, tau_ajustado = popt
```

```
            erro_amp_a_ajustado, erro_amp_b_ajustado, erro_c_ajustado,
erro_d_ajustado, erro_tau_ajustado = np.sqrt(np.diag(pcov))
            fitted_params.append(popt)
            covariances.append(pcov)
            if erro_tau_ajustado < tau_ajustado and 0 < tau_ajustado <= 0.001:
                constante_tempo.append(tau_ajustado)
                erro_constante_tempo.append(erro_tau_ajustado)
                Constante_de_tempo_coleta.append(tau_ajustado)
                erro_Constante_de_tempo_coleta.append(erro_tau_ajustado)

            # gerar o modelo ajustado
            y_fit = transition_model(regime_time_zeroed, *popt)

        except RuntimeError:
            print(f"Ajuste falhou para o intervalo {i+1}")
            continue
        if erro_tau_ajustado < tau_ajustado and 0 < tau_ajustado <= 0.001:
            plt.figure(figsize=(10, 10))
            plt.plot(regime_time_zeroed, normalized_data, label='Sinal',
color='#0c3fa5')
            plt.plot(regime_time_zeroed, y_fit, label=f'Ajuste do intervalo {i+1}, tau =
{tau_ajustado:.7} ± {erro_tau_ajustado:.7} ', color='#ef8c14', linestyle='--')
            plt.xlabel('Tempo')
            plt.ylabel('Tensão')
            plt.legend()
```

```
            plt.title('Ajuste dos Intervalos com Decaimento Exponencial')
            #  plt.show()
            # Salvar as constantes de tempo em um arquivo CSV
            output_file = os.path.join(folder_destiny, f"Constantes_de_tempo_da {arquivo.split('_')[4]} {arquivo.split('_')[5]}_intervalo {i+1}.csv")
            resultado_df = pd.DataFrame({'x': regime_time_zeroed, 'sinal': normalized_data})

            if os.path.exists(output_file):
                resultado_df.to_csv(output_file, mode='a', header=False, index=False, sep=';')
            else:
                resultado_df.to_csv(output_file, index=False, sep=';')

            nome_grafico_lifetime = f'Intervalo {i+1} da {arquivo.split('_')[4]} {arquivo.split('_')[5]}_foton lifetime.png'
            output_grafico_lifetime = os.path.join(folder_destiny_graficos, nome_grafico_lifetime)
            plt.savefig(output_grafico_lifetime)
            plt.close()

        # Calcular a média da constante de tempo
        if len(constante_tempo) >= 1:
            pesos = 1/(np.array(erro_constante_tempo))**2
            Constante_de_tempo_arquivo = np.sum(np.array(constante_tempo)*pesos)/np.sum(pesos)
```

```
            erro_Constante_de_tempo_arquivo = np.sqrt(1/np.sum(pesos))
        else:
            print(f"Não foi possível calcular a constante de tempo para a {arquivo.split('_')[4]} {arquivo.split('_')[5]}")

        # Exibir os parâmetros ajustados
        for i, params in enumerate(fitted_params):
            errors = np.sqrt(np.diag(pcov))
            print(f"Intervalo {i+1} - Parâmetros Ajustados (normalizados):")
            print(f"Amplitude Alta (a) = {params[0]:.7f} ± {errors[0]:.7f}")
            print(f"Amplitude Baixa (b) = {params[1]:.7f} ± {errors[1]:.7f}")
            print(f"Tempo de Transição (c) = {params[2]:.7f} ± {errors[2]:.7f}")
            print(f"Offset (d) = {params[3]:.7f} ± {errors[3]:.7f}")
            print(f"Constante de Tempo (tau) = {params[4]:.7f} ± {errors[4]:.7f}")
        if len(constante_tempo) >= 1:
            for constante, erro in zip(constante_tempo, erro_constante_tempo):
                print(f'Constantes de tempo usados para analisar o ARQUIVO: Coleta: {constante:.7f}, Erro: {erro:.7f}')
            print(f"Constante de Tempo do arquivo (tau) = {Constante_de_tempo_arquivo:.7f} ± {erro_Constante_de_tempo_arquivo:.7f}")
    # else:
    #     os.remove(caminho_arquivo)
    #     print(f"Arquivo {arquivo} removido por não ter valor máximo maior que 0.0050")

if len(Constante_de_tempo_coleta) >= 1:
```

```
    pesos_coleta = 1/(np.array(erro_Constante_de_tempo_coleta))**2

    Tau_Coleta =
sum(np.array(Constante_de_tempo_coleta)*pesos_coleta)/sum(pesos_coleta)

    erro_Tau_Coleta = np.sqrt(1/sum(pesos_coleta))

    Tau_Coleta_a = np.mean(Constante_de_tempo_coleta)

    erro_Tau_Coleta_a = np.mean(erro_Constante_de_tempo_coleta)

    for constante, erro in zip(Constante_de_tempo_coleta,
erro_Constante_de_tempo_coleta):

        print(f"Constantes de tempo usados para analisar a COLETA: Coleta:
{constante:.7f}, Erro: {erro:.7f}")

    print(f"Quantidade de regimes analisados: {len(Constante_de_tempo_coleta)}")

    print(f"Constante de Tempo da Coleta (tau) - Média Aritmética =
{Tau_Coleta_a:.10f} ± {erro_Tau_Coleta_a:.10f}")

    print(f"Constante de Tempo da Coleta (tau) - Média Ponderada =
{Tau_Coleta:.10f} ± {erro_Tau_Coleta:.10f}")
```